MASTER THESIS IN CHEMISTRY

A project in renewable fuels: A study of the catalytic activity of sulfated H-Ni-Mo catalyst on ZrO_2 support in the LtL-process, and development of ESI-MS method for biooils

by
Audun Kronstad

September 2015

Institute of chemistry

University of Bergen

Summary

Biofuels produced from lignocellulosic materials have the potential to serve as a good substitute or supplement to the fuels produced from conventional sources. The chemical similarity between biooil and conventional oil also allows for the potential production of a wide range of platform chemicals. The utilization of the carbohydrates in the lignocellulosic biomass is near commercialized, but 1/3 of the biomass consists of the component lignin.

Lignin-to-liquid is a termochemical solvolysis process that utilizes formic acid as a hydrogen donor to depolymerize and deoxygenize the lignin polymers. The oxygen content of the oils produced by lignin-to-liquid is generally higher than that of conventional oils, reducing the quality of the oil. Further oimprovement of the process can be obtained using catalysts to increase hydrogenation and oxygen removal.

The hydrogenated Ni-Mo catalyst on a zirconia support was tested for catalytic activity in the range 300-380 ºC and 2-10 hours reaction time. A good experimental result is characterized by high yield and H/C-ratio, and a low O/C-ratio. The yield of the catalyzed experiments was higher than the uncatalyzed, as well as the H/C-ratio. The O/C-ratio was higher for the catalyzed experiments.

Characterization of the oils was done by GC-MS, GPC and elemental analysis.

The development of an ESI-MS method for analysis of the oils was attempted. No method was successfully developed to allow for ionization of the compounds in the mixture not containing nitrogen.

Acknowledgements

First and foremost I would like to thank prof. Tanja Barth for allowing me to do my master thesis under her supervision. Your guidance and help along the way have meant a lot, and your positive spirits is a great help when facing adversities, and appreciated in general. So thank you so much for your guidance and the time you have invested in supervising this project.

Secondly I would like to thank Mikel Oregui Bengoechea (PhDc) for his hard work and patience. Thank you for the tutoring in both lab and analytical procedures as well as a plethora of fun trivia about Spain.

I would also like to thank my parents. Their support have meant the world, and I can honestly say that without their help, both monetary and otherwise, I would not be where I am today. My sisters and brother, who have also kept me in good spirit as the project has progressed. Thanks also to my grandparents for constantly checking up on me.

The friends I've met at UiB have been great sparring partners, both during the master thesis and bachelor program. The friends from elsewhere who don't really care about chemistry, but still let me talk about it.

Abbreviations

LtL	= Lignin to liquid
IPCC	= Intergovernmental Panel on Climate Change
PV	= Photovolatic energy
HDO	= Hydrodeoxygenation
GC-MS	= Gas chromatography-mass spectrometry
GPC	= Gel permeation chromatography
EA	= Elemental analysis
RT	= Retention time
MS	= Mass spectrometry
ESI	= Electrospray ionization
CRM	= Charged residue model
IEM	= Ion evaporation model
TIC	= Total ion current
THF	= Tetrahydrofuran
EtAc	= Ethylacetate
M_w	= Molecular weight
NIST	= National Institute of Standards and Technology
O/C	= Oxygen to carbon ratio
H/C	= Hydrogen to carbon ratio
BHT	= Butylated hydroxytuolene
PC	= Principal component
PLS	= Partial least squares
PCA	= Principal component analysis
DCM	= Dichloromethane

Table of contents

1 Introduction

1.1 Energy consumption

The last 100 years there has been a vast increase in energy usage. With more and more processes becoming automatized, and the eternal chase for bigger and better, this is not looking to change in the years to come. In the same period of time we have progressively become better at finding and retrieving the fossil fuels present underground, and so we have been able to keep up with the increased demand.

It lies in the nature of fossil fuels to be a limited resource. It is formed as organic matter is subjected to high pressure and temperature over millions of years. A major part of the earths reservoirs have probably already been discovered, and quite possibly a large fraction has also been retrieved and used. To what degree this is true does however depend on what analyst you are willing to believe.
One such prediction is shown in Figure 1.1.

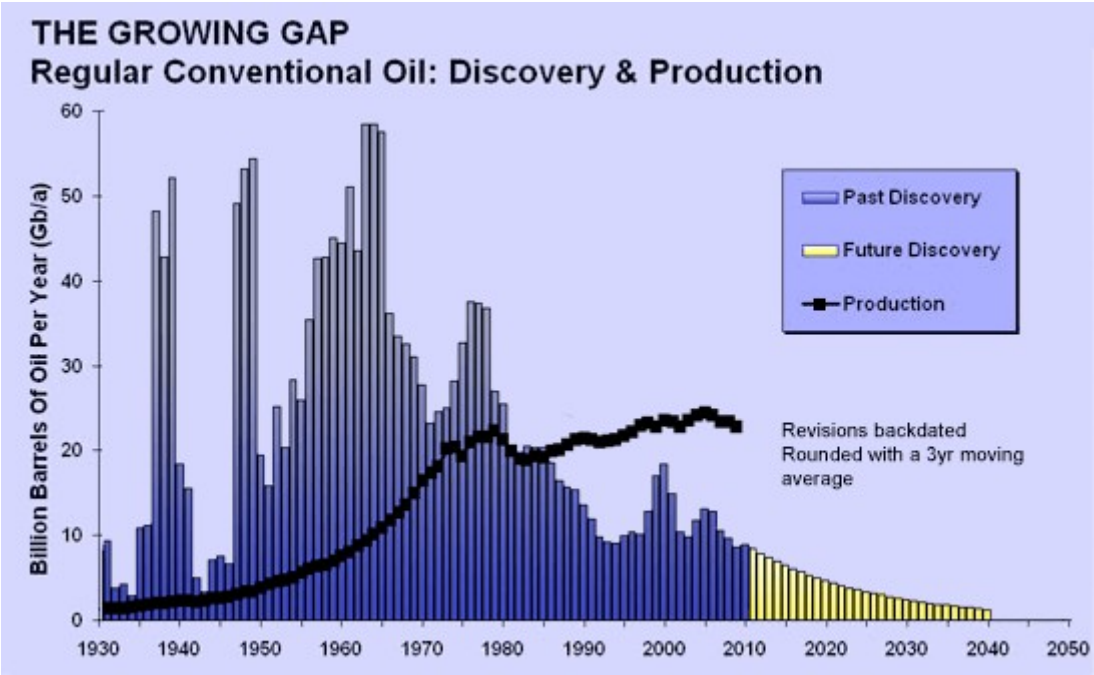

Figure 1.1: Oil reserves and production [1]

The last 20 years the rate of major discoveries have slowed down significantly, and it

is largely due to technical advancements allowing us to retrieve a bigger fraction of the resources that we have been able to keep up with the rise in demand. The advances in technology have also allowed us to extract petroleum from unconventional sources to an increasing degree. In particular the shale oil and gas production in the US have increased over the last few years as show in Figure 1.2.

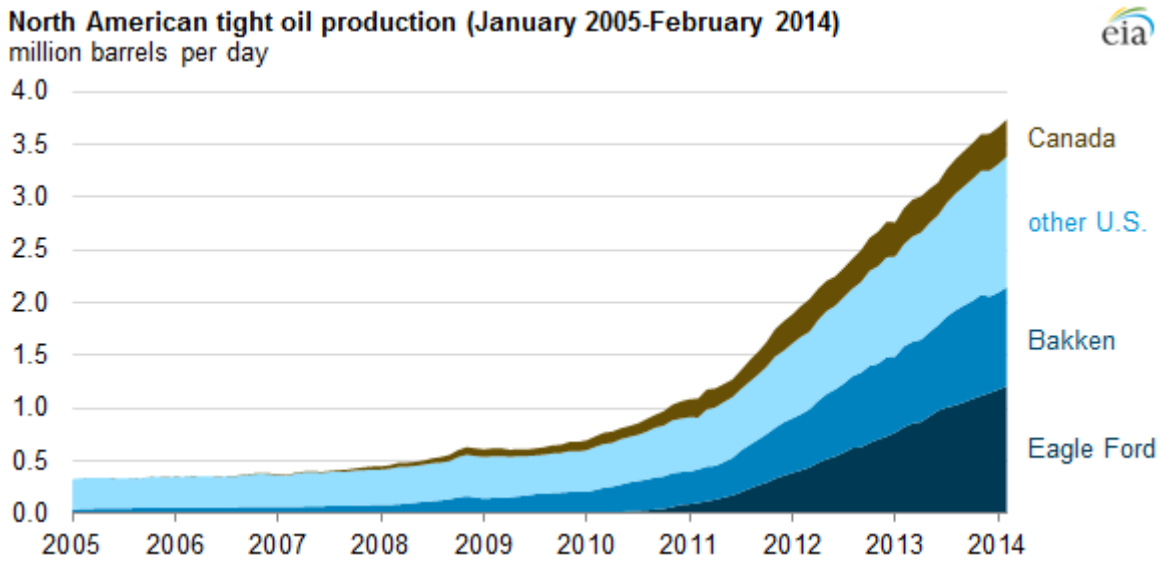

Figure 1.2: Production of US shale oil [2]

The production of oil from conventional sources was steadily increasing until a record was reached in 2008. After 2008 it has been steadily decreasing. Due to the sharp increase in shale oil production there was a new record set in 2013. Despite the advances in technology and use of unconventional sources many analysts are reaching the conclusion that we may have, or will soon, reach max production, or peak oil, and that the production will decrease steadily from now on.

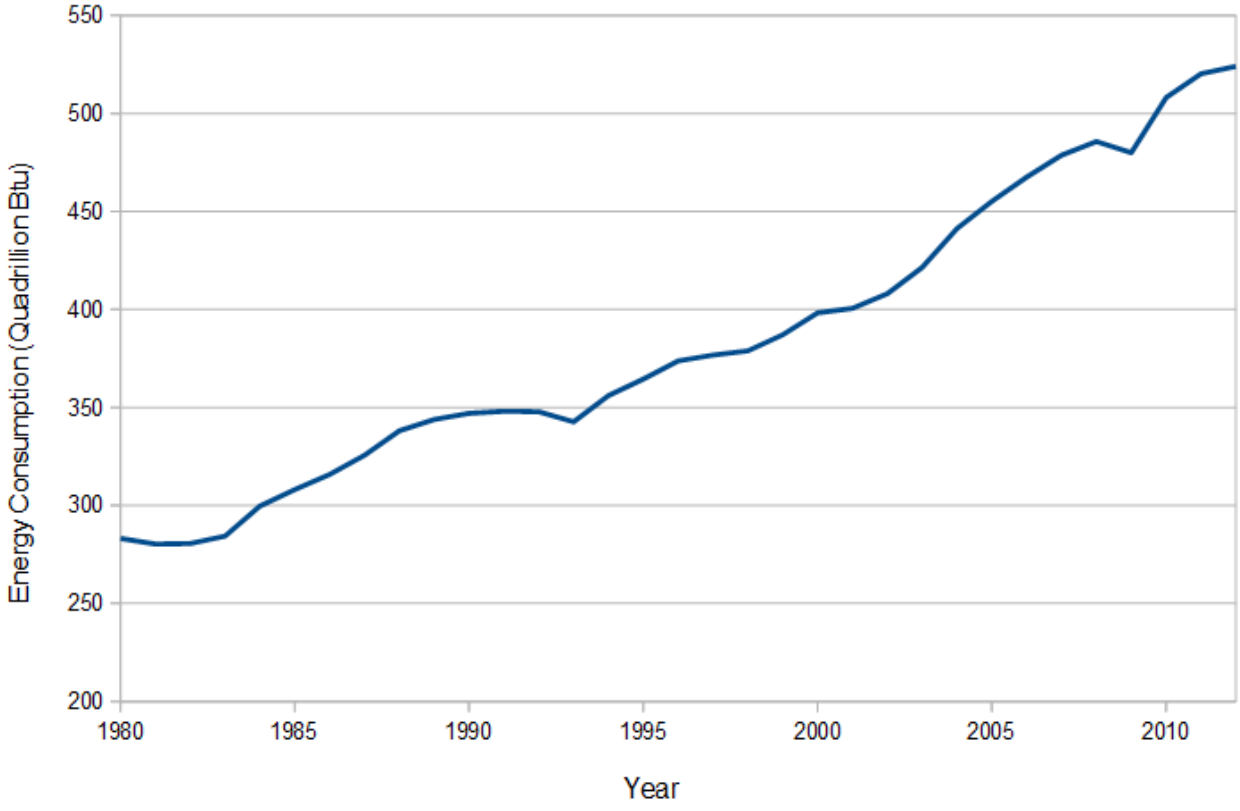

Figure 1.3: World energy consumption 1980-2012 [3]

From 1980 to 2012 the world's energy demand has increased by over 80 % (Figure 1.3). [3] Countries with huge populations, like China and India, have had a growing middle class, and with increased purchasing power comes increased energy usage. By now China has a slowing growth in energy consumption, and in 2014 China in fact experienced a 0 % growth in energy consumption for the first time in 17 years. [4] At the same time the world's energy consumption continues to rise, and it is unlikely that it will stop in the coming years.

1.2 Fossil fuels

With fossilized fuels being both a limited resource and a major contributor to both air pollution and global warming, it is probable and most likely desirable, that we look for other primary sources for the energy of the future. Fuels produced from biomass

can help relieve part of the problems encountered from use of fossil fuels. When plants grow they capture CO_2 from the atmosphere, and store it as organic molecules. The CO_2 released from internal combustion engines running on biofuels has in other words quite recently been a part of the atmospheric carbon cycle, and is in that sense carbon neutral. Fossil fuels contains carbon that have been out of the cycle for millions of years, and during this time it has not had any effect on the atmosphere. A schematic representation of the carbon cycle can be seen in Figure 1.4.

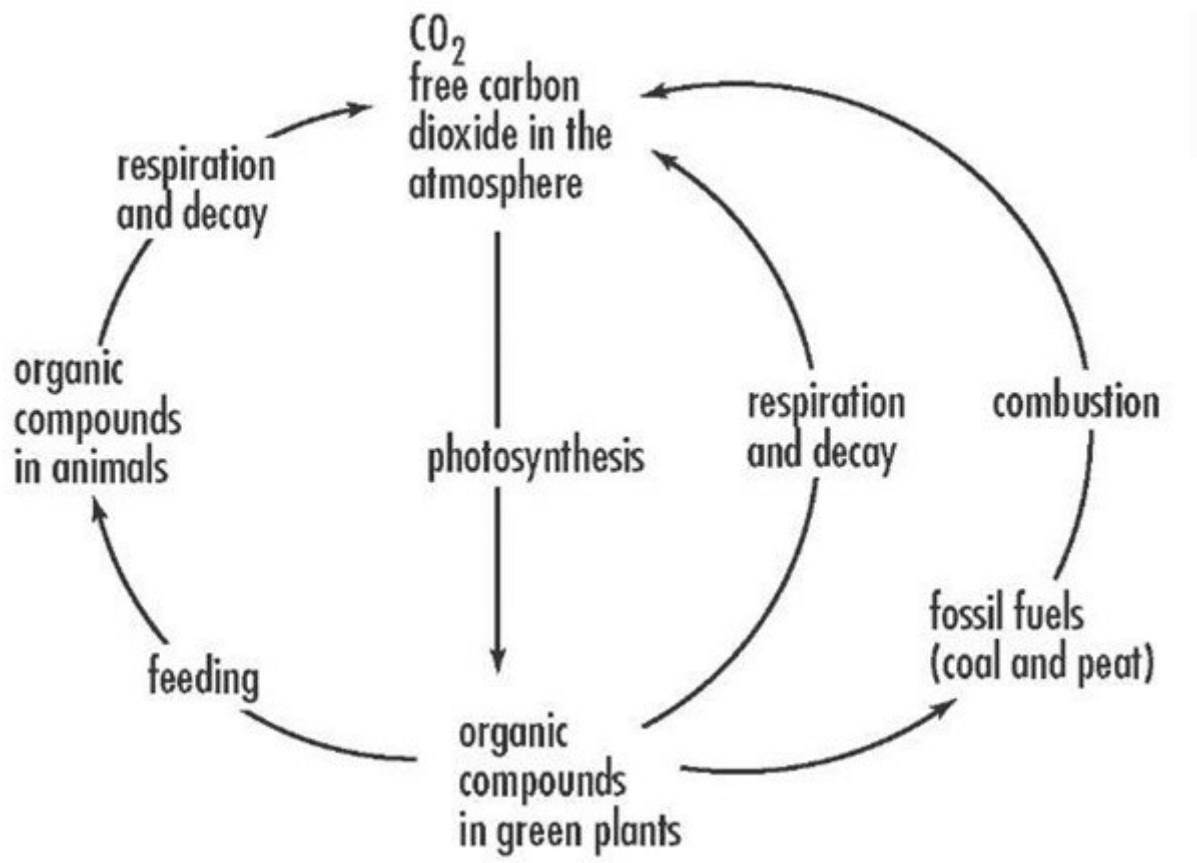

Figure 1.4: The carbon cycle [5]

At the same time biomass is renewable resource, and a commercially viable production would most certainly help meet the future energy needs.

Large parts of the scientific community are convinced that the increase in temperature

we're experiencing at a global scale can in large parts be accredited to the greenhouse effect. There are a lot of different gases causing the greenhouse effect, and many of them occur naturally in the atmosphere, including CO_2. The problem we're encountering today is that carbon which has been removed from the natural carbon cycle for millions of years is being reintroduced as CO_2, leading to a progressively increased concentration in the atmosphere as we retrieve fossilized carbon from the ground. A graph showing the CO_2 emissions from 1850-2010 can be seen in Figure 1.5.

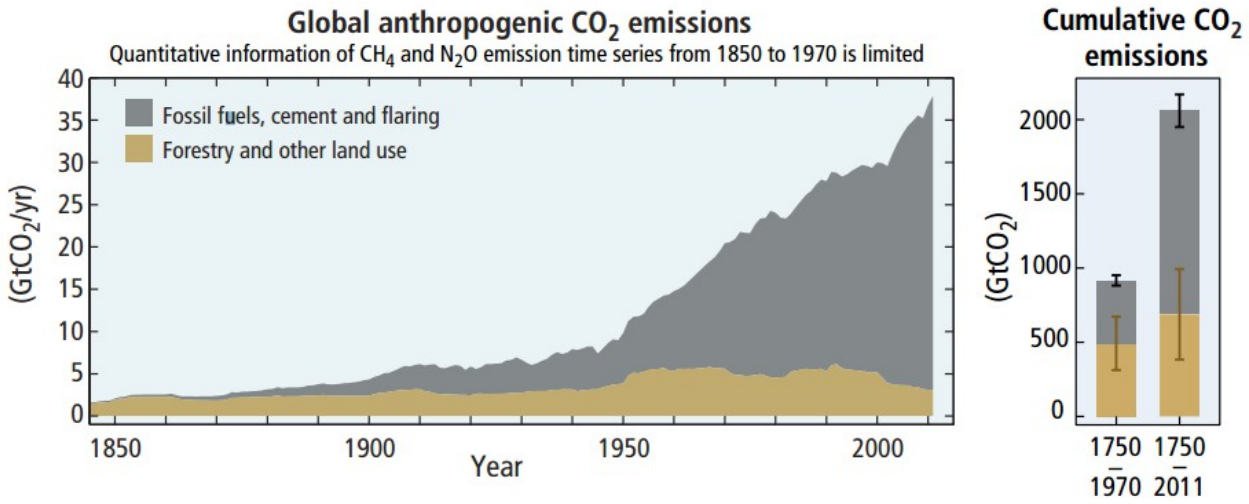

Figure 1.5: The increase in CO_2 emissions over time [6]

At the 2009 U.N. Climate Change Conference in Copenhagen a decision was made to make attempts at keeping the global rise in temperature below 2 degrees, this is referred to as the “2-degree goal”. IPCC claims that to keep inside of this goal a 40-70% cut in climate gas release from the 2010 numbers before 2050 is necessary, and a subsequent progression towards zero release in 2100. They even suggest that CO_2 might have to be removed from the atmosphere. [7]

1.3 Renewable sources of energy

A move towards renewable sources of energy is necessary to keep the global rise in temperature below the 2-degree goal. As it stands now, most renewable sources of energy are less economically viable than using fossil fuels. This will change in the future as the supply of fossil fuels decrease while the demand for energy continues to increase.

In Norway, where we have a lot of mountains and precipitation, hydropower have delivered much of the electrical energy needed for a long time. Hydropower is a very clean source of energy regarding pollution and global warming. It does however require big interventions in the landscape around the power plants, which is not always too popular. The efficiency of a hydropower plant is greatly affected by the surrounding landscape. With no big changes in altitude one should look towards other sources of power.

Nuclear energy is another source of potentially clean energy that can provide a large part of the future energy production, but with the disasters of Chernobyl, Sellafield and Fukushima in mind this is often met with skepticism.

Solar power, or photovolatic energy (PV), is a very promising source of renewable energy. The energy output is highly dependent on the amount of solar light the solar cells are exposed to, the weather conditions are in other words directly related to the energy output. To obtain a good efficiency with the current technology PV should be developed in areas with much direct sunlight. This raises questions concerning, amongst others, storage and transport.

The primary problem when moving towards a society running on renewable energy is the long distance transport. Assuming zero release production of electricity can be achieved, there is still a long way to go until big ships and airplanes are running on

electricity. The major advantages to bio oils is that they are not only more environmentally friendly than petroleum products, but they can also be utilized by the technology already in place. This lowers the transitional costs considerably, and can be a significant catalyst for companies and other entities to choose more environmentally friendly.

Petroleum is not only a vast source of energy in today's society, it is also the origin of a lot of useful chemicals and materials. With bio oils produced from biomass having similar chemical properties to petroleum, it will be possible to produce platform chemicals from bio oil.

1.4 Biofuels

Biomass is composed of organic molecules, and as such are mostly carbon, hydrogen, oxygen, with traces of nitrogen and some minerals.
The oxygen content of biomass is larger than petroleum, and as the energy organic molecules provides is inversely correlated to the oxygen content, the energy content of biomass is lower than that of petroleum.

Biofuels are generally characterized depending on the biomass they are derived from.

- First generation biofuels are produced from food crops like corn or sugar cane.
- Second generation biofuels are produced from biomass that is not usually used for food.
- Third generation biofuels are derived from algae

First generation biofuels present an ethical dilemma. As millions of people are suffering form starvation, it could be considered unethical to use biomass that could potentially be used as food. It has also been hypothesized that their production have increased food prices as the demand rises.

Second generation biofuels escape many of the problems faced by first gen. They do not directly compete with food sources in the market, and can generally be grown on soil not suitable for growing food. As a consequence lignocellulosic biomass is attracting attention as a possible feedstock for biofuels.

1.5 Lignocellulosic biomass

Lignocellulosic biomass consists of three major components:

- Cellulose: 40-50 %
- Hemicellulose: 25-30 %
- Lignin: 20-30 %

Cellulose is a polysaccharide that is the major component of the cellular wall in plants, see Figure 1.6.

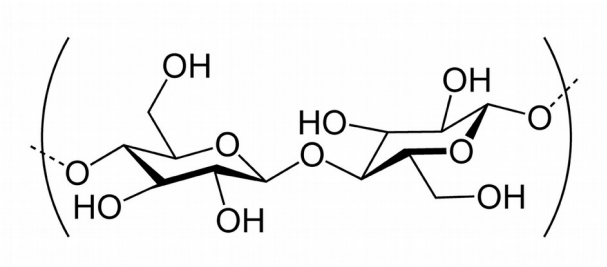

Figure 1.6: Cellulose [10]

Hemicellulose is a group of heteropolymers comprising of polymerized monosaccharides, an example can be seen in Figure 1.7

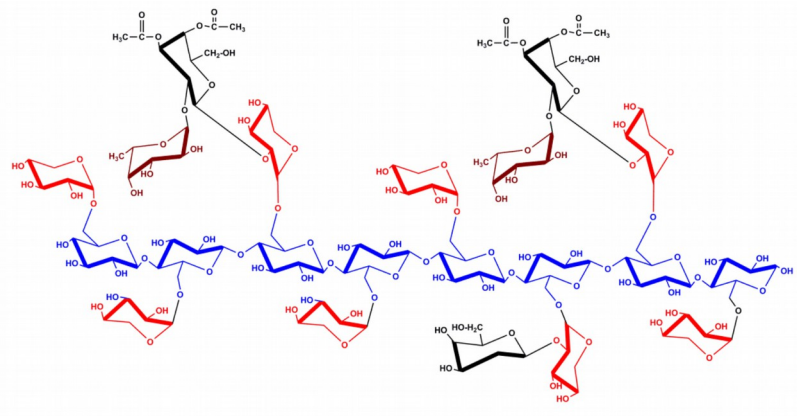

Figure 1.7: The structure of xyloglucan. The β-D-glucan backbone is shown in blue, α-D-xylose in red, α-D-galactose in black and α-L-fucose residues in brown [11]

Lignin is a class of compounds of cross-linked phenol polymers. It's function is to strengthen the cell wall and, due to its hydrophobic nature, limit transport of water. A schematic representation can be seen in Figure 1.8.

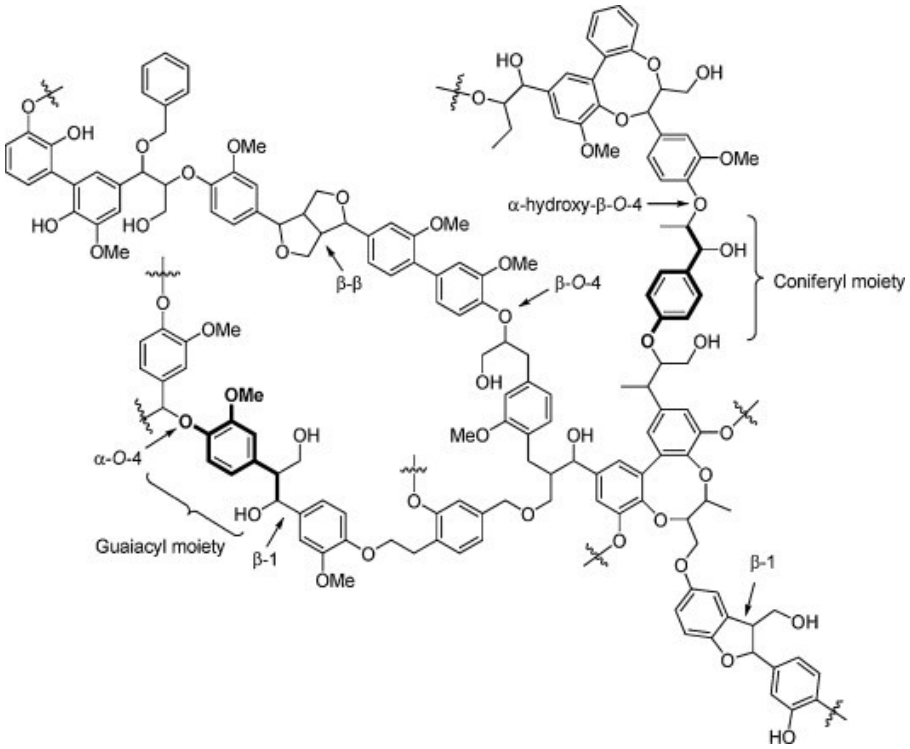

Figure 1.8: Schematic representation of a typical softwood lignin macro structure [13]

There are additional classes of compounds in lignocellulosic biomass, however due to the high abundance of these three the main effort have been focused on utilizing them to the fullest.

1.6 Harnessing the energy stored in biomass

At the present time there have been quite a few methods developed to create biofuels from biomass. Some of these are shown in Figure 1.9.

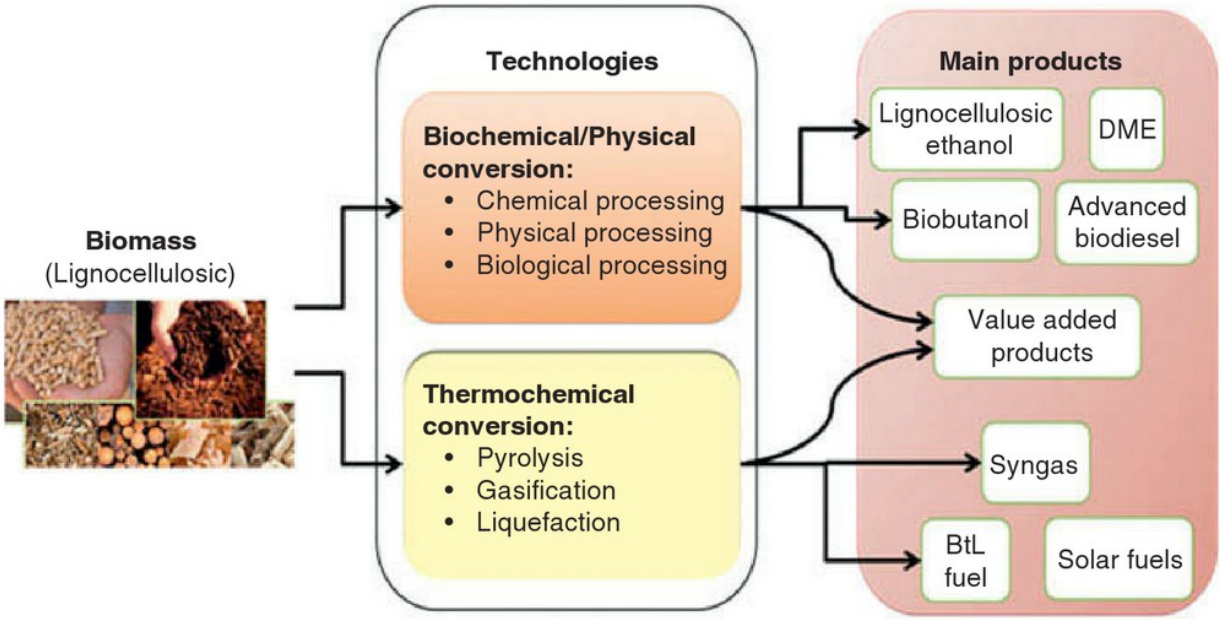

Figure 1.9: A summary of the available processes for the conversion of lignocellulosic materials into biofuels [12]

1.7 Lignin-to-liquid (LtL)

This project utilizes the LTL method of conversion. It is one of the most promising methods for conversion of the lignin in biomass. The main goals of the process is to produce a liquid from the lignin and to reduce the O/C-ratio, while increasing the H/C-ratio, thus making the products soluble in conventional petroleum, and increasing the energy density.

The general reaction for the process is shown in Figure 1.10.

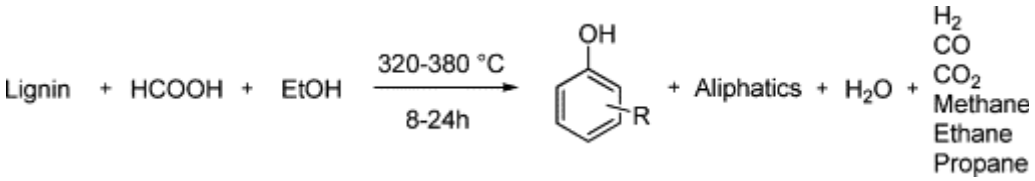

Figure 1.10: The general reaction for the LtL-conversion [13]

The reaction takes place in a closed reactor subjected to heat. The lignin is dissolved in a solvent together with a hydrogen donor and catalyst.

Various solvents have been attempted, and ethanol and water have been shown to be suitable as solvents.[8] Water has later been found to inhibit some of the potential catalysts used for the process, and as a consequence ethanol is used in this project.

To achieve a good biooil composition from the LtL-process it is necessary to reduce the oxygen content. This process is aided by adding a hydrogen donor. In this project formic acid have been used.

1.8 Catalysts for the LtL-conversion

Various catalysts have been tried to maximize the potential of the process. Hydrodeoxygenation (HDO) is a combined process of hydrogenation and deoxygenation. The purpose of HDO is to hydrogenate the unstable unsaturated bonds and to reduce the oxygen in the pyrolysis oils. There are two common types of catalysts used to catalyze HDO reactions. [14] [15] [16]

1. Sulfide catalysts e.g., $NiMoS/Al_2O_3$.
2. Noble metal catalysts, e.g. palladium, rhodium.

The first category is a well studied system that has proven to work well for systems analogous to biofuels. The relatively high oxygen content in biooil can deactivate the catalysts during the reaction, as can water. They are significantly cheaper than the noble metals.

The second category of catalysts can be used for HDO even with water as a solvent. Noble metals require less severe reactions conditions, and have a high activity for HDO. It is however very sensitive to sulfur, resulting in a need to remove sulfur before starting the reaction for certain feedstock with high sulfur content. [9]

For this project a sulfide catalyst was used. Specifically a sulfided Ni-Mo catalyst on zirconia substrate. Other types of sulfide catalysts, including $NiMoS/Al_2O_3$ were tested by others in the research group, and the cumulative results are to be evaluated by Mikel O. Bengoechea. The main exeperimental series was performed with a hydrogenated version of the catalyst, synthesized by Mikel O. Bengoechea. The effect of the support and unhydrogenated catalyst on the support was also examined.

1.9 Analytical challenges

The oils produced by the LtL-conversion consist of a diverse mix of compounds. Lignins are not a definite structure like cellulose. The products produced from the depolymerization and HDO processes are dependent on the structure of the lignin they are derived from, and as lignin is already a diverse group more diversity can be expected in the products. As the complexity of a mixture increases the challenge of obtaining e.g. a complete separation in chromatographic analysis increase with it.

2 Purpose of the study

In this study the effect on the LtL-conversion process of a hydrogenated NiMo catalyst on zirconia support (HNMZr4) was tested. The degree of catalytic activity was tested in an experimental design with two variables, reaction time and temperature. The results of the catalyzed experiments was also compared to experiments catalyzed by the NiMo catalyst on zirconia support without hydrogenation, just the zirconia support and uncatalyzed experiments.

The study of the catalyst is a part of a wider catalytic study performed in the research group.

The aim of the catalytic study is to examine the output at various combinations of reaction conditions (temperature: 300 – 380 ºC, reaction time: 2 – 10 hours). A good result would be the catalyst resulting in less severe reaction conditions yielding the same or better output in terms of quantity and quality.

The yield produced by the experiments, as well as the chemical composition of the produced oils are taken into consideration when evaluating the experiments.

An attempt was made to develop an electrospray ionization method for analysis of the oil samples produced by the LtL-conversion.

3 Methods

3.1 Solvolysis and experimental design

The lignin used for the experimental series is derived from rice straw. It is produced by strong acid hydrolysis of lignocellulosic materials at Bergen University College. Before usage it was pulverized in a blender to increase surface area. [41]

The experiment was set up as a 2^2 factorial design with temperature and reaction time as variables. [18] The values used for the levels can be seen in Table 3.1.

Table 3.1: Values of variables set up for the factorial design

Level	Temperature [ºC]	Reaction Time [hrs]
-	300	2
0	340	6
+	380	8

3.2 LtL-conversion

The reaction is performed in a 4742 reactor from Parr Instrument Company. It has a inner volume of 25 mL and are designed for pressures up to 125 bar at the maximum temperature of 540 ˚C. At lower temperatures it tolerates significantly higher pressures, at 350 ˚C the max pressure is 585 bar. [19]

The sealing of the reactors was performed in a specific rigid pattern involving cross tightening of the bolts with increasing resistance on a torque wrench.
The resistance increase in 3 steps, 15, 30 and 40 Nm. The last tightening was performed 3 times to ensure proper sealing of the reactor.

Table 3.2 shows a summary of the quantities of reactants that were put into the

reactor for each experiment.

Table 3.2: Quantities of reactants added for each experiment

Substance	Amount [g]
Lignin	2,0
Catalyst	0,2
Formic Acid	1,5
Ethanol	2,5

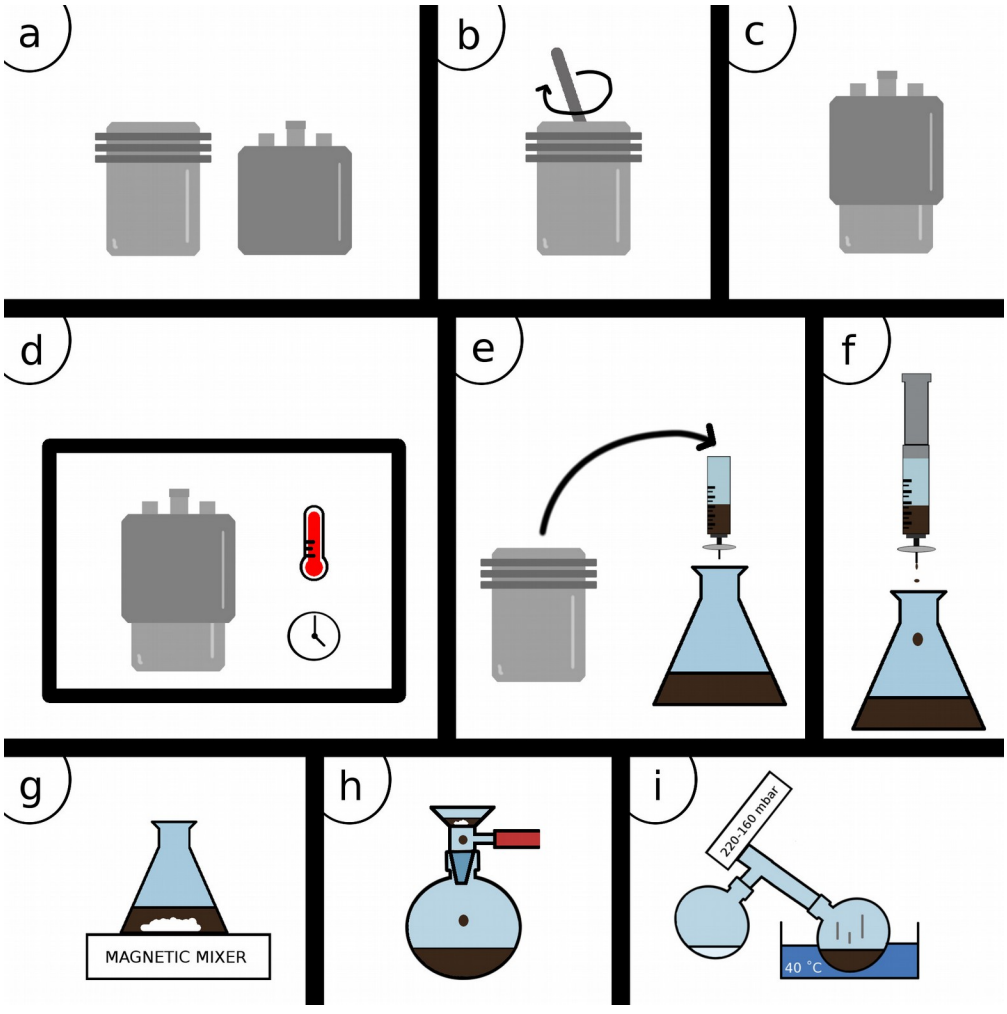

Figure 3.1: A graphical step by step representation of the LtL-conversion

A graphical representation of the process can be seen in Figure 3.1.

The procedure is based on that described for a water system in Bengoechea et al. [20]

3.2.1 Preparation of experiment

The lignin was weighed and added to the reactor along with the catalyst. The ethanol and formic was then weighed and added, save a small quantity of the formic acid, before a spatula was used to mix the contents of the reactor. The remainder of the formic acid was then used to clean of the spatula to minimize the loss of reactants. The reactor was then closed quickly after lubricating the seal with WD-40. It was then weighed before it was put into an oven preheated to the desired temperature.

After the reaction, the reactor was removed from the oven, and left to cool for approximately a day. It was then weighed before opening, to make sure there had been no significant loss of mass. The reactor was then moved to a fume hood and the valve on the reactor was then opened slightly to relieve the pressure at a slow rate. After approximately five minutes, when the excess gas had seeped out and the pressure was relieved, the reactor was fully opened. A final weighing of the reactor measures the released gas that was produced during the reaction.

3.2.2 Workup

Before starting the workup procedure the following equipment was weighed:

- 3 Pasteur pipettes
- Syringe
- 3 Pasteur pipettes, one with the tip broken off to prevent blockage (Pasteur pipette #1)
- Piston
- Nylon Filter (Whatman Puradisc 25, 0,45 μm pores)
- A vial for the oil phase, 20 mL

After opening the reactor the contents was transferred to a glass syringe connected to a nylon filter (Whatman Puradisc 25, 0,45 μm pores) using Pasteur pipette #1. A solvent consisting of EtAc and THF in a 90:10 ratio was added to solve and transfer as much as possible of the products. While transferring a piston is used on the syringe to help the speed up the filtering. The filtrate is drained into an Erlenmeyer flask

Upon completion of the transfer sodium sulphate was added to the Erlenmeyer flask to remove water. It was left for an hour while stirred with a magnetic mixer. The resulting mix was vacuum filtered into another flask through a glass filter (Whatman glass microfiber GF/F, pore size 0,7 μm).
After filtration the mix was rotavapored at 40 ˚C with a gradual decrease in pressure from 220 to 160 mbar, and the resulting oil phase was transferred to the weighed vial.

The final product was left under nitrogen gas flow for three days before the vial was weighed, sealed and refrigerated.

The rest of the weighed equipment was left for three days in a fume hood before it was weighed again, thus determining the remnants of the mix left on the equipment, as well as the solids filtered in the syringe.

3.3 Analysis

The analysis performed on the oils were gas chromatography- mass spectrometry (GC-MS), gel permeation chromatography (GPC), elemental analysis (EA) and electrospray ionization mass spectrometry (ESI-MS).

3.3.1 Gas chromatography – Mass spectrometry (GC-MS)

Method

Chromatography is one of the most important methods of analysis of chemical mixtures. It is a way of physically separating analytes in a mixture. A chromatographic system is composed of two phases called the mobile and stationary phase. The mobile phase is a liquid or gas depending on the type of chromatography. The mobile phase moves through the stationary phase, which can be either liquid or solid. As the analytes are moving through the stationary phase they are retained depending on their interaction with the stationary phase. If one analyte has a stronger interaction with the stationary phase than another analyte, it will emerge at the other end at a later time. The time it takes for a given analyte to travel from the point of injection to the detector is called retention time (RT). [21]

The choice of mobile and stationary phase is of high consequence to the separation of the compounds, especially in liquid chromatography. The chemical properties of the compounds to be analyzed are the main factors influencing this decision. For gas chromatography it is common to use inert gasses, such as nitrogen or noble gasses as mobile phases. [22]

As the sample is introduced it is vaporized and carried towards the column by the mobile phase. As the sample reaches the column the various compounds are retained depending on their chemical properties, and their interaction with the stationary phase. The resulting flow carrying the analytes towards the detector ideally contains analytes completely separated, so the detector can analyze them one by one. [23]
See Figure 3.2 for a schematic representation of a GC-system.

The detector used for this analysis was a MS. The principles of MS are discussed under ESI-MS in chapter 3.3.3.

Instrument and conditions

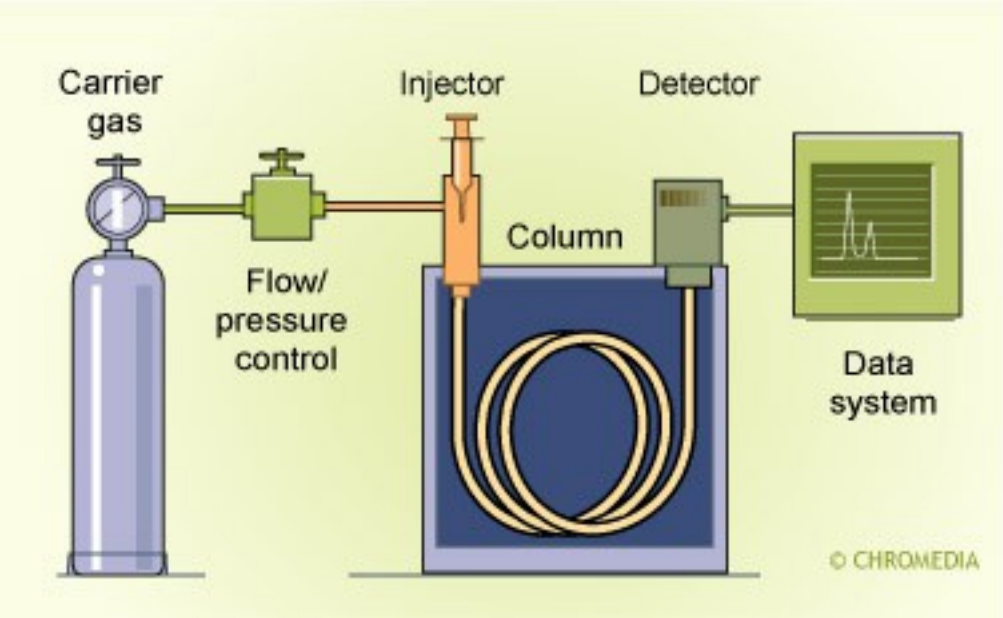

Figure 3.2: Schematic representation of a GC-instrument. [24]

For the analysis performed in this project, a mass spectrometer (MS) was used The GC-MS analysis was performed on an *Agilent 5977A* system. The sample was vaporized in an antechamber with a temperature of 280 ˚C and a pressure of 0,5 bar. Helium with a flow of 1 mL/min was used as a mobile phase. The column was a 30 m *HP-5MS*, with (5%-phenyl)-methylpolysiloxane as the stationary phase, an inner diameter of 0,250 mm and a stationary phase thickness of 0,25 µm. It is an open tubular column, meaning that it's not packed, the stationary phase is instead coating the wall. The ionization in the MS-detector was an electron ionization (EI) source running with 70 eV ionization energy. The detector was set to scan a range between 45-400 m/z. Hexadecane was used as an internal standard.

The instrument procedure used for the analysis is called TANJA2. It starts with a column temperature of 40 ˚C, with a gradual increase in temperature of 6 ˚C/min up to 280 ˚C. After 280 it increases with 40 ˚C/min up to 300 ˚C, which was kept for the remaining 5 minutes.

Sample preparation

The internal standard hexadecane was solved with a concentration of 4 µg/L in EtAc:THF (90:10). The resulting solution was then diluted to 1 µg/L and used to make the samples, with a concentration of 1 mg/mL.

3.3.2 Gel Permeation Chromatography (GPC)

Method

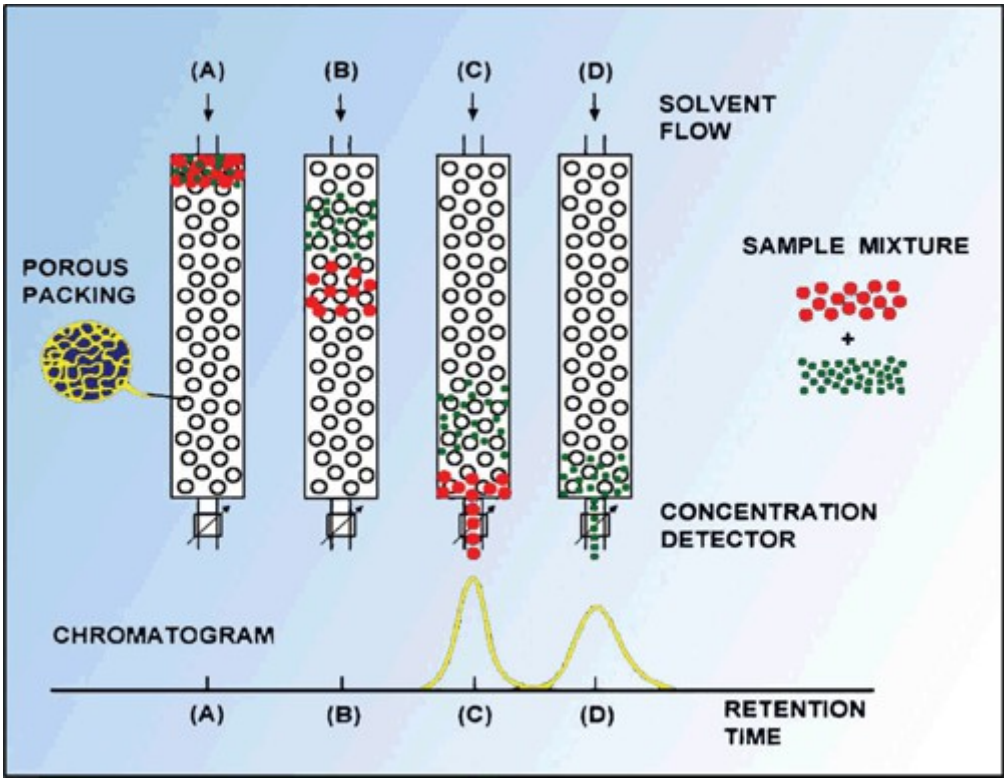

Figure 3.3: Gel permeation chromatography [25]

Where common chromatography separates analytes depending on chemical interaction with the stationary phase, GPC separates compounds depending on their size.

The stationary phase consists of a porous material, with known pore size. Larger molecules who are too big to enter the pores are not retained, and will elute together with the mobile phase. Smaller molecules are however able to enter the pores, and as the they spend time in the pores the mobile phase continues to move. This results in them eluting with a comparatively longer RT. [26] The principle is illustrated in Figure 3.3. For this analysis a spectrophotometer was used as a detector. A spectrophotometer is a common type of detector that measures the absorbance of light traveling through the flow. The absorbance is proportional to the concentration of analytes according to the Beer-Lambert law.

$$A = \varepsilon l c$$

Where ε is molar absorption coefficient, l is distance the light travels through the solution and c is the concentration of the analyte given in mol/L.

GPC produce a relative molecular weight distribution. To establish a qualitative mass distribution a calibration curve using known substances must be created. The calibration curve is used to convert detector signal vs retention time to a molecular weight distribution. An example of such a calibration curve is seen in Figure 3.4. [39]

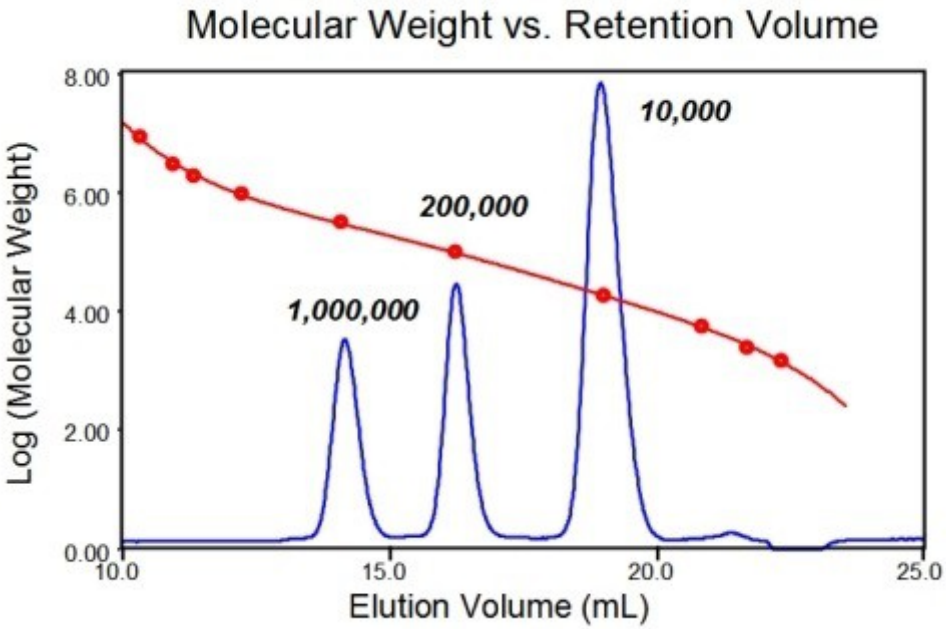

Figure 3.4: Example of a calibration curve for GPC [40]

Four polystyrene standards were chosen to establish the standardized curve. The standards had a molar mass of 162, 580, 1060 and 1480 g/mol.

Instrument and conditions

The GPC analysis was performed on a *Dionex UltiMate 3000 LC system*. The column was an *Agilent MiniMIX-E* (250x4,6 mm, PLgel 3 µm). The method used was *MedDAD2_7_2*, which is a 30 minute long program with 0,5 mL/min isocratic flow. The mobile phase used was THF. The detectors measure the absorbance at 255 and 272 nm.

Sample preparation

Both the samples and the standards were solved in THF, with a concentration of 1 mg/mL.

3.3.3 Electrospray ionization – Mass spectrometry (ESI-MS)

Method

ESI-MS is a commonly used analytical technique for mixtures of compounds. The separation effect from the chromatography combines well with MS as a detector with it's ability to analyze compounds in real time with both qualitative and quantitative aspects.

The instrument used for this analysis was a LC-MS capable of liquid chromatography. However the samples were bypassing the column, so no chromatographic separation took place. A discussion of chromatographic principles can however be seen under GC-MS (chapter 3.3.1).

Mass Spectrometry

A mass spectrometer can be divided into three regions depending on their purpose. [29] The ion source is the part of the instrument that creates the ions necessary for analysis. Several different ionization methods have been used to great effect, and the choice of which to use is generally dependent on the chemical properties of the sample to be analyzed, and what is available. [30] The mass filter separates the ions depending on the mass to charge ratio. Again there is a range of mass filters available, with varying degrees of accuracy and sensitivity. The type used for this project was a quadrupole. [31]
The detector detects the signal from the filtered ions and converts it to usable data.

Ionization method: ESI

One often makes a distinction between soft and hard ionization methods. The various methods used for ionization transfer different amounts of energy to the compound, and depending on the energy transferred the compound can form fragments, or

remain a molecular ion. Soft ionization methods, like electrospray ionization (ESI), are methods that commonly transfer a relatively small amount of energy, and consequently result in a lesser degree of fragmentation. Hard ionization methods transfer a larger amount of energy to the compounds during the ionization, and result in a higher degree of fragmentation. [32]

A schematic representation of the ESI ionization technique can be seen in Figure 3.5.

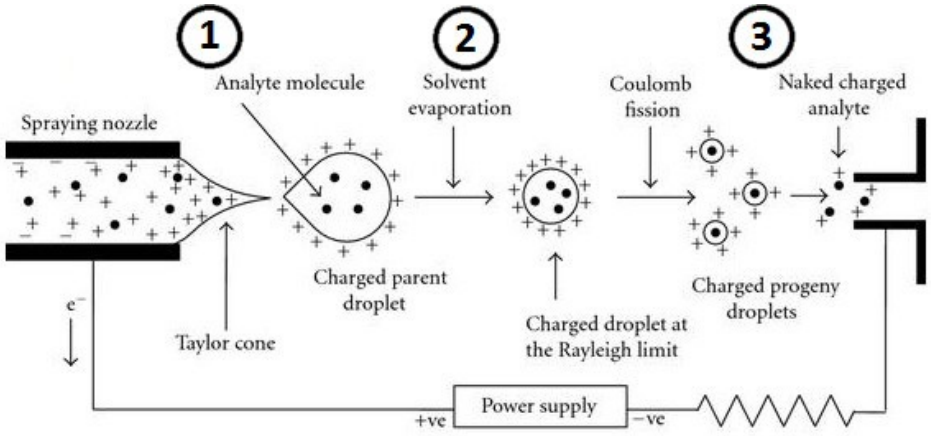

Figure 3.5: A schematic representation of the ESI ionization technique [33]

ESI was chosen as a means of ionization because it is a very soft method of ionization that leads to little fragmentation. It is also well suited towards polar and non-volatile compounds, which is expected in the oil. The process of ionization by ESI takes place through three stages: [34]

1. Formation of charged droplets at the capillary tip
2. Shrinkage of the charged droplets
3. Production of gas phase ions from the diminished small droplets

Production of charged droplets at the capillary tip

The capillary tip is charged with a voltage with a counter electrode placed at the inlet to the MS. The electric field between the two electrodes will affect the solution near the capillary tip, resulting in an alignment of the dipoles in the solution according to the direction of the field making the solution increasingly conducting. Positive ions will congregate towards the meniscus by the capillary tip, and negative ions will move away. The result of this movement is a distortion of the meniscus into what is called a Taylor cone. If the applied field is big enough a jet of fine droplets break free from the cone tip, with surfaces charged by an excess of positive ions. [35]

Shrinkage of the charged droplets

The solvent captured in the droplets evaporate while the charged ions remain, concentrating the charge further. The ionization chamber is heated to facilitate this process. As the droplets shrink the repulsive forces between the cations increase. When the repulsive forces exceed the cohesive force of the surface tension, what is called a Coulomb fission occurs, resulting in smaller droplets. This process is repeated until very small droplets are formed that ultimately will free charged gaseous analytes. [36]

Production of gas-phase ions from the diminished small droplets

The mechanism behind the formation of gas-phase ions from the very small and highly charged droplets are disputed. There are two main theories that have been proposed. *The charged residue model*, and *The ion evaporation model*. [37]

The charged residue model (CRM)

The charged residue model assumes the formation of droplets so small they can only contain one analyte molecule and some ionic charges. Further solvent evaporation will then result in a gas-phase analyte ion with the charge originating from the cations on the surface of the evaporated droplet. [38]

The Ion Evaporation model (IEM)

The IEM model predicts that when the radius of the evaporating droplet is reduced enough direct ion emission becomes possible. [38]

ESI operational modes

ESI can be performed in both positive and negative mode. The name of the mode of operation derives from the charge of the ionized compounds, which again is dependent on the polarity of the opposing electrodes.

The general reactions for the two operational modes can be written as follows:

Positive:

$M + H^+ \rightarrow MH^+$

Addition of some other cations, like sodium, has also been known to happen, as well as multiple charge ions.

Negative:

$M \rightarrow M^- + H^+$

Mass filter

Inside the ionization chamber an electric field acts on the charged particles, accelerating them towards a lens system that is focusing the beam.

To obtain usable data from the detector there needs to be a separation of the ions. There are several types of MS that achieves this in different ways, but the underlying principle is the same. Lorentz force law shows us that the force acting on an ion is related to the ionic charge while Newton's 2nd law shows that the acceleration of a particle is dependent on the mass and force acting on the ion. Mass filters distinguish ions depending on their mass to charge ratio, m/z.

Lorentz Force law: **F** = e (**E** + **v** x **B**)

Newton's 2nd law: **F** = m * **a**

where **F** is the force acting on the ion, e is the ionic charge, **E** is the electric field, **v** is the ion velocity, **B** is an applied magnetic field, m is the mass of the ion and **a** is the acceleration of the ion.

The instrument used for the data analysis is a triple quadrupole (QqQ). A QqQ is an instrument with three quadrupoles connected to each other, two capable of resolving ion masses, while a third one in between the former, called a collision cell. The main function of the collision cell is to allow for further fragmentation of the ions selected in the first quadrupole. A schematic representation of a typical quadrupole can be seen in Figure 3.6.

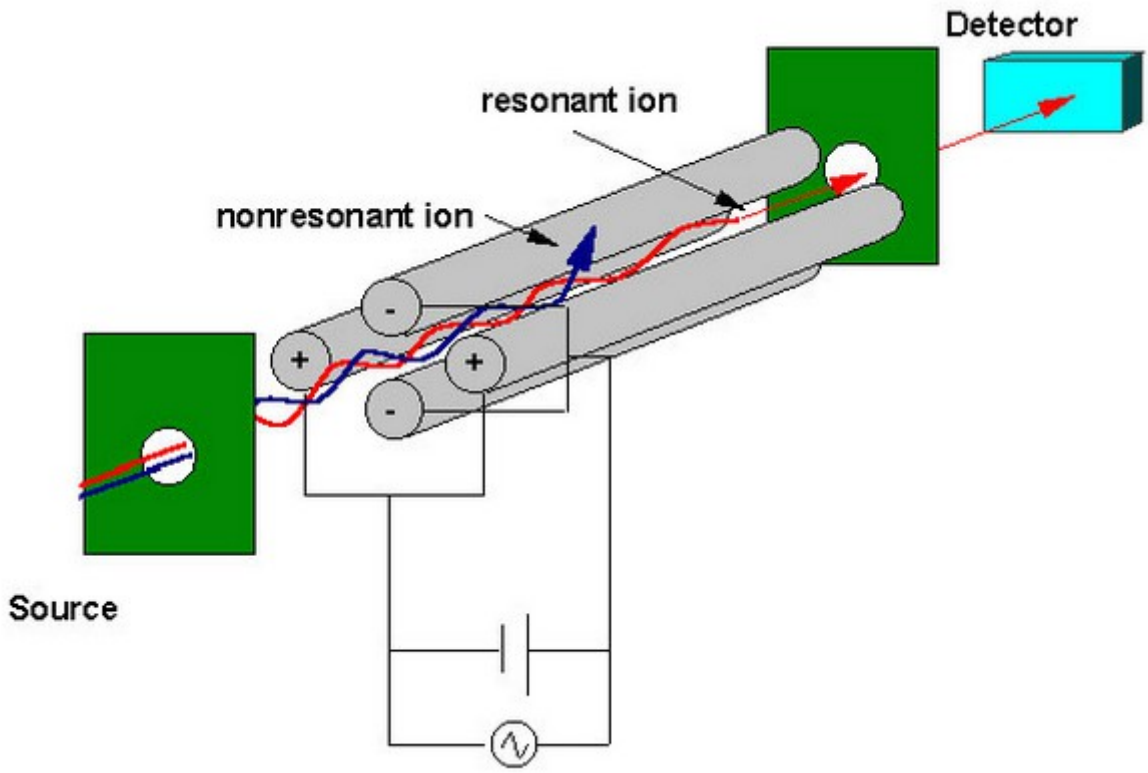

Figure 3.6: Schematic representation of a quadrupole [42]

A quadrupole consists of four parallel metal rods. Opposite rods have the same charge, while rods lying next to each other have opposite. The potentials on the rods can be varied to allow for only ions with certain m/z values to reach the detector.

The solvent used for the LC-MS procedure was methanol (MeOH) and acetonitrile (ACN) in a 1:1 ratio.

Instrument

MS

The analysis was performed on a *Agilent 6420A* mass spectrometer set up for direct infusion. 1 µL of the sample was injected into a mobile phase flow of 0,3 mL/min. The instrument was run in positive ion mode and the main series of spectra have been analyzed with the following parameters. Fragmentor: 140, cell accelerator voltage 7, nebulizer flow: 6 L/min with a temperature of 300 ºC. A voltage of 3500 V was put on the capillary needle and the scan time was set to 500.

Preparation of the samples

The samples were weighed into a 25 mL volumetric flask. Approximately 0,0375 g for the oil samples, and 0,0125 g for standard compounds. The flask was then filled with a solution of acetonitrile, methanol and dichloromethane in a 1:1:1 ratio. The dichloromethane was added to the solvent to facilitate dissolution on the samples. 1000 µL of the resulting solution was removed with an autopipette and moved to a second 25 mL volumetric flask, where it was diluted with 1:1 MeOH and ACN. The final solution was moved to a vial to be analyzed.

The data from the instruments is given as a chromatogram with total ion current (TIC) plotted against time. [28] The TIC at a given time is the integral of the corresponding mass specter. As no LC was performed in the method used, the

assumption is made that the ionized compounds have not been separated, and will arrive at the MS at the same time. The spectra at or around the maximum of the chromatogram can then be assumed to be the best representation of the sample.

3.3.4 Elemental analysis

Elemental analysis is an analytical method that shows the elemental composition of the sample. The elemental analysis instrument used for this analysis only measures hydrogen, oxygen, carbon and sulfur, although it was not calibrated for sulfur measurement, so the results for sulfur are not used. Any traces of metals and other elements were also not measured. Oxygen is assumed to make up the remainder of the weight. When ready for analysis a tin container with the sample is dropped into an oven with a CO_2 atmosphere. The tin container melts and the sample evaporates before oxygen is added. When oxygen is added the tin is oxidized to SnO_2 and the sample burns. The various elements of the sample are oxidized into gases by reactions shown in table 3, with the following overall reaction:

$$C, H, N, S \rightarrow CO_2(g) + H_2O(g) + NO_x(g) + SO_x(g)$$

Metallic copper is then used to reduce SO_3 to SO_2, NO_x to N_2 and remove residual oxygen as CuO.

The various gases are separated and measured individually. The detector used is a Thermal conductivity detector (TCD). It measures the gases ability to conduct heat. The gases are carried by a wolfram filament. Depending on the thermal conductivity of the gas mixture the temperature in the filament will either rise or decrease, and that effect is compared to that of the pure carrier gas in a reference chamber. [17]

Instrument

The analysis was performed on a *elementar Vario EL III* element analyzer.

Sample preparation

A tin container is filled with 4-10 mg of the sample and closed, then weighed, before being put into a slot on the instrument.

4 Results

4.1 Results from the LtL-conversion

4.1.1 Organization of the data

In this project the word char is used to describe the solid products after the LtL-conversion. It will contain unconverted lignin, catalyst and char produced during the reaction.

The char and oil yield are presented as the mass percent of the added lignin.

The overall mass balance is calculated as the mass of the products divided by the mass of the reactants.

The lignin recovery is the sum of the oil and gas yield.

The results of some experiments were discarded due to gas leakage during heating, or various problems during the workup. Those results are not reported.

The name of the experiments catalyzed by the HNMZr4 catalyst is on the form H(temp)-(time). So the name of the experiment catalyzed by HNMZr4 on 340 ºC with 6 hours reaction time is H340-6.

The experiments conducted with other catalysts, or uncatalyzed, are all on 340 ºC and 6 hours, so they will be named only after the catalyst.

4.1.2 Yields from the experiments

Table 4.1 shows a summary of the product yields from the LtL experiments.

Table 4.1: Reaction results from the LtL-conversion

Type of Catalyst	Reaction time [hrs]	Temperature [ºC]	Oil yield [%]	Char yield [%]	Gass yield [%]	Lignin recovery [%]	Overall mass balance [%]
NoCat	6	340	40,0	33,0	25,0	73,0	49,5
Zr4-1	6	340	37,77	30,66	24,43	68,43	47,42
Zr4-2	6	340	36,59	33,85	22,49	70,44	45,95
NMZr4-1	6	340	45,99	33,74	28,79	79,74	54,64
NMZr4-2	6	340	47,97	26,69	24,91	74,67	48,89
HNMZr4	2	300	33,2	45,91	24,25	79,10	50,03
HNMZr4	6	300	46,97	30,11	25,59	77,09	50,68
HNMZr4-1	10	300	51,75	24,68	23,69	76,44	48,13
HNMZr4-2	10	300	50,95	23,57	25,88	74,52	49,90
HNMZr4	2	340	49,15	32,17	22,45	81,33	49,53
HNMZr4-1	6	340	66,6	20,02	25,70	86,62	54,14
HNMZr4-2	6	340	71,89	29,92	27,08	101,81	60,00
HNMZr4-3	6	340	65,51	24,07	26,53	89,58	55,52
HNMZr4	10	340	56,46	22,68	25,44	79,14	51,31
HNMZr4	2	380	44,81	27,47	31,08	72,29	53,62
HNMZr4	6	380	45,42	29,43	36,70	74,85	60,80
HNMZr4	10	380	45,44	37,82	41,72	83,25	69,13

A graphical representation of the oil, char and gas yields from Table 4.1 can be seen in Figure 4.1.

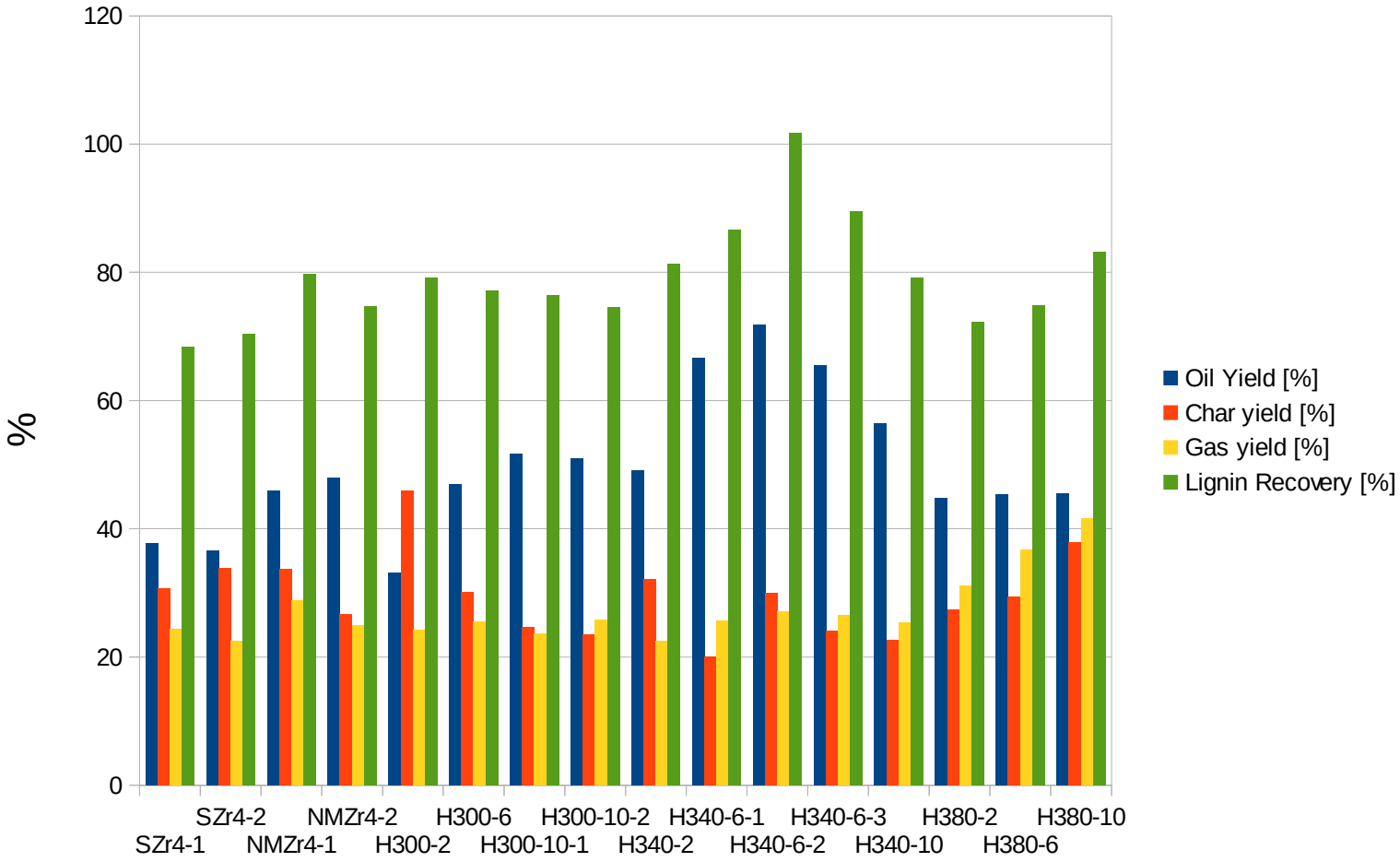

Figure 4.1: A graphical representation of the oil, char and gas yields from the experiments performed.

Table 4.2 shows an overview of the gas produced during the experiments. The gas yield is given in both mass and as a percentage of the added reactants. The percentage of formic acid released as gas relative to the adde amount is also shown.

Table 4.2: Gas yield from the LtL-conversion

Type of catalyst	Temperature [°C]	Reaction time [hrs]	FA [g]	Gas phase [g]	Gas phase [%]	Gas phase [% FA]
-	340	6	1,496	1,50	25,0	1,00
Szr4	340	6	1,48	1,5	24,43	98
SZr4	340	6	1,43	1,4	22,49	102
NMZr4	340	6	1,48	1,8	28,79	82
NMZr4	340	6	1,52	1,6	24,91	95
HNMZr4	300	2	1,42	1,5	24,25	94
HNMZR4	300	6	1,5	1,6	25,59	94
HNMZR4	300	10	1,53	1,5	23,69	102
HNMZR4	300	10	1,49	1,6	25,88	93
HNMZr4	340	2	1,45	1,4	22,45	103
HNMZR4	340	6	1,54	1,6	25,7	97
HNMZr4	340	6	1,57	1,7	27,08	92
HNMZr4	340	6	1,56	1,7	26,53	92
HNMZr4	340	10	1,43	1,6	25,44	89
HNMZR4	380	2	1,59	2	31,08	79
HNMZR4	380	6	1,48	2,3	36,7	64
HNMZr4	380	10	1,46	2,6	41,72	56

4.1.3 Water system

Before the catalyst was found to be inactivated in a water system around 10 successful experiments were performed with this system.

4.2 Elemental analysis

Most of the oils were analyzed in parallels. The complete data set from the elemental analysis can be seen in appendix.A1 and A2. Table 4.3 shows a summarized version displaying the mean value between the parallels.

*Table 4.3: The elemental abundance in the oil samples created by the LtL-conversion, given in mol percentage. * The analysis for the lignin was performed by Mikel Oregui Bengoechea.*

Sample	Nitrogen	Carbon	Hydrogen	Oxygen	O/C	H/C
Lignin*	0,2	62,0	5,5	32,2	0,39	1,05
NoCat	0,64	41,71	51,67	5,97	0,143	1,239
SZr4	0,55	42,11	51,92	5,41	0,129	1,233
NMZr4	0,58	41,94	52,32	5,14	0,123	1,248
H300-2	0,46	40,05	49,88	9,61	0,240	1,246
H300-6	0,48	40,97	50,11	8,44	0,206	1,223
H300-10	0,52	41,18	51,37	6,92	0,168	1,248
H340-2	0,52	41,84	50,31	7,32	0,175	1,202
H340-6	0,50	41,32	51,91	6,26	0,152	1,257
H340-10	0,54	42,07	52,39	4,99	0,119	1,245
H380-2	0,58	42,46	51,88	5,06	0,119	1,222
H380-6	0,53	40,8	53,35	5,31	0,130	1,308
H380-10	0,53	40,92	54,24	4,3	0,105	1,326

A graphical representation of the oxygen to carbon- and hydrogen to carbon-ratios can be seen in a Van Krevelen diagram in Figure 4.2.

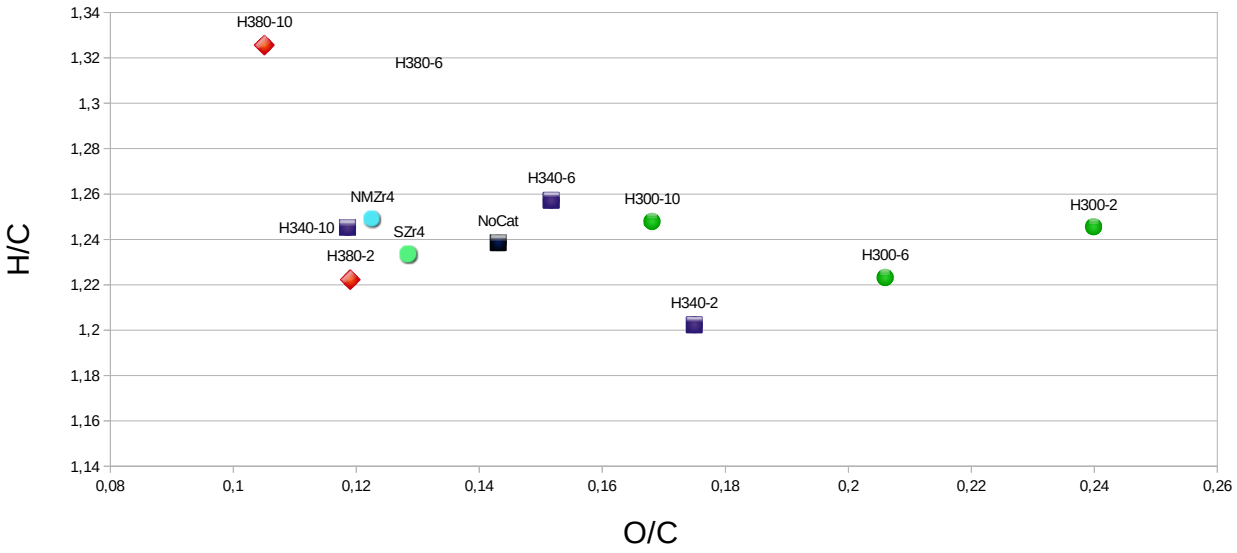

Figure 4.2: Van Krevelen Diagram of the oil samples created by the LtL-conversion.

4.3 GPC

4.3.1 Calibration curve

To form the calibration curve the chromatograms of the standards were examined. The mean mass was assumed to be represented by the peak of the chromatograms. The mean retention time of the two parallels were used. The data obtained for the standards can be seen in Table 4.3.

Table 4.3: Experimental retention times for the standard samples.

Sample		**Retention time [min]**		
Sample	**Mw [g/mol]**	**Sample 1**	**Sample 2**	**Peak mean**
mp162	162	5,34	5,16	5,25
mp580	580	4,7	4,77	4,74
mp1060	1060	4,59	4,63	4,61
mp1480	1480	4,36	4,4	4,38
mp2360	2360	4,22	4,23	4,23

The logarithm of the molecular weight was plotted against the retention time, as seen in Figure 4.3.

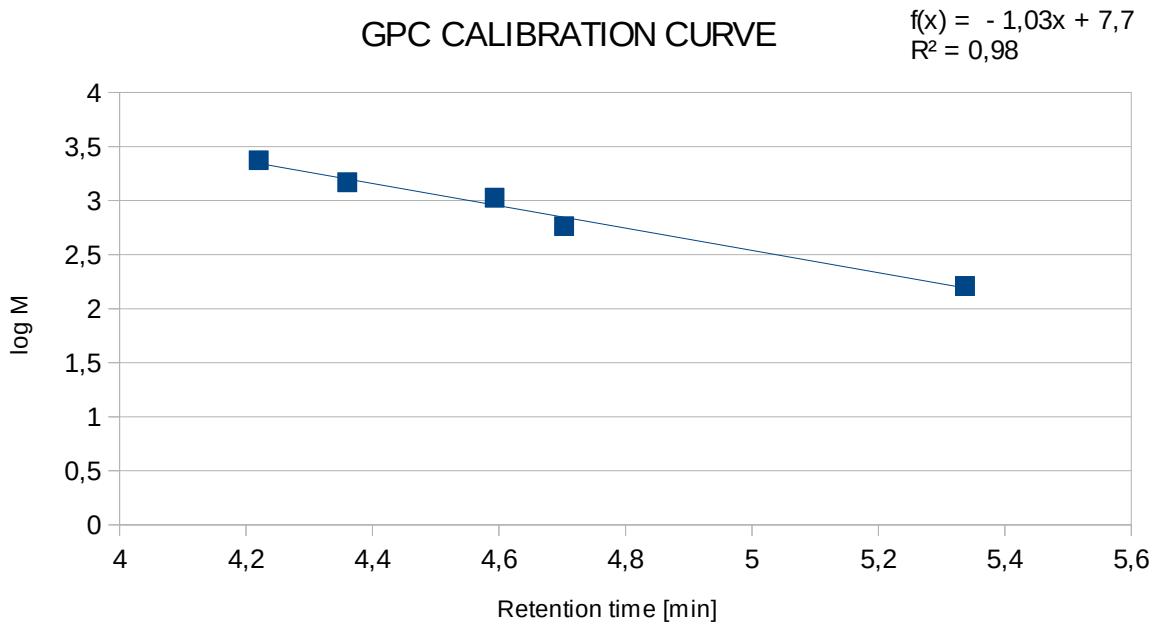

Figure 4.3: GPC calibration curve created by plotting the logarithm of the molecular weights against the retention times

A least squares approximation was used to find the following equation.

$log\ M_w = 7{,}696 - 1{,}031 * r$ *equation 5.1*

M_w is the molecular weight of the compound, and r is the retention time.

4.3.2 Oil Samples

The retention time for the peak on the spectra of the oil samples were recorded. As with the standards, the peak was assumed to represent the mean molecular weight in the sample. The results can be seen in table 4.4.

*Table 4.4: Retention time of peaks in oil spectra, and mean molecular weight calculated from equation 5.1, the uncatalyzed analysis was performed by Sveinung Fosen Simonsen, and is calculated by another calibration curve **

Sample	Retention time [min]	log Mw	Mw [g/mol]
NoCat*	4,87	2,54	346
SZr4	4,97	2,57	373
NMZr4	4,90	2,64	441
H300-2	4,80	2,75	563
H300-6	4,82	2,72	528
H300-10	4,80	2,75	565
H340-2	4,85	2,69	493
H340-6	4,89	2,66	454
H340-10	4,94	2,61	404
H380-2	4,97	2,58	376
H380-6	5,03	2,51	324
H380-10	5,13	2,41	257

A graphical representation of the mean molecular weights shown in Table 4.4 can be seen in Figure 4.4.

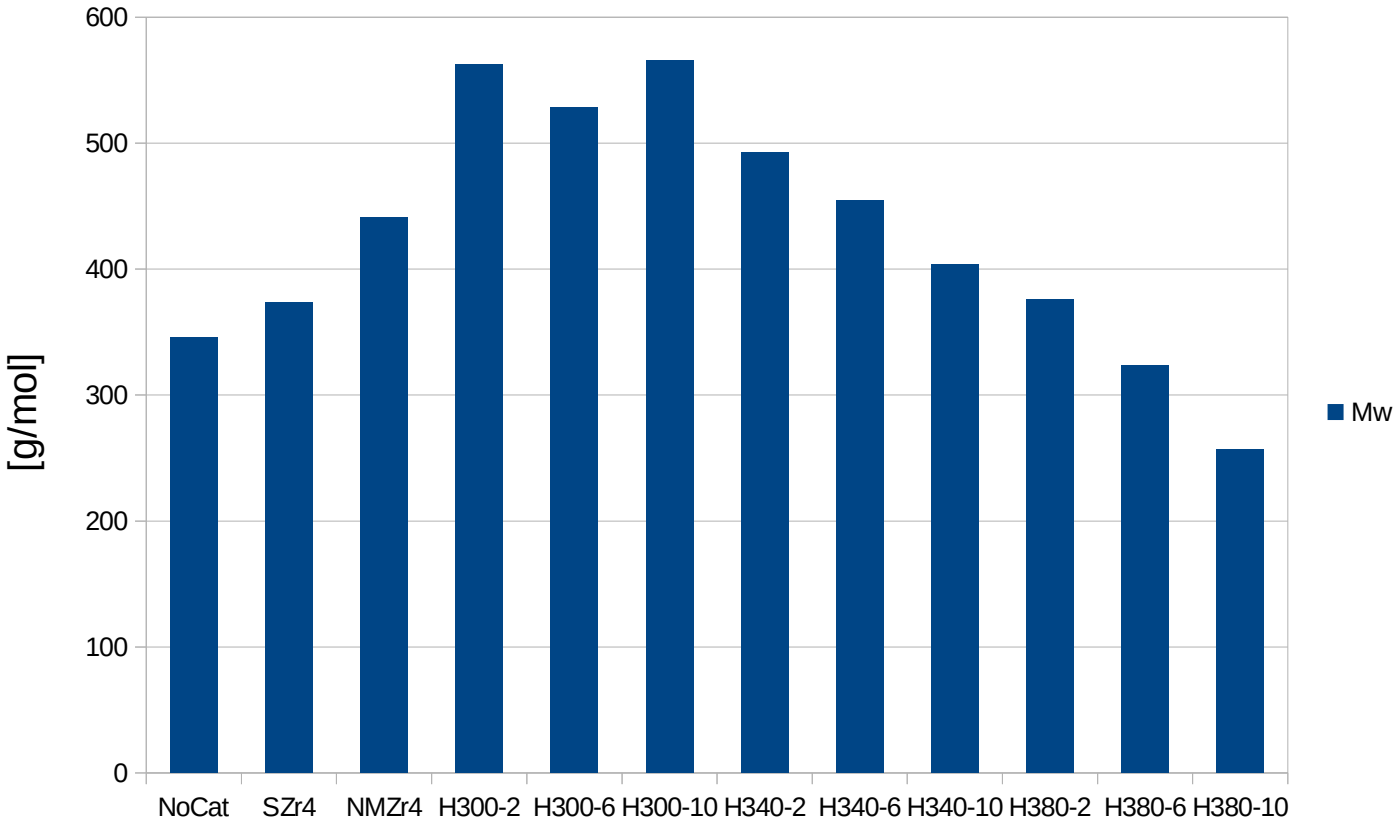

Figure 4.4: Mean molecular mass calculated for the samples, values shown in Table 4.4.

4.4 GC-MS

The major peaks in the chromatograms of the analyzed samples was analyzed by library searches. The chromatogram of H300-10-1 can be seen in Figure 4.5.

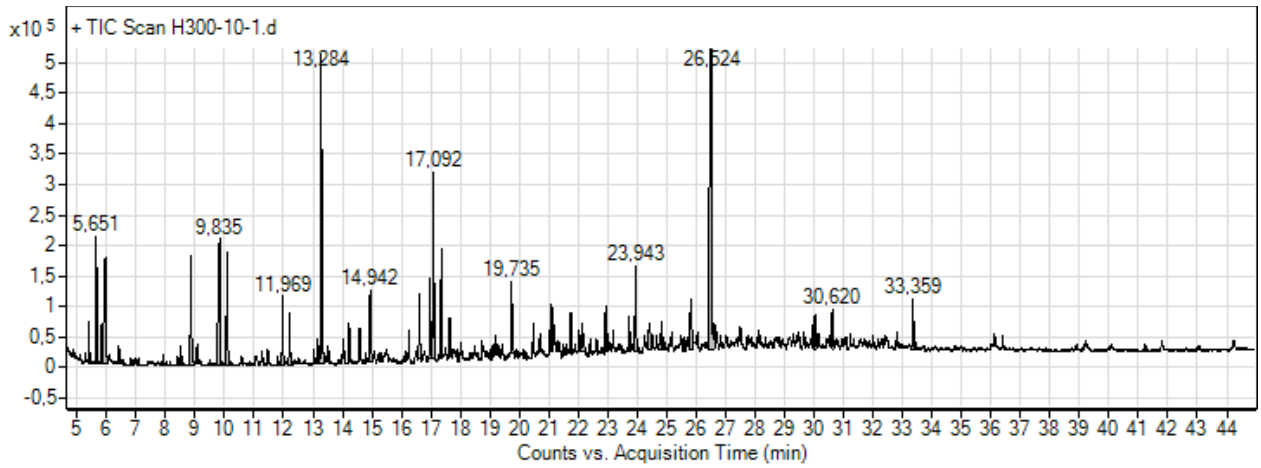

Figure 4.5: The chromatogram of H300-10-1, TIC vs retention time.

The mass spectra of the chromatographic peaks in the data was matched with the NIST library entries. Many of the substances eluting before 10 minutes seemed to be related to THF and EtAc. Due to this it was decided to focus the analysis on the compounds eluting after this point. In general the 10 most prevalent peaks in each chromatogram with a retention time higher than 10 minutes was analyzed, although some exceptions was made where there seemed to be a higher or lower number of important peaks.

This way of choosing peaks can potentially leave out valuable or useful products represented by smaller peaks, but it will better represent the total composition of the mix. A list of compounds found to be present over all the samples can be found in Table 4.5.

Table 4.5: Compounds identified by GC-MS analysis of the oil samples.

RT [min]	Compound	RT [min]	Compound	RT [min]	Compound
11,97	Phenol	19,25	3-ethyl-5-methyl-Phenol	24,3	2,4-bis(1-methylethyl)-Phenol
13,28	2-ethyl-1-hexanol	19,74	4-ethyl, 2-methoxyphenol	24,82	4-methoxy-2,3,6-trimethyl-Phenol
14,22	Levulinic acid	20,48	2,5-Diethylphenol	25,02	2,6-Diisopropylanisole
14,94	2-methoxyphenol	20,72	2,5-Diethylphenol	25,09	5-tert-Butylpyrogallol
16,26	2-ethyl-Phenol	21,24	3,5-diethyl-Phenol	25,19	1-(4-hydroxy-3-methoxyphenyl)-2-Propanone
16,61	2-ethoxyphenol	21,37	phenol, 2,6-dimethoxy	25,69	3-tert-Butyl-4-hydroxyanisole
16,97	4-ethylphenol	21,75	2-methoxy-4-propylphenol	25,82	4-methoxy-2,3,6-trimethyl-Phenol
17,04	3-ethyl-Phenol	22,85	4-tert-Butylbenzyl alcohol	26,53	**Hexadecane (Internal standard)**
17,09	Ethyl benzoate	22,93	Methylphthalimide	29,3	Ethyl-β-(4-hydroxy-3-methoxy-phenyl)-propionate
17,36	Succinic acid	22,95	2,4-bis(1-methylethyl)-Phenol	33,36	Hexadecanoic acid, ethyl ester
17,65	Creosol	23,73	2',4'-Dihydroxy-3'-methylacetophenone	34,87	Phthalic acid, ethyl 2-propylpentyl ester
19,18	3,5-diethyl-Phenol	23,95	N-Ethylphthalimide	41,25	Diisooctyl phthalate

The peaks in different chromatograms with corresponding retention time were found to represent the same compound. The compounds found in Table 4.5 are in other words a complete list of the identified compounds. A summation of the analyzed peaks for the various oils can be found in Table 4.6.

Table 4.6: Analyzed peaks for the oil samples. The corresponding compounds can be found in Table 4.5.

Retention time [min]	H300-10	H300-2	H300-6-2	H340-10	H340-2	H340-6
11,97	x	x	x			x
13,28	x	x	x	x	x	x
14,22		x	x			
14,94	x	x	x		x	
16,26				x		
16,61	x		x			
16,97	x	x	x			x
17,04						x
17,09	x	x	x	x		x
17,36	x	x	x		x	
17,65		x	x			
19,18						
19,25				x		x
19,74	x	x	x		x	
20,48				x		x
20,72				x		x
21,24				x		x
21,37		x				
21,75		x				
22,85						
22,93		x	x		x	
22,95						
23,73						
23,95	x	x	x		x	
24,3				x		
24,82						
25,02						
25,09		x				
25,19		x				
25,69						
25,82	x	x				
26,53	x	x	x	x	x	x
29,3		x				
33,36		x				x
34,87		x				
41,25		x	x		x	

Table 4.6 continued

Retensjonstid	H380-10	H380-2	H380-6	NMZr4	SZR4	NoCat
11,97		x	x		x	x
13,28				x	x	x
14,22						
14,94						
16,26	x	x	x			x
16,61						
16,97		x			x	x
17,04		x	x			
17,09		x		x	x	x
17,36						x
17,65						
19,18	x		x			
19,25		x				
19,74						
20,48	x	x	x	x	x	x
20,72	x	x	x	x		
21,24	x	x	x	x	x	
21,37						
21,75						
22,85	x		x			
22,93						
22,95	x		x		x	x
23,73					x	x
23,95					x	
24,3	x	x	x	x		
24,82					x	x
25,02	x					
25,09						
25,19						
25,69					x	
25,82						
26,53	x	x	x	x	x	
29,3						
33,36						x
34,87						
41,25						

The chromatograms of the oil samples can be seen in appendix.C.

4.5 ESI-MS

4.5.1 Development of method

The method used for capturing the spectra from the ESI-MS was found by tweaking parameters of the ion source and MS. The main parameters varied was changing between positive or negative ion mode, adjusting the fragmentor setting as well as the voltage applied to the needle. In addition 0,1 % formic acid was added to the methanol to increase the availability of positive charges in an attempt to facilitate ionization of compounds containing even numbers of nitrogen.

A series of spectra from the variation of the fragmentor setting can be seen in appendix.D3. In appendix.D4 some spectra from the attempts with formic acid in the solvent can be seen.

4.5.2 Oil samples

The spectra of oil samples were gathered, along with spectra of certain known compounds. A spectrum captured from H380-6 can be seen in Figure 4.5 as an example. The rest of the spectra can be seen in appendix.D1 (oil samples) and D2 (standards). The background of the spectra have been subtracted.

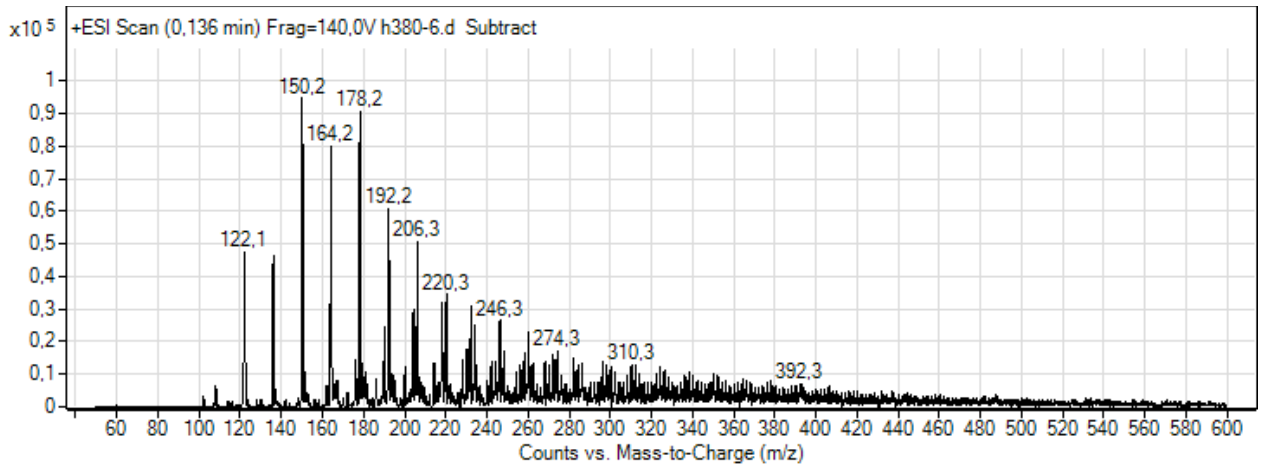

Figure 4.5: The ESI-MS spectrum captured for H380-6

The MS is run in positive mode. The addition of a H^+ means that an organic molecule with an even number of nitrogen (including 0) should produce an odd numbered peak. As seen in Figure 4.5 the majority of the peaks are even numbered. This was a general trend for the oil samples.

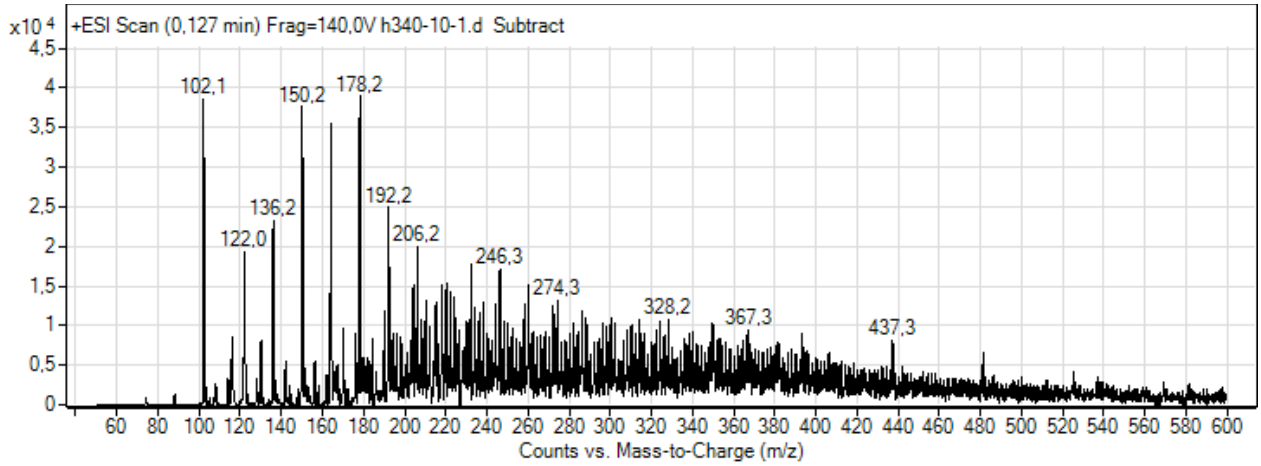

Figure 4.6: The ESI-MS spectrum captured for H340-10-1

The same trend can be seen in Figure 4.6, the spectrum captured from H340-10-1. The peak 102,1 as seen in Figure 6 was inflated in some spectra due to contamination of the instrument. However the background correction should account for most of it, so the peaks seen in the spectra can be seen as representative.

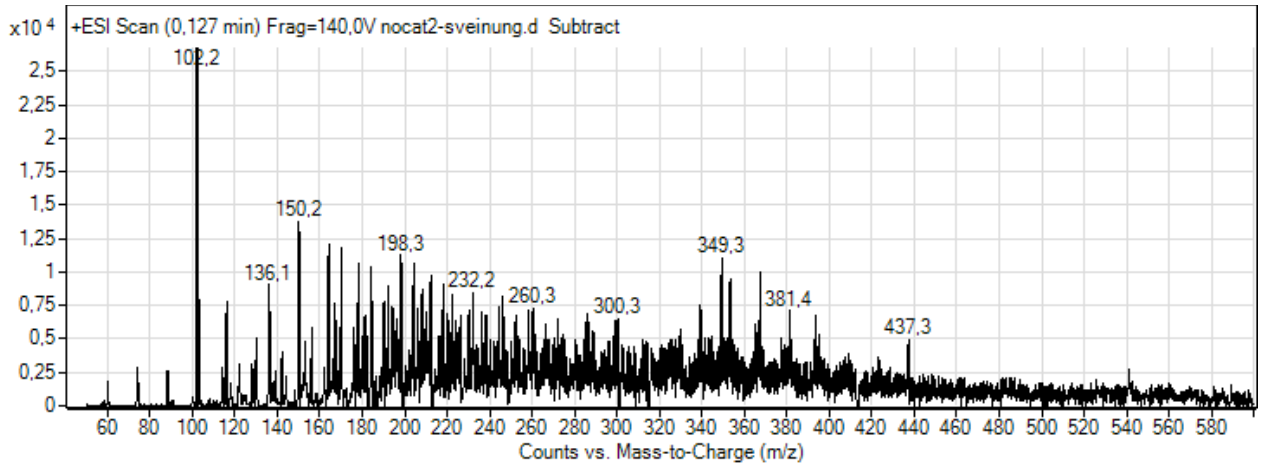

Figure 4.7: The ESI-MS spectrum captured for the uncatalyzed sample

The MS-spectrum for the uncatalyzed samples, as seen in Figure 4.7 has a peak at 102,2 overshadowing the other peaks. The sample was run several times to double check if there was a problem with the sample preparation, but the spectra was similar between all of them. An attempt was made to examine the ion at 102,2 m/z with the precursor ion setting on the MS. This allows for the ion to be singled out in the first mass filter, before introducing more energy in the collision cell to induce fragmentation. The chromatogram for one of these attempts can be seen in Figure 4.8. As seen there are no major peaks, and at either of the smaller peaks the only ion seen in the mass spectrum is 102,2.

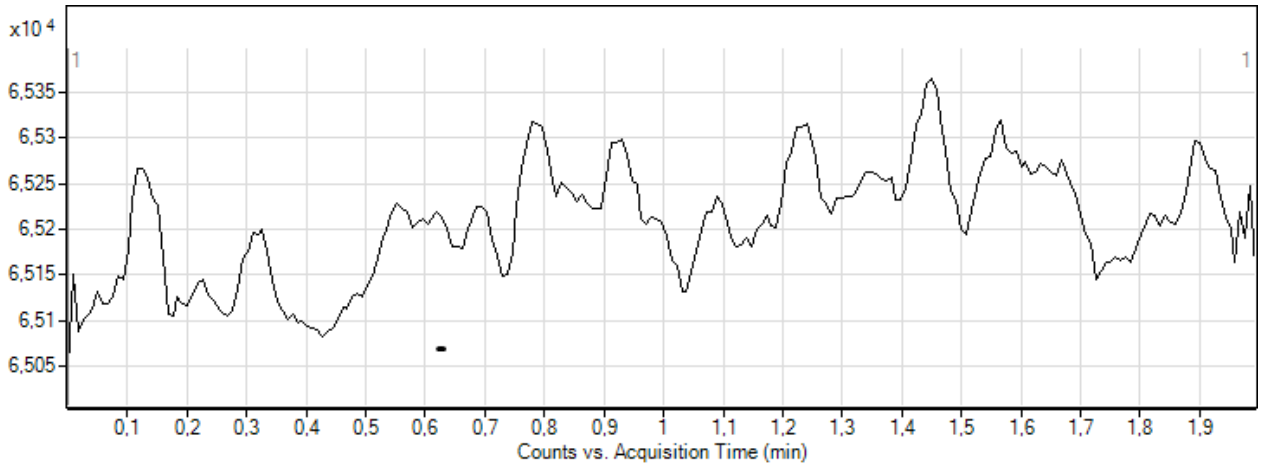

Figure 4.8: Chromatogram of the NoCat sample run in precursor ion mode for 102,2 m/z, showing no significant peaks

The complete list of spectra can be found in appendix.D.

4.5.3 Standards

In Table 4.7 a summary of the standards that was analyzed can be found. All of the standards that produced ions detected in the spectrum contained nitrogen.

Table 4.7: The standards that were tested, and if their ions produced a signal in the spectra

Compound	Molecular weight [g/mol]	Signal
Triethylamine	101,2	Yes
O-nitrophenol	139,1	No
3-aminophenol	109,1	Yes
2,6-dimethylphenol	122,2	No
Pyridine	79,1	No
Quinoline	129,16	Yes
Carbazole	167,206	No
Guaiacol 2-isopropylphenol 2,6-diisopropylphenol	124,14 136,1 178,3	No

Figure 4.9-11 shows the captured spectra of pyridine, quinoline and carbazole, the complete collection of spectra can be found in appendix.D. As seen in Figure 4.9 no peak can be seen at 80,1. The spectrum of quinoline in Figure 4.10 show a clear peak at the expected value of 130. The spectrum of carbazole have no peak at 168.

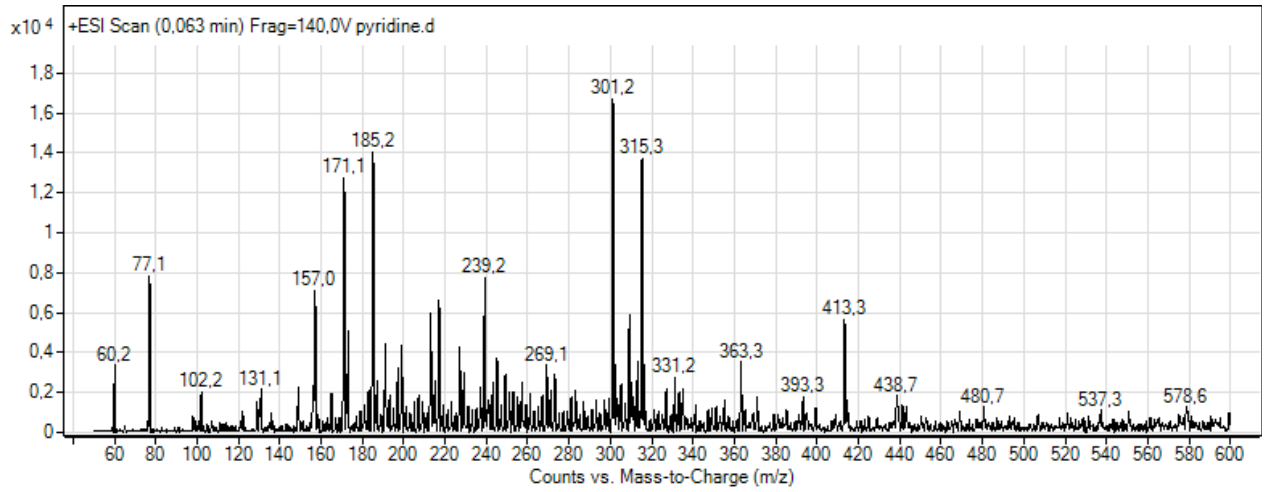

Figure 4.9: The spectrum of pyridine

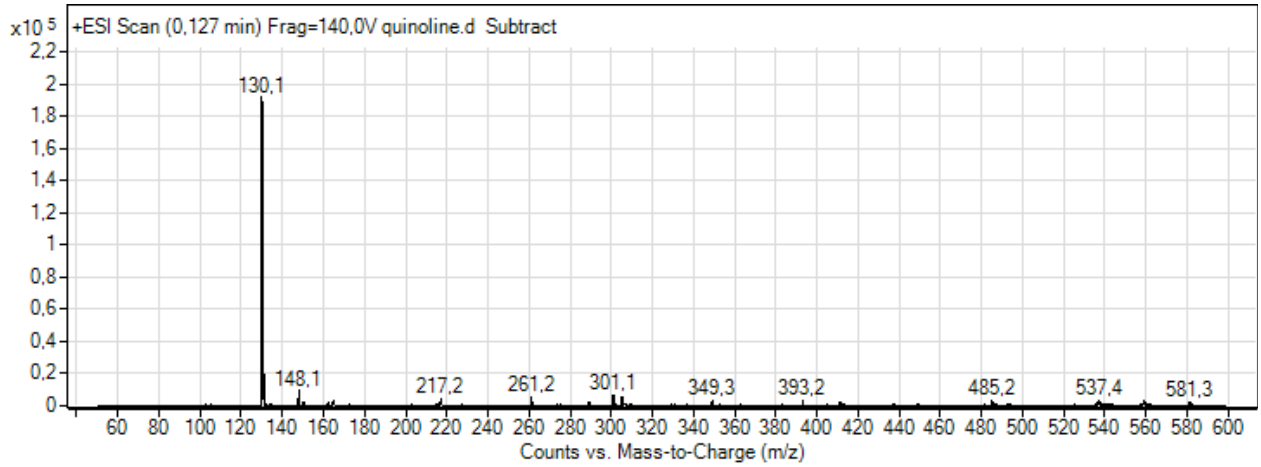

Figure 4.10: The spectrum of quinoline

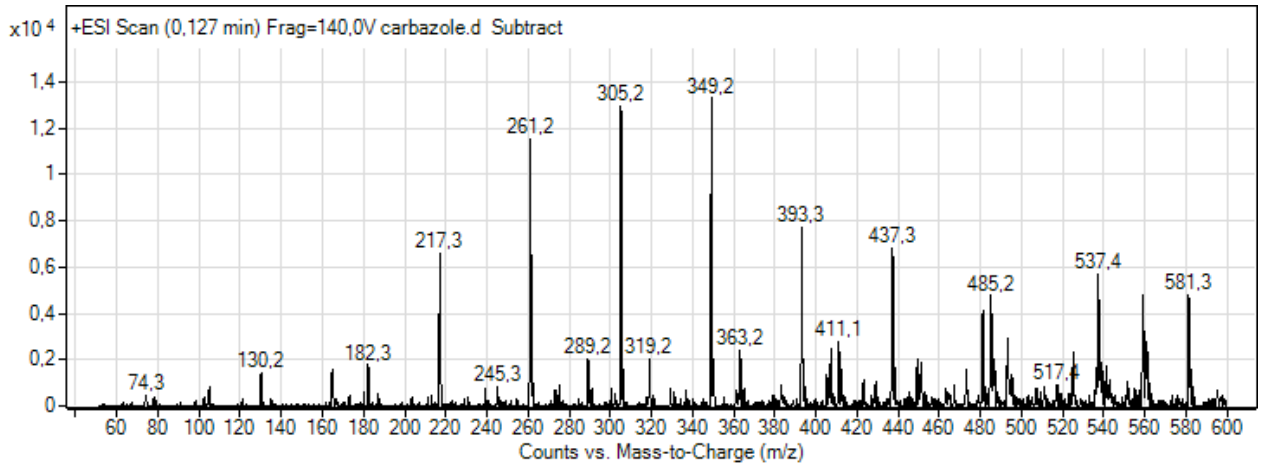

Figure 4.11: The spectrum of carbazole

5 Discussion

5.1 Introduction

Discarded experiments

During the experimental series a number of experiments were discarded due to gas leakage during heating. It was discovered that one reactor in particular was having this problem. As the number of reactors available was limited, and used by others some solutions were tried in hopes of alleviating the problem. In the end another reactor was acquired, and the reactor causing problems was put aside.

A number of experiments were conducted with water as a solvent in place of ethanol. The catalyst was found to be inactivated in a water system, and so the solvent was changed to ethanol.

The discussion of the successful experiments is essentially divided into two main parts. The first part, 6.2, discusses the results from the LtL-conversion and analysis of the oils produced. The second part, 6.3, discusses the process of developing the method for capturing ESI-MS spectra of the oils, and the results from the analysis.

5.2 LtL-Conversion

5.2.1 Introduction: Determining the optimal oil output

The oil yield of LtL-conversion can be measured according to two main criteria:

1. The amount of reactants converted to products
2. The quality of the oil

A good reaction setup should naturally convert as much of the reactants into products as possible. In this project this is measured as the oil yield, which is presented as the mass percent of product compared to the added reactants. The oil yields of the performed experiments can be found in Table 4.1.

The quality of the oil is harder to evaluate as several factors play a role. The density of the oil, acidity, and sulfur content are commonly used for conventional crude oil. Another important factor when determining oil quality is the hydrogen to carbon ratio (H/C). A high hydrogen to carbon ratio indicates a high degree of saturation. The oxygen content, presented as the oxygen to carbon ratio (O/C), is another indicator of quality, with a low O/C preferred.
While considering the output amount and quality it is important to make effort to reduce the severity of the reactions conditions.

5.2.2 Elemental composition

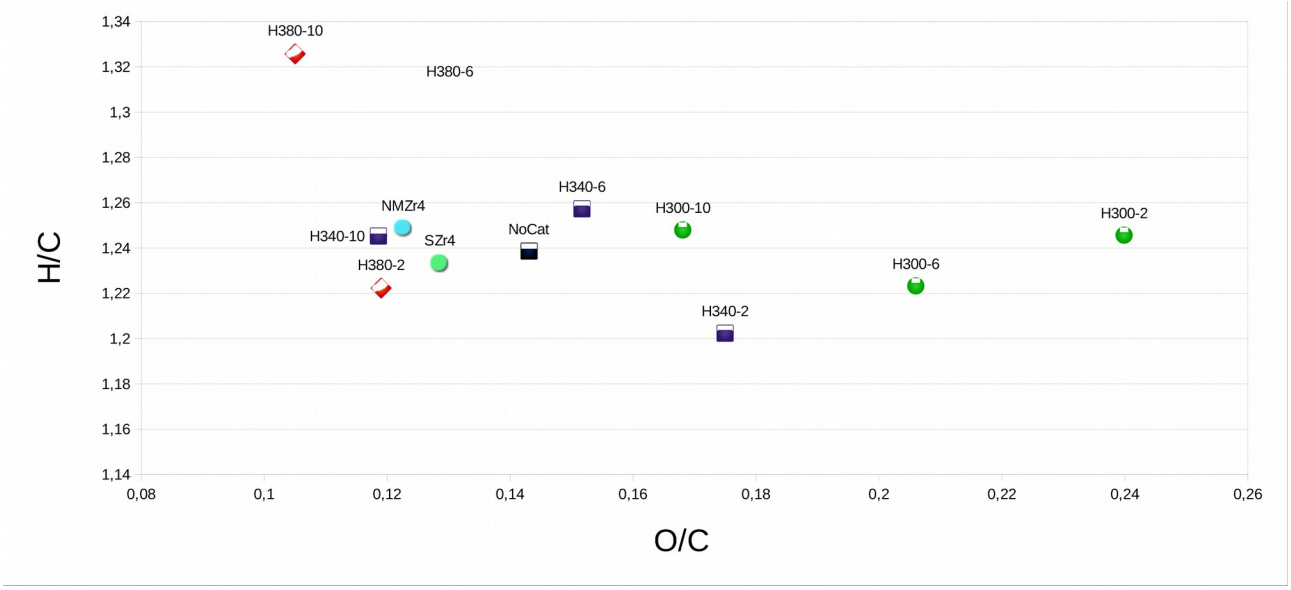

Figure 5.1: Van Krevelen diagram plotting the H/C- vs the O/C-ratios for the produced oils.

The data from the elemental analysis is presented in Table 4.3. The H/C-ratio of the oils produced by the experiments are higher than that of lignin (1,05) showing that hydrogenation has taken place during the reaction. The O/C-ratio of the oils is lower than that of lignin (0,39) indicating that deoxygenation has occurred as well.

As seen in Figure 5.1 there is a trend for the O/C ratio of samples to decline as the reaction time is increased for the oils produced at 300 and 340 ºC. The oils produced at 380 ºC do not follow this trend however. Higher temperature seems to decrease the O/C-ratio as well.

An important observation is that the uncatalyzed oil seem to have a lower O/C-ratio than both oils produced with HNMZr4 at 300 ºC and at 340 ºC with reaction time 2 and 6 hours. This can be taken as an indication that the catalyst doesn't induce deoxygenation. However, as the oils produced from the catalyzed reactions have a higher oil yield (apart from H300-2), this is probably not the case. HDO-activity is needed for the conversion of lignin into oil. An example of this is when the ether bond between the lignin monomers are broken (Figure 1.9). The higher O/C-ratio does in other words not necessarily mean that the deoxygenation activity of the catalyst is low, as a higher amount of products are formed. The reactions performed with SZr4 and NMZr4 catalysts are both at lower O/C-ratios than the oil produced without a catalyst.

The temperature seems to have an effect on the hydrogenation. Especially the oils produced at 380 ºC show a significant increase.

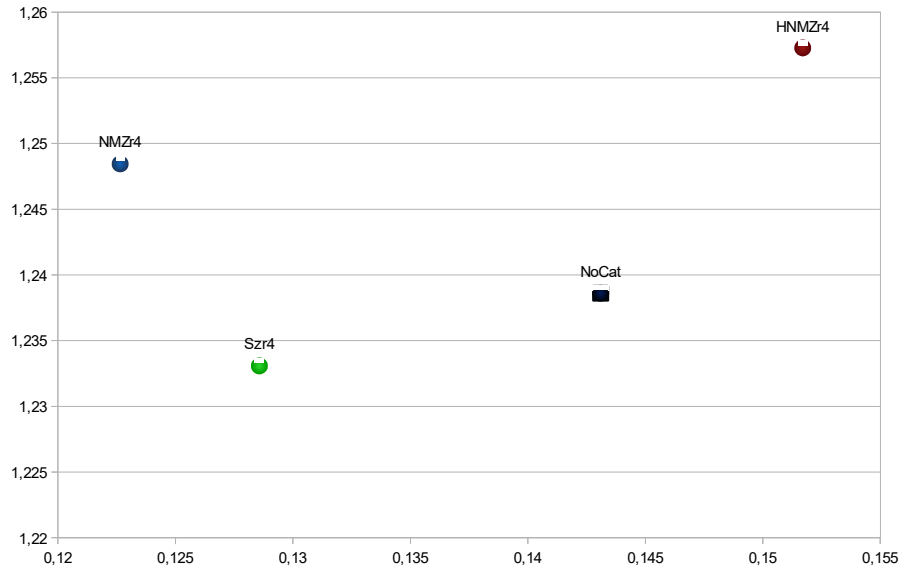

Figure 5.2: Van Krevelen diagram plotting the H/C- vs the O/C-ratios for the oils produced with the various catalysts at 340 ºC and 6 hours, as well as the uncatalyzed

The values for the oils produced at 340 ºC and 6 hours are plotted in a Van Krevelen diagram in Figure 5.2. The same trend is observable here, the oils catalyzed by the NMZr4 catalyst seems to have a slightly higher oxygen content. In Figure 5.2 it is possible to see an increase in the H/C-ratio that is hard to read from Figure 5.1, indicating that both the NMZr4 and HNMZr4 catalysts perform hydrogenation.

5.2.3 GPC: Mean molecular weight

The standard compounds used for establishing the calibration curve are polystyrenes with a more linear characteristic than the average compounds found in the oils produced. The less linear form of the oil compounds results in a lower molecular volume, enabling them to enter the pores in the stationary phase more easily, and be retained to a higher degree. This causes the system to underestimate the mean molecular weight of the compounds found in the oil. To what degree this effect lowers the calculated molecular weights is hard to say. It is however reasonable to assume that the effect will increase with the length of the polystyrenes.

The data gathered for the oil samples can be seen in Table 4.4.
The mean standard deviation for the samples that were analyzed in parallels were 1,5 sec. This results in a mass difference of 15 g/mol. This is a rather large margin of error, and the results from the analysis of the GPC results cannot be interpreted as proof of a definite molecular weight, but rather as an indication of the area in which it will lie.

As the method separates the compounds based on size and not chemical interaction with the column, it can be hard to increase their separation. A longer column could help, but the uncertainty of the results is likely to increase with a similar factor as the separation. A possibly better alternative is to try to find a column with a more suitable pore size distribution.

To improve the predictive power of the calibration curve the polystyrenes should be changed for a standard more similar to the compounds analyzed to make the calculated mean molecular weights a more accurate estimation.

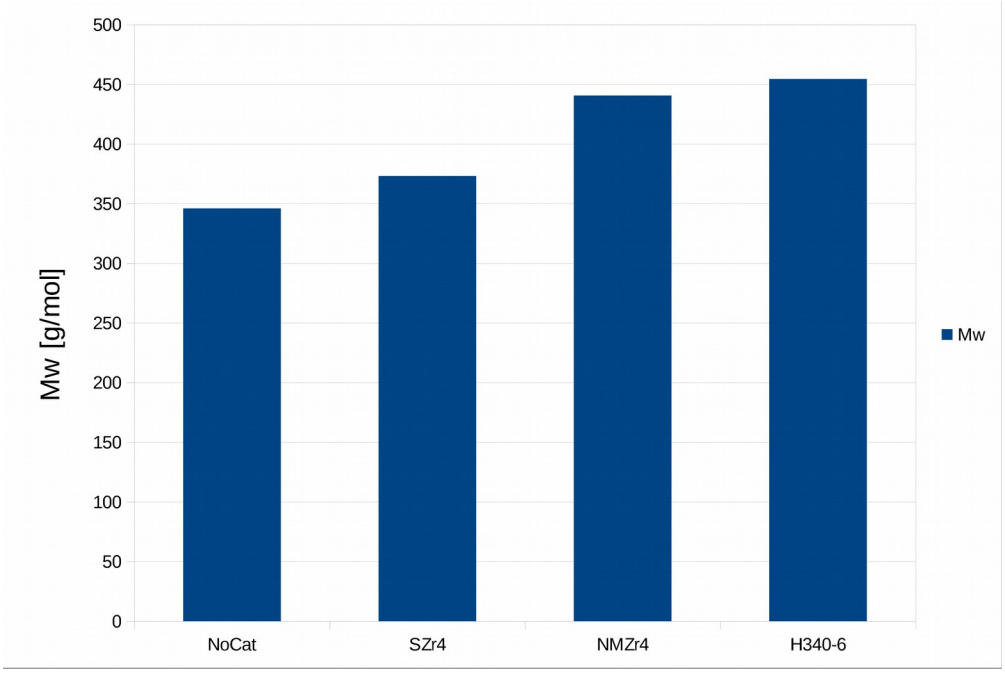

Figure 5.3: The calculated molecular weights of the experiments performed at 340 ºC and 6 hours

As seen in Figure 5.3 the mean molecular weight of the compounds formed in the reactions performed at 640 ºC and with 6 hours reaction time are larger when catalyzed compared to the uncatalyzed experiment. The addition of Ni-Mo onto the substrate of SZr increases the effect even more, while there seems to be only a small effect of the hydrogenation of the catalyst.

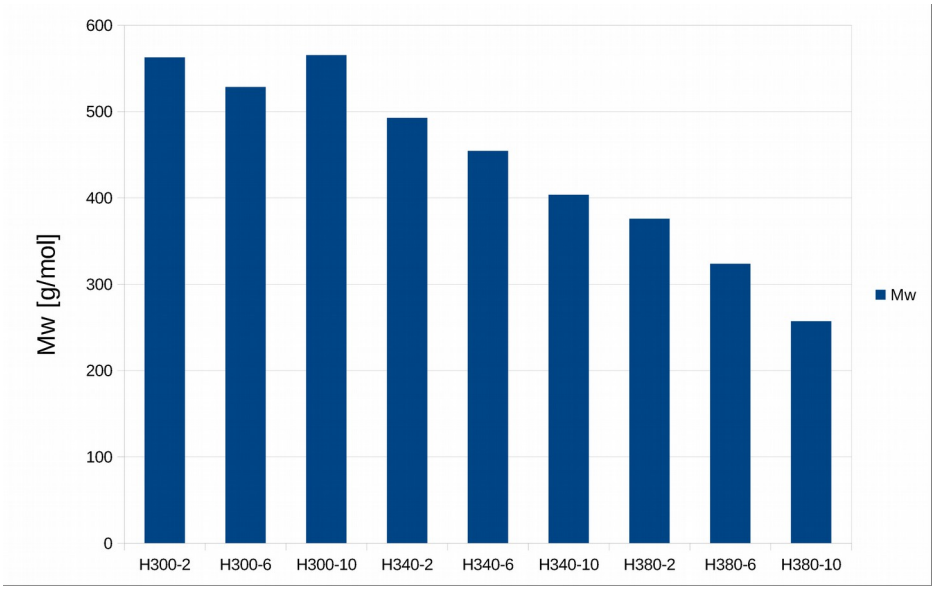

Figure 5.4: The calculated molecular weights of the oils produced with the catalyst HNMZr4.

In Figure 5.4 the evolution of the mean molecular mass of the oils produced with the catalyst HNMZr4 is examined as the temperature and reaction time is varied. There is a clear trend that both the temperature and reaction time decreases the mean molecular weight of the overall oil composition.

An examination of the relationship between time, temperature and mean molecular weight by PCA gave the biplot shown in Figure 5.5

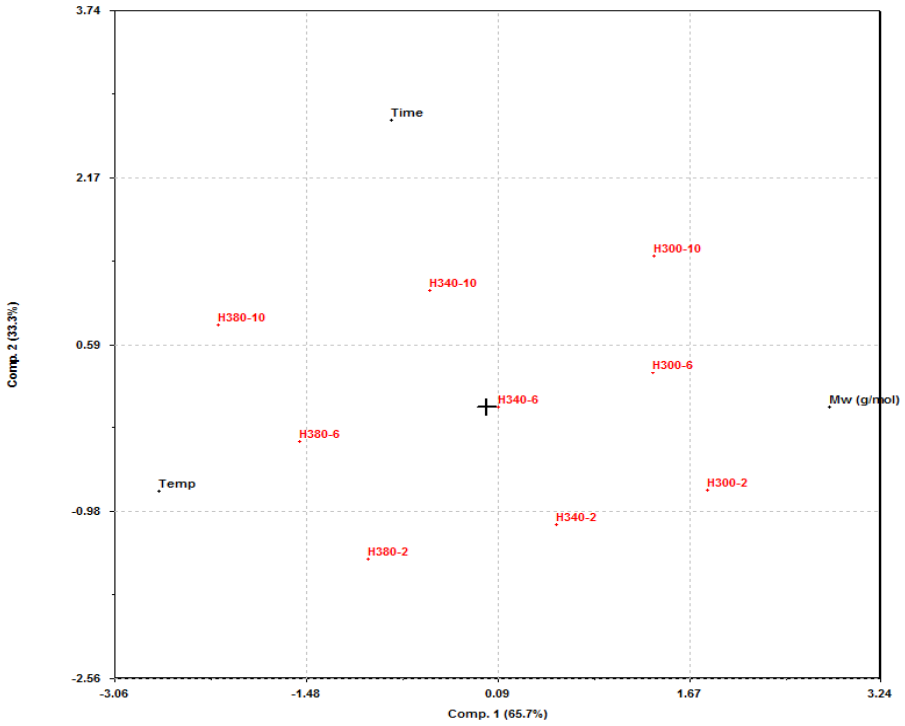

Figure 5.5: The biplot of a PCA analysis of the experiments performed with HNMZr4, and the variables Temperature (Temp), reaction time (Time) and mean molecular weight (Mw (g/mol))

The angle between temperature and M_w is measured to be 158 showing a strong negative correlation. The angle between time and M_w is measured to be 101, showing that this factor might not be as prevalent as inferred from Figure 5.4. Looking at Figure 5.4 this might in large part be due to the effect of H300-10, which does not fit into the general pattern. When a new PCA was performed removing H300-10 from the objects used, the angle between time and M_w increased to 144, showing a strong negative correlation. The calculated M_w of H300-10 might be an outlier.

5.2.4 GC-MS: Compounds in the oil

The compounds identified by GC-MS was identified by a search in the NIST-library. The MS data in the analysis consists of scans performed form m/z 40 to m/z 400. The data in the NIST library contains scans at lower m/z than this. If there are any peaks

in this region in the standard spectrum the search will not necessarily find a high correlation between the measured spectrum and the standard spectrum. As a consequence of this factor, and to be as sure as possible that the compound identified was correct, all the spectra was compared to each other manually as well. For some peaks none of the suggested spectra seemed to contain all peaks with the right ratio between them. The choice was made to identify the compounds by the most similar spectra where the similarity was deemed high enough. If any compounds have been misidentified it is still plausible that they share a lot of characteristics with the actual compound, as they would need to be quite similar to produce the same kind of fragmentation pattern.

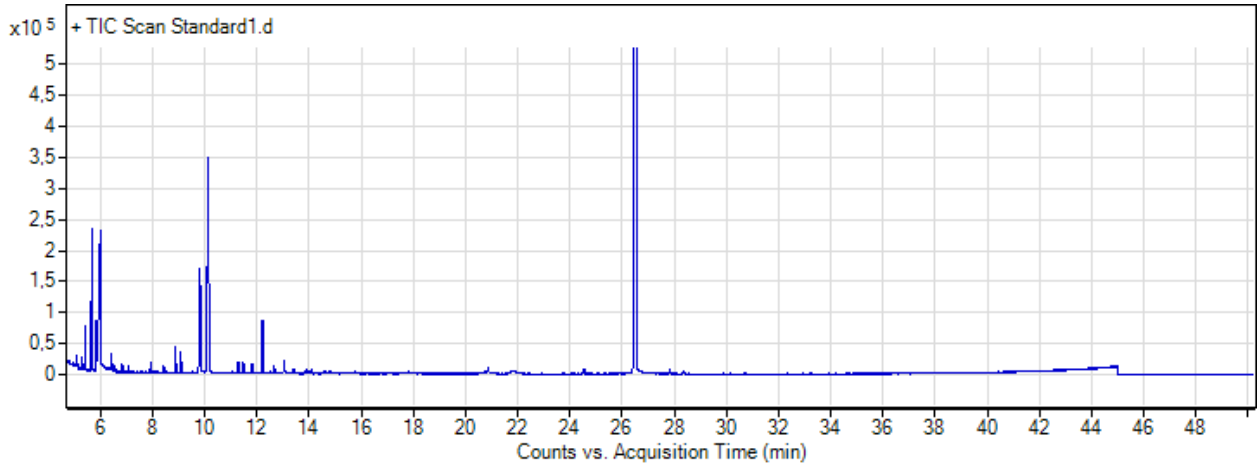

Figure 5.6: Chromatogram of the standard solution.

The chromatogram of the standard solution shown in Figure 5.6 shows that there are some compounds eluting before 10 minutes in particular, and one peak at 12,2 minutes. These compounds show similarities to THF and EtAc which was used as solvents in the preparation of the samples. The peaks did not show up when using only DCM as solvent. The THF used in the solvent was not stabilized with butylated hydroxytuolene (BHT), and it is probable that the THF has decomposed over time creating some of the compounds seen in the chromatogram. These peaks are generally present in all the chromatograms of the samples, and can be thought of as

noise.

The experiments performed in the earlier part of the process used a THF with added BTH. The BHT was removed by means of a rotavapor before the THF was used, however it is possible that some BHT would remain and would be detectable in the GC-MS. It was not observed, but as not all peaks were analyzed it is possible that a small amount is present in some samples.

The column used for the GC-MS is not polar, and does not retain the compounds to a significant degree. The main factor in separation of the compounds is their boiling point, with compounds with a low boiling point having a lower retention time (RT). In general most of the significant peaks in the oil samples eluted before the internal standard hexadecane, which had a RT of 26,53 minutes. Hexadecane has a boiling point of 287 ºC [43], so it is natural to assume that the substances eluting before hexadecane will have a lower boiling point. Phenol which which elutes with a RT of 11,97 minutes has a boiling point of 182 ºC. [44] The latest eluting substance identified by GC-MS was diisooctyl-phthalate with a retention time of 41,25 minutes, and a boiling point of 370 ºC. [45]

Some compounds in the oil may have too high boiling points for them to be analyzed with this method, and some compounds may have a boiling point that is so low they elute with the solvent. The solvent-delay in the chromatogram was set to 4,7 minutes, and as mentioned the area before 10 minutes was not analyzed.

Compounds

A table containing all the identified compounds can be seen in Table 4.5.

The oil from the uncatalyzed experiment seems to contain many forms of substituted phenols. Many of them are substituted with ethyl groups which may come from the

ethanol used as solvent. Some esters are also observed. Many of the identified compounds can be found in several of the oils.

The oils produced at 300 ºC also show a high amount of phenols. For the experiments catalyzed with HNMZr4 the experiments at 300 ºC and H340-2 were the only oils with phthalamide peaks that were analyzed, indicating that the relative amount produced of this compound was higher with less severe reaction conditions. This includes diisooctylphthalamide that was the slowest eluting compound identified. The same is true for guaiacol eluting at 14,94 minutes. Creosol was observed only in H300-2 and H300-6 along with 4-oxo-pentanoic acid ethyl ester.

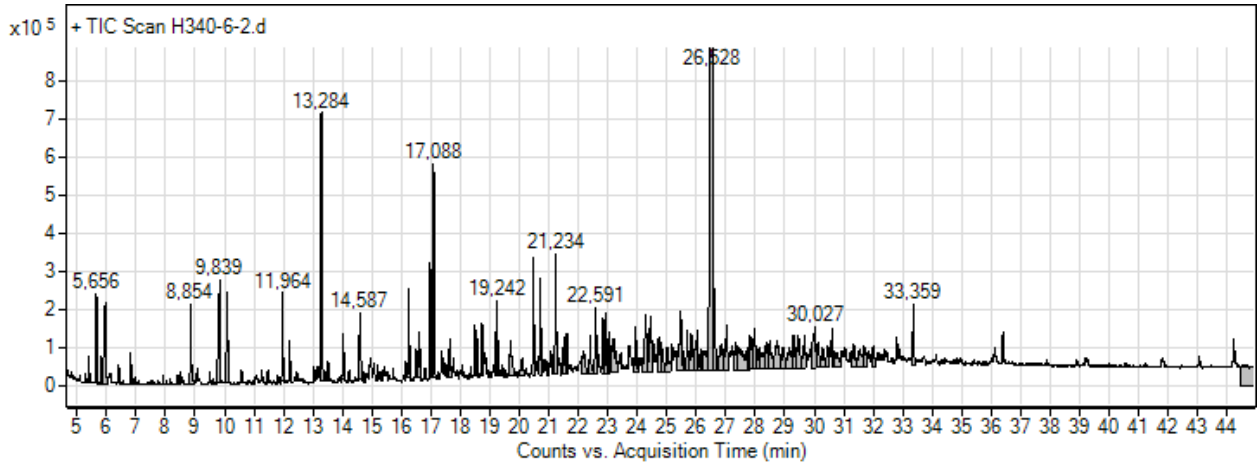

Figure 5.7: The chromatogram of H340-6-2

The oils produced 340 ºC shows a higher degree of substitution on the phenols, like 2,5-diethylphenol and 3-ethyl-5-methylphenol. An example is shown in Figure 5.7 with the chromatogram of H340-6-2.

The oils produced at 380 ºC share a lot of characteristics with the oils produced 340 ºC. Some additional diethylphenols are observed, like 3,5-diethylphenol. At 6 and 10 hours 4-tert-Butylbenzyl alcohol are identified.

The general trend seems to be that a higher temperature leads to a higher degree of substitution of phenols.

5.2.5 Modelling the oil yield

A linear predictive model for the oil yield for the experiments catalyzed with HNMZr4, with temperature and reaction time as variables was attempted, but the fit was not good. A PLS-model containing a cross-product between time and temperature resulted in one principal component (PC) explaining 26,85% of the variance. In Figure 5.8 the plot of predicted vs. measured output is shown.

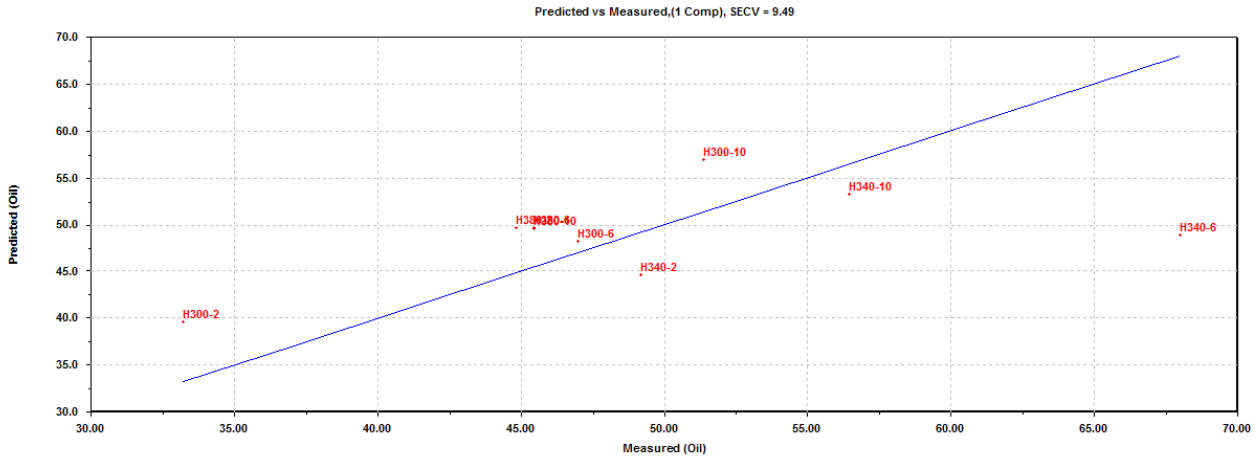

Figure 5.8: Predicted vs measured for Oil regression

As seen in Figure 5.8 the predictive power of the model was poor. A surface response model was attempted in its place. The model was built based on the data presented in Table 5.1. The calculation of the surface response model was performed by Mikel Oregui Bengoechea. One data point as been used for each of the points outside of the center point, and three for the center point. The data was fitted to a quadratic model with a 95% confidence level (significance level 0,05).

Table 5.1: The experimental data used for building the surface response model

Number	***Temperature***	***Time***	***Oil Yield***	***Char Yield***	***x0***	***x1***	***x2***	***x12***	***x11***	***x22***
1	*300*	*2*	***33,2***	***45,9***	*1*	*-1*	*-1*	*1*	*1*	*1*
2	*300*	*6*	***47***	***30,1***	*1*	*-1*	*0*	*0*	*1*	*0*
3	*300*	*10*	***51,3***	***24,1***	*1*	*-1*	*1*	*-1*	*1*	*1*
4	*340*	*2*	***49,1***	***32,2***	*1*	*0*	*-1*	*0*	*0*	*1*
5	*340*	*6*	***66,6***	***20***	*1*	*0*	*0*	*0*	*0*	*0*
6	*340*	*6*	***71,9***	***29,9***	*1*	*0*	*0*	*0*	*0*	*0*
7	*340*	*6*	***65,5***	***24***	*1*	*0*	*0*	*0*	*0*	*0*
8	*340*	*10*	***56,5***	***22,7***	*1*	*0*	*1*	*0*	*0*	*1*
9	*380*	*2*	***44,8***	***27,5***	*1*	*1*	*-1*	*-1*	*1*	*1*
10	*380*	*6*	***45,4***	***29,4***	*1*	*1*	*0*	*0*	*1*	*0*
11	*380*	*10*	***45,4***	***37,8***	*1*	*1*	*1*	*1*	*1*	*1*

Figure 5.9 shows a plot of the resulting surface response model.

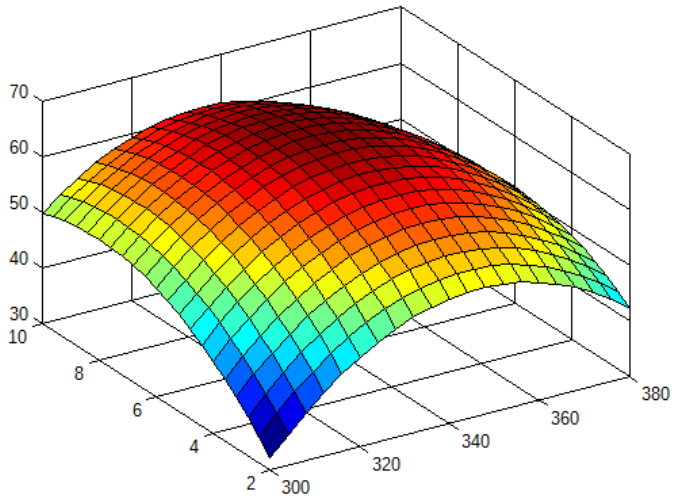

Figure 5.9: The plotted surface response model for oil yield.

The model is given by equation 5.1.

Equation 5.1: Oil yield = 65,33 + 0,68X_1 + 4,35X_2 – 15,13X_1^2 -8,53X_2^2 – 4,37X_1X_2

Where X_1 is the temperature and X_2 is the reaction time.

The significance of the individual regression coefficients were also examined. The coefficients marked with green in Equation 5.1 were deemed significant for a confidence level of 95%, while the coefficients marked red were not.
The p-value was found to be 0,015, indicating the the model is significant.

As seen in Figure 5.9 the model describes an optimal output in terms of quantity in the middle of the model. Is<covered in the design

A model for the char yield was also developed with the surface response plot shown in Figure 5.10.

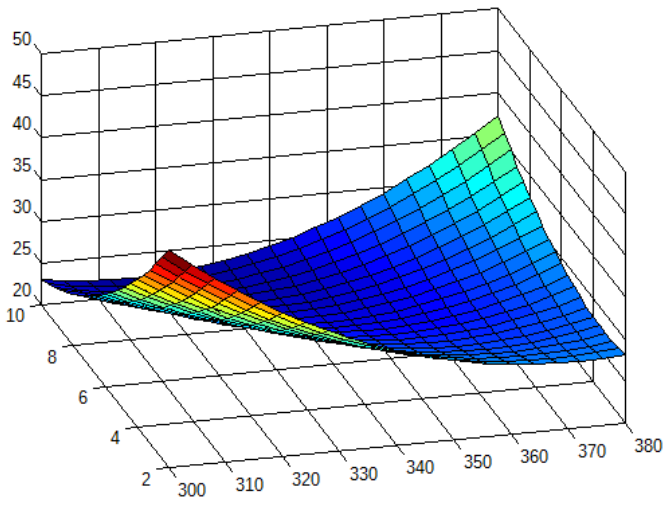

Figure 5.10: The plotted surface response model for char yield

As seen in Figure 5.10 the model seems to have two maxima for the least severe, and most severe reaction conditions. This is however probably a false result. The char measured for this project includes the ligning remnants that did not react during the experiment, which is probably the main factor contributing to the peak towards H300-2. In reality the char yield is likely to increase with the severity. The predicted char yield for H380-2 is higher than that for H300-10, indicating that temperature might be making the biggest contribution towards the char yield.

5.2.6 Modelling the H/C-ratio by PLS

A model predicting the H/C-ratio of a given experiment was created for a significance level of 0,5. The plot of predicted vs. measured value can be seen in Figure 5.11.

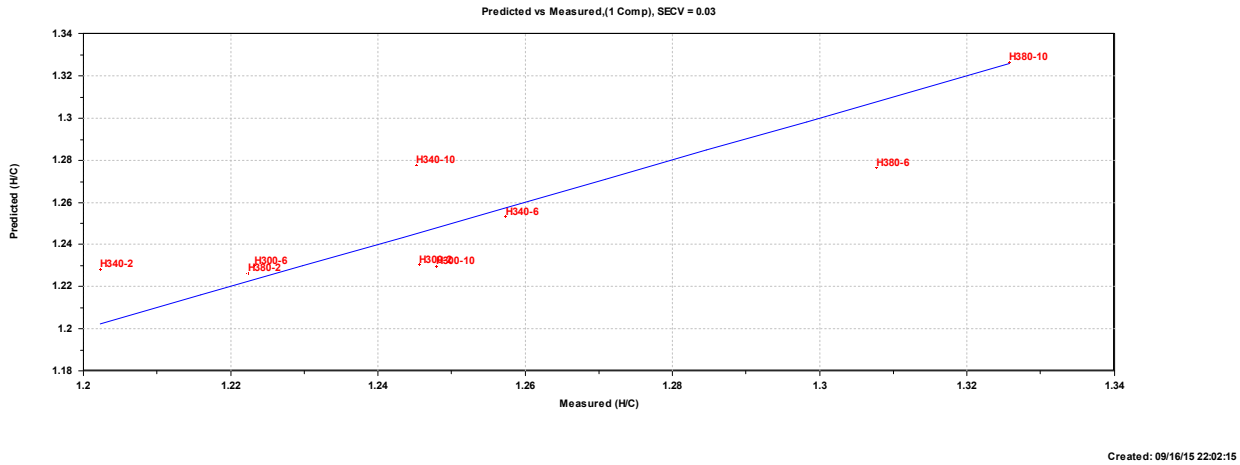

Figure 5.11: Plot of predicted vs measured values for the PLS-model of the H/C-ratios (R=0,858)

As seen in Figure 5.11 the fit is much better than the model developed for the oil yield. The first PC explains 73,65% of the variance in the data, and is the only PC taken into consideration. The equation found by the regression is found below (built with weighted variables)

Equation 6.2: $H/C = 25.4 + 0.54 * Time + 0.50 * Temp + 0.45 * Temp * Time$

A PCA analysis performed indicates that time has the strongest correlation to the resulting H/C-ratio.

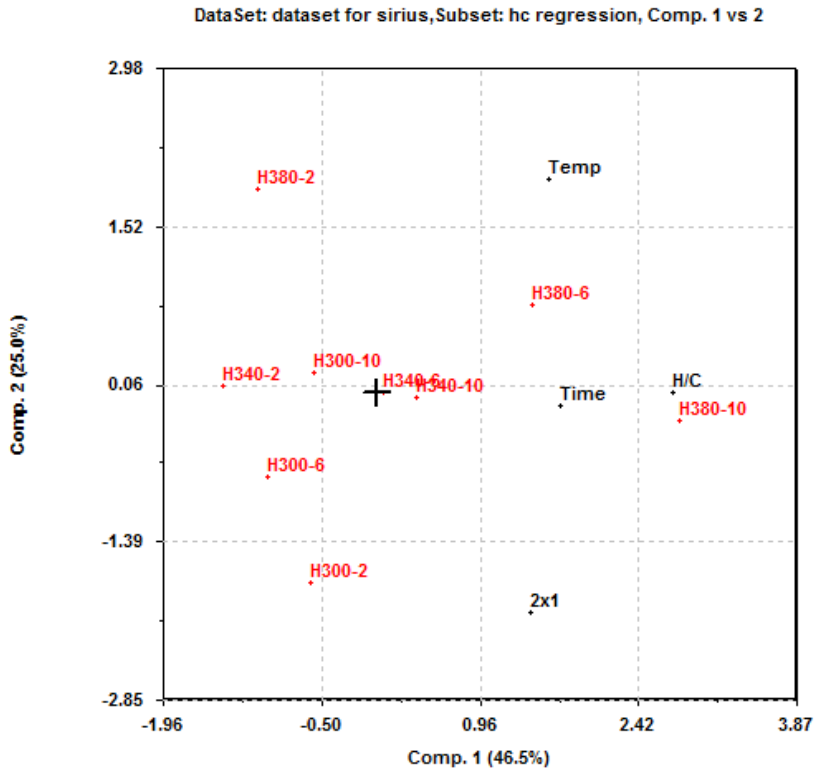

Figure 5.12: Biplot for the PCA model developed for the reaction variables and H/C factor. 2x1 is the cross factor of temperature and time.

5.2.7 Summary of the results from the LtL-conversion

The oils produced during the LtL-conversion experiments were analyzed with elemental analysis, GPC and GC-MS. In addition they were analyzed with ESI-MS, the results of which is discussed in 6.3.

The results from the elemental analysis shows that the O/C-ratio in the oils produced with the HNMZr4 have the highest O/C-ratio of the catalysts included. The oil also has a higher O/C-ratio than the uncatalyzed oil. (Figure 5.2) It was postulated that this is not necessarily due to a low deoxygenation effect, as HDO-reactions are a necessity for the production of oil, and the oil yields of the HNMZr4 experiments are significantly higher.

The trends of the H/C-ratio is harder to read from the Van Krevelen diagram in Figure 5.1, but the effect of the variables were modeled using PLS and PCA in 6.2.6. The analysis shows that both time and temperature is positively correlated to the resulting H/C-ratio. The PLS model indicates that the effects are quite similar in magnitude with the reaction time slightly more important. PCA indicates a strong correlation between the reaction time and the H/C-ratio, while the temperature is much less correlated with an angle of 42 º.

Modelling the oil yield shows that a maximum is found inside the range of parameters set by the experimental design (Figure 5.9). The equation for the model is given in equation 6.1, using weighted variables. The model shows that the oil yield increases with the severity of the parameters up to a point. At this point the formation of char increases, resulting in a decrease of the final oil yield.

The catalyst seems to have had an effect on the yield when comparing catalyzed and uncatalyzed experiments. While the uncatalyzed reported an oil yield of 40,0% the oil yield for the H340-6 experiments was over 65 % for all three parallels.

The mean molecular weights of the compounds was found using GPC. The calculated mean molecular weights was found to be inaccurate, they are however still as indications as to what the real mean molecular weight would be. The PCA biplot shown in Figure 5.5 indicates that the mean molecular weight of the oils have a strong negative correlation to the reaction temperature. The reaction time seems to slightly negatively correlated.

The GC-MS analysis showed that the general profile of the identified compounds was quite similar between the oils. The substitution on the phenols identified seemed to increase with the temperature.

5.3 ESI-MS discussion

5.3.1 Introduction

The MS-spectra from the ESI-MS analysis was expected to mirror the results from the other analytical methods. An example of how a spectrum was expected to look is given in Figure 5.13, it shows an ESI-MS-spectrum captured in positive ion mode on another instrument for an oil produced by Mikel Oregui Bengoechea. The analysis was performed by Bjarte Holmelid. A spectrum captured for this project can be seen in Figure 5.14.

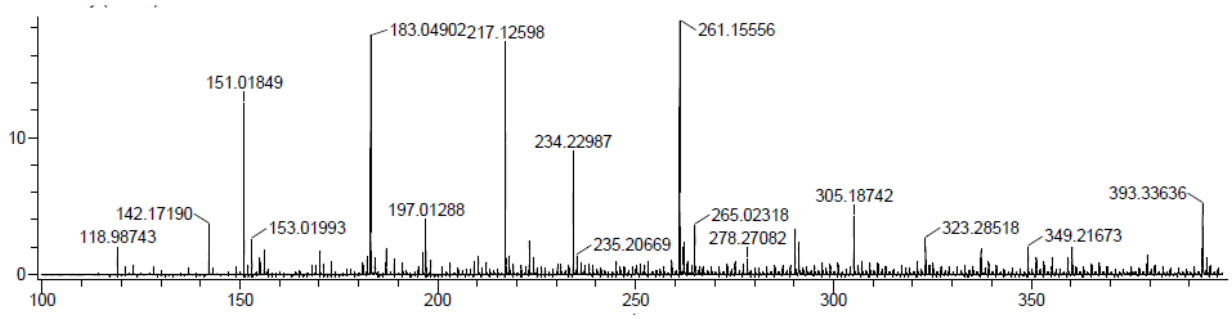

Figure 5.13: MS-spectrum captured for an oil produced by Mikel Oregui Bengoechea.

As seen in Figure 5.13 the peaks are odd numbered. For a compound with the formula CxH_yO_z odd numbered peaks are expected when the instrument is run in positive ion mode (ions are mainly detected as $M+H^+$). The spectra captured on the Agilent instrument used for the analysis of the oils in this project (e.g. Figure 5.14) showed mainly even numbered peaks, indicating that the compounds shown have the formula $C_xH_yO_zN_i$, where *i* is an odd number.

5.3.2 Developing the method

The initial attempts at establishing a method consisted of running standards expected to be in the mix, including among others guaiacol. A spectrum showing an attempt at getting a signal from a standard solution consisting of guaiacol, isopropylphenol and

2,6-diisopropylphenol can be seen in appendix.D2. The standard was run with varying parameters, none of which produced a detectable signal at the expected m/z values (the expected m/z values can be seen in Table 4.7). A decision was made to postpone the analysis of standards and rather start analyzing the oils. Analyzing in this order would enable the tailoring of standards towards what were actually present in the specta.

The parameters of the MS was varied in an attempt to allow ionization of compounds with no nitrogen. The attempts were not successful, as no combination of parameters seemed to be able to produce a significant increase in the odd numbered peaks in the spectra.
An addition of formic acid to the solvent can help facilitate the ionization by increasing the charge density in the solvent. Methanol containing 0,1%vol formic acid was attempted, but did not produce odd numbered peaks.

Negative ion mode was not attempted, as the DCM used to solve the oils in the sample preparation is not suitable for negative ion mode. It was however attempted for some of the standards, with no significant result.

5.3.3 Expected compounds

As explained in 6.2.2 the analysis was expected to mirror the results of the GC-MS to a certain degree, allowing for the difference in ionization methods to create a difference.

The majority of the compounds identified by the GC-MS analysis did not contain nitrogen. The elemental analysis shows that the analyzed oils have a molar percent of nitrogen below 0,7 %. It is in other words unlikely that the spectra captured is a good representation of the oil. The most likely explanation is that the ionization method

was only able to ionize the nitrogen containing groups to a significant degree.

5.3.4 Analysis of the spectra

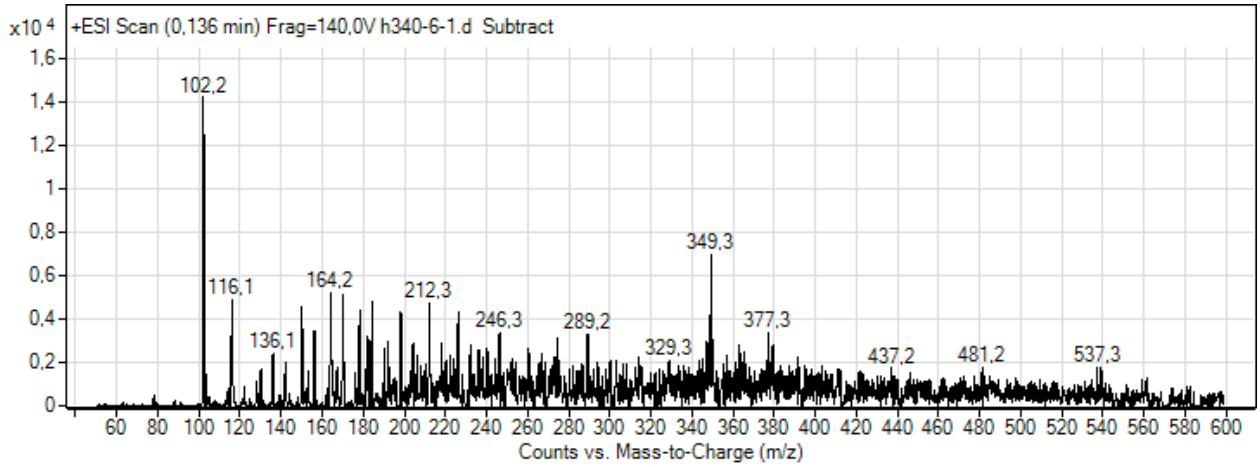

Figure 5.14: Captured MS-spectrum for H340-6-1

As seen in the spectrum in Figure 5.14 the peaks below 250 have a m/z value with an even number. A spectrum showing the area between 100 and 300 m/z for the same spectrum is shown in Figure 5.15, showing that the peaks are indeed almost exclusively even numbered.

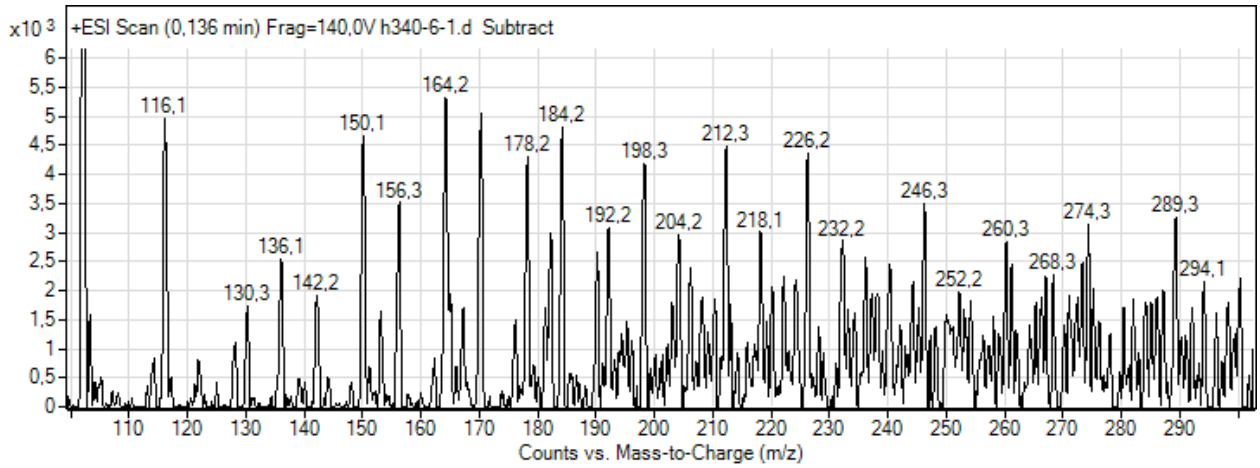

Figure 5.15: ESI-MS spectrum for H340-6-1, m/z range: 100 - 300

What determines if a compound gets ionized or not is the local chemical

environment. That is, the type of functional group, and the effect of any surrounding resonance or electron rich areas. Following that train of thought there is no logical reason for the formation of odd numbered peaks exclusively at a higher m/z. A possible reason for this might be the formation of single charged dimers. This seemed to be a general trend for all the oil spectra.

As seen in 6.15, some of the peaks are separated with 14 m/z, e.g. the peaks at 150, 164, 178 and 192. This indicates that some of the compounds formed during the LtL-conversion might constitute a homologous series with a starting compound and the addition of an increasing number of methyl groups. This process can be assumed to take place for the non-nitrogen containing compounds as well given that the functional group does not necessarily play a part in the reaction.

A comparison between the distributions of the ions in the oil spectra compared to the mean molecular mass of the oil was performed. There did not seem to be a close relation between the two. If the premise that the spectra only shows the nitrogen containing compounds in the mixture is true, then the logical conclusion that the spectra does not necessarily represent the actual mix in a good way holds true. As a consequence the only conclusion that can be drawn is that the m/z distribution of the nitrogen containing ions in a MS-spectrum of the oil is not necessarily closely related to the mean molecular mass of the oil.

5.3.5 Standards

A list of the standard compounds analyzed can be found in Table 4.7. The table also shows what standards produced a signal in the spectrum captured.

Pyridine, quinoline and carbazole

Three of the standards analyzed were pyridine, quinoline and carbazole, the structure

of which can be seen in Figure 5.16.

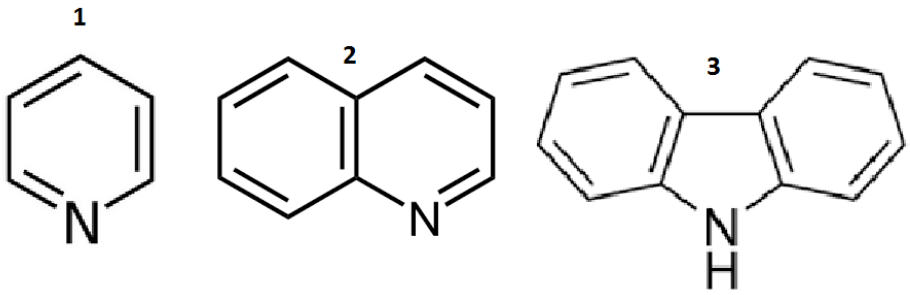

Figure 5.16: The structure of pyridine (1), quinoline (2) and carbazole (3)

The three compounds shown in Figure 5.16 have a very similar structure. Assuming that the factor influencing the ionization of the compound is the local chemical properties around the site of ionization pyridine and quinolone seems to be most closely related in that context. The degree of resonance between the two seems to be quite similar as well, with a slightly larger resonance in quinoline. However as seen in Figure 4.9-11 the only compound that produced a detectable peak in the MS-spectrum was quinoline. The increase in resonance from pyridine to quinoline might be the difference between ionization and no ionization.

As expected in light of the ion peaks in the spectra none of the standards without nitrogen produced a peak when analyzed. Of the nitrogen-containing compounds, triethylamine, 3-aminophenol and quinoline were detected in the standard spectra. Triethylamine has a molecular weight of 101,2, with a peak in the MS-spectra of 102,2. This peak is observed in a majority of the spectra, and the most prevalent one in several. Particularly the spectra from the oils produced at less severe reaction conditions. For the oils produced at 380 ºC the peak only seems to be present in the spectrum of H380-2.

5.3.6 Summary of the ESI-MS analysis

The analytical power of the ESI-MS spectra was severely limited by the fact that no method could be developed to ionize non-nitrogen containing compounds. As a result the spectra reported were not representative for the major components of the oil.

As shown by the failure to ionize o-nitrphenol, pyridine and carbazole the resulting spectra does not represent the complete range of potential nitrogen containing compounds in the mix. The spectra are likely to consist mostly of amines.

6 Further work

6.1 Problems to be solved

ESI-MS:

The inability to ionize non-nitrogen containing compounds were a great limitation upon the analytical power of the analysis. As shown in Figure 6.13 a mass spectrum with mostly odd numbered peaks, as expected, was achieved on another instrument by Bjarte Holmelid. In the future this instrument could be used to analyze the oils. Based on the GC-MS results the majority of the compounds identified were not containing nitrogen, and as such Figure 6.13 seems to be a much better representation of the oils as a whole.

Inaccuracy of GPC

The inaccuracy of the GPC analysis can be reduced by choosing standard compounds more similar to the analyzed compounds. Increasing the separation could also be a viable option for increasing the accuracy.

6.2 Multivariate analysis

The potential of multivariate analysis of the data from the ESI-MS was explored by Gasson, J.R. and Carlson, J.E. et al. [46] The same problem with even numbered peaks and inability to ionize expected standards was encountered in the same ways for the projects behind the article. The homologous series described in the article seems to be present in the analysis performed for this project as well. If a better ionization is achieved the multivariate approach can yield easily accessible results that can be make the assessment of the general characteristics of the oil easier.

6.3 Catalyst

If one or more of the catalysts tested by the research group shows more promise than the rest a more extensive testing will be performed. This includes a finer tuning of the experimental design towards finding optimal parameters for the output, as well as allowing for variation of other parameters to examine their effect.

7 References

1: http://www.resilience.org/primer

2: http://www.eia.gov/todayinenergy/detail.cfm?id=15571

3: http://www.eia.gov/cfapps/ipdbproject/iedindex3.cfm?tid=44&pid=44&aid=2&cid=regions&syid=1980&eyid=2012&unit=QBTU

4: https://yearbook.enerdata.net/

5: http://what-when-how.com/biology/binomial-binomial-name-to-blood-biology/

6: IPCC climate chagen 2014: synthesis report, page 19

7: IPCC press release, 13th April 2014

8: Gasson, J.R., *Solvolytic lignin degradation in an alcohol/formic acid medium*, University of Bergen, 2012 (Page 9)

9: Ragauskas, Arthur J, *Materials for Biofuels*, World Scientific Publishing Company, 2014, page 250-252

10: https://commons.wikimedia.org/wiki/File:Cellulose-2D-skeletal.png

11: Villareal, M.O. et al., *Plant Cell Wall Polymers: Function, Structure and Biological Activity of Their Derivatives*, INTECH Open Access Publisher, 2012, Chapter 3.2.1

12: Babu, Vikash, Thapliyal, Ashish, Patel, Girijesh Kumar, *Biofuels Production*, page 24
13: Kleinert, M.; Gasson, J. R.; Barth, T., *Optimizing solvolysis conditions for integrated depolymerisation and hydrodeoxygenation of lignin to produce liquid biofuel*, Journal of Analytical and Applied Pyrolysis 2009, 108-117.

14: Choudhary, T.V., Phillips, C.B., *Renewable fuels via catalytic hydrodeoxygenation*, Applied catalysis A: General, Vol. 397, Issues 1-2 30th April 2011, pages 1-12

15: Liguori, L., Barth, T., *Palladium-Nafion SAC-13 catalysed depolymerisation of lignin to phenols in formic acid and water*, Journal of Analytical and Applied Pyrolysis, Volume 92, Issue 2, November 2011, Pages 477–484

16: Oregui, M.B. et al., *Simultaneous catalytic de-polymerization and hydrodeoxygenation of lignin in water/formic acid media with Rh/Al2O3, Ru/Al2O3 and Pd/Al2O3 as bifunctional catalysts*, Journal of Analytical and Applied Pyrolysis, Volume 113, May 2015, Pages 713–722

17. Instrument manual, available at the following URL: http://www.isoprime.co.uk/Resolve/index.php?/Knowledgebase/Article/GetAttachment/48/2532

18. Barrentine, Larry B.. Introduction to Design of Experiments : A Simplified Approach. Milwaukee, WI, USA: ASQ Quality Press, 2014. ProQuest ebrary. Web. 23 August 2015. chapter 2

19. http://www.parrinst.com/products/non-stirred-pressure-vessels/series-4740-25-75-ml-hpht-vessels/specifications-15/ (accessed 29.07.15)

20. Oregui Bengoechea,M.; Hertzberg, A. and Barth, T. (2015) *Simultaneous catalytic depolymerization and hydrodeoxygenation of lignin in water/formic acid media with Rh/Al2O3, Ru/Al2O3 and Pd/Al2O3 as bifunctional catalysts.,* J. Anal. App. Pyrolysis 113 (20159)713-722

21. McNair, Harold M., and Miller, James M.. Basic Gas Chromatography (2nd Edition). Hoboken, NJ, USA: Wiley, 2009. Chapter 1, pages 3-4

22. McNair, Harold M., and Miller, James M.. Basic Gas Chromatography (2nd Edition). Hoboken, NJ, USA: Wiley, 2009. Chapter 4

23. McNair, Harold M., and Miller, James M.. Basic Gas Chromatography (2nd Edition). Hoboken, NJ, USA: Wiley, 2009. Chapter 1, pages 5-6

24. http://www.chromedia.org/chromedia?waxtrapp=wlqdcDsHqnOxmOlIEcClBwFjE&subNav=rwhpbjDsHqnOxmOlIEcClBwFjEQ

25. http://www.mtpgroup.nl/amm-laboratory-course.aspx

26. Striegel, Andre, Yau, Wallace W., and Kirkland, Joseph J.. Modern Size-Exclusion Liquid Chromatography : Practice of Gel Permeation and Gel Filtration Chromatography (2nd Edition). Hoboken, NJ, USA: Wiley, 2009., Chapter 2.4, page 26

27. Katz, Elena, Eksteen, Roy, and Schoenmakers, Peter, eds. Handbook of HPLC. New York, NY, USA: CRC Press, 1998. Chapter 7.v

28. http://particularsciences.ie/psl/technology/sec-gpc/conventional-cal/

29. Ekman, Rolf, Silberring, Jerzy, and Brinkmalm, Ann M., eds. Mass Spectrometry: Instrumentation, Interpretation, and Applications. Hoboken, NJ, USA: Wiley, 2009. Chapter 2

30. Ekman, Rolf, Silberring, Jerzy, and Brinkmalm, Ann M., eds. Mass Spectrometry: Instrumentation, Interpretation, and Applications. Hoboken, NJ, USA: Wiley, 2009. Table 2.1, pages 17-18

31. Ekman, Rolf, Silberring, Jerzy, and Brinkmalm, Ann M., eds. Mass Spectrometry: Instrumentation, Interpretation, and Applications. Hoboken, NJ, USA: Wiley, 2009. Table 2.2, page 39

32. Ekman, Rolf, Silberring, Jerzy, and Brinkmalm, Ann M., eds. Mass Spectrometry: Instrumentation, Interpretation, and Applications. Hoboken, NJ, USA: Wiley, 2009. Chapter 2.1, Pages 15-16

33. Banerjee, S., Mazumdar, S., *Electrospray Ionization Mass Spectrometry: A Technique to Access the Information beyond the Molecular Weight of the Analyte*, International Journal of Analytical Chemistry, Volume 2012 (2012), Article ID 282574

34. Cole, Richard B.. Electrospray and MALDI Mass Spectrometry : Fundamentals, Instrumentation, Practicalities, and Biological Applications (2nd Edition). Hoboken, NJ, USA: John Wiley & Sons, 2010. Chapter 1.2.1, pages 6-7

35. Cole, Richard B.. Electrospray and MALDI Mass Spectrometry : Fundamentals, Instrumentation, Practicalities, and Biological Applications (2nd Edition). Hoboken, NJ, USA: John Wiley & Sons, 2010. Chapter 1.2.2, pages 7-10

36. Cole, Richard B.. Electrospray and MALDI Mass Spectrometry : Fundamentals, Instrumentation, Practicalities, and Biological Applications (2nd Edition). Hoboken, NJ, USA: John Wiley & Sons, 2010. Chapter 1.2.6, pages 13-16

37. Cole, Richard B.. Electrospray and MALDI Mass Spectrometry : Fundamentals, Instrumentation, Practicalities, and Biological Applications (2nd Edition). Hoboken, NJ, USA: John Wiley & Sons, 2010. chapter 1.2.7, pages 17-18

38. Cole, Richard B.. Electrospray and MALDI Mass Spectrometry : Fundamentals, Instrumentation, Practicalities, and Biological Applications (2nd Edition). Hoboken, NJ, USA: John Wiley & Sons, 2010. Chapter 1.2.8, page 19

39. Ekman, Rolf, Silberring, Jerzy, and Brinkmalm, Ann M., eds. Mass Spectrometry : Instrumentation, Interpretation, and Applications. Hoboken, NJ, USA: Wiley, 2009. Chapter 2.2.3, page 49

40. Ekman, Rolf, Silberring, Jerzy, and Brinkmalm, Ann M., eds. Mass Spectrometry : Instrumentation, Interpretation, and Applications. Hoboken, NJ, USA: Wiley, 2009. Chapter 5.2.2, page 123

41. Rinaldi, R., Schüth, F., *Acid Hydrolysis of Cellulose as the Entry Point into Biorefinery Schemes*, ChemSusChem, Volume 2, Issue 12, pages 1096–1107, December 21, 2009

42. http://www.chemicool.com/definition/quadrupole_mass_spectrometry.html

43: https://www.sigmaaldrich.com/content/dam/sigma-aldrich/docs/Sigma/**Product**_Information_Sheet/2/h0255pis.pdf

44: https://**www**.sigmaaldrich.com/content/dam/sigma-aldrich/docs/Sigma-Aldrich/Product_Information_Sheet/p1037pis.pdf

45: http://pubchem.ncbi.nlm.nih.gov/compound/Diisooctyl_phthalate#section=Physical-Description

46: Gasson, J.R. and Carlson, J.E. et al., Chemometrics and Intelligent Laboratory Systems, vol 114, pages 36-43

7 Appendix
A. Elemental analysis:
A1. Raw data in weight %

Sample	N [%wt]	C [%wt]	S [%wt]	H [%wt]	C/N ratio
NoCat	1,37	76,19	0,04	7,86	55,65
SZr4-1	1,09	77,37	0,05	7,76	70,73
SZr4-1	1	77,83	0,08	7,88	77,8
SZr4-2	1,27	77,77	0,03	8,09	61,44
SZr4-2	1,37	77,12	0,02	8,12	56,3
NmZr4-1	1,25	77,93	0,04	8,23	62,17
NmZr4-1	1,31	77,78	0,03	8,47	59,42
NmZr4-2	1,33	78,27	0,12	7,69	58,74
NmZr4-2	1,13	77,46	0,04	8,01	68,45
H300-2-1	0,87	69,58	0,03	7,2	80,21
H300-2-1	0,98	69,56	0,03	7,24	70,68
H300-6-2	1,09	71,29	0,04	7,35	65,38
H300-6-2	0,93	70,99	0,03	7,21	76,44
H300-6-3	0,78	71,85	0,03	7,17	92,67
H300-6-3	1,14	73,13	0,02	7,67	64,18
H300-10-1	1,18	73,86	0,03	7,96	62,85
H300-10-1	1,01	74,32	0,05	7,71	73,27
H300-10-2	1,2	74,76	0,03	7,82	62,24
H300-10-2	1,02	74,82	0,03	7,48	73,59
H340-2-1	1,13	74,17	0,02	7,51	65,61
H340-2-1	1,04	74,14	0,04	7,35	71,22
H340-6-1	1,01	73,64	0,06	7,59	72,72
H340-6-1	1,02	73,31	0,03	7,72	71,63
H340-6-1	1,11	72,81	0,07	7,93	65,82
H340-6-2	1,39	78,33	0,03	8,25	56,37
H340-6-3	0,93	77,29	0,06	7,51	82,97
H340-6-3	0,81	76,62	0,06	7,65	94,42
H340-6-3	1,32	77,34	0,03	8,37	58,66
H340-10-1	1,28	77,92	0,07	8,12	60,72
H340-10-1	1,05	78,63	0,05	8,13	74,62
H380-2-1	1,36	78,38	0,06	8,2	57,61
H380-2-1	1,16	78,19	0,05	7,74	67,62
H380-6-1	1,21	77,08	0,1	8,41	63,61
H380-6-1	1,12	76,91	0,07	8,37	64,16
H380-10-1	1,21	78,94	0,06	8,78	65,27
H380-10-1	1,2	78,98	0,05	8,67	65,93

A2. Computed data in molecular %

Sample	Nitrogen [%mol]	Carbon [%mol]	Sulfur [%mol]	Hydrogen [%mol]	Oxygen [%mol]
NoCat	0,642	41,714	0,008	51,666	5,969
SZr4-1	0,52	42,57	0,01	51,24	5,66
SZr4-1	0,47	42,48	0,02	51,63	5,41
SZr4-2	0,58	41,9	0,01	52,32	5,19
SZr4-2	0,63	41,51	0	52,46	5,4
NmZr4-1	0,57	41,63	0,01	52,76	5,03
NmZr4-1	0,59	40,98	0,01	53,52	4,91
NmZr4-2	0,63	43,2	0,02	50,94	5,21
NmZr4-2	0,53	41,96	0,01	52,08	5,43
H300-2-1	0,43	40,1	0,01	49,81	9,65
H300-2-1	0,48	39,99	0,01	49,95	9,56
H300-6-2	0,53	40,61	0,01	50,21	8,65
H300-6-2	0,46	40,81	0,01	49,74	8,98
H300-6-3	0,38	41,37	0,01	49,53	8,71
H300-6-3	0,54	40,7	0	51,22	7,53
H300-10-1	0,55	40,34	0,01	52,15	6,95
H300-10-1	0,48	41,2	0,01	51,28	7,03
H300-10-2	0,57	41,14	0,01	51,6	6,69
H300-10-2	0,49	42,04	0,01	50,45	7,02
H340-2-1	0,54	41,62	0	50,6	7,23
H340-2-1	0,51	42,06	0,01	50,01	7,42
H340-6-1	0,49	41,16	0,01	50,92	7,42
H340-6-1	0,49	40,67	0,01	51,38	7,46
H340-6-1	0,52	39,89	0,01	52,15	7,43
H340-6-2	0,64	41,77	0,01	52,79	4,8
H340-6-3	0,45	43,21	0,01	50,37	5,96
H340-6-3	0,39	42,51	0,01	50,91	6,18
H340-6-3	0,6	41	0,01	53,25	5,15
H340-10-1	0,59	41,91	0,01	52,4	5,09
H340-10-1	0,49	42,24	0,01	52,38	4,89
H380-2-1	0,62	41,91	0,01	52,64	4,81
H380-2-1	0,55	43,02	0,01	51,12	5,3
H380-6-1	0,55	40,79	0,02	53,4	5,24
H380-6-1	0,51	40,8	0,01	53,3	5,38
H380-10-1	0,54	40,78	0,01	54,4	4,27
H380-10-1	0,53	41,05	0,01	54,08	4,33

B. GPC: Chromatograms

B1. Standards:

mp162

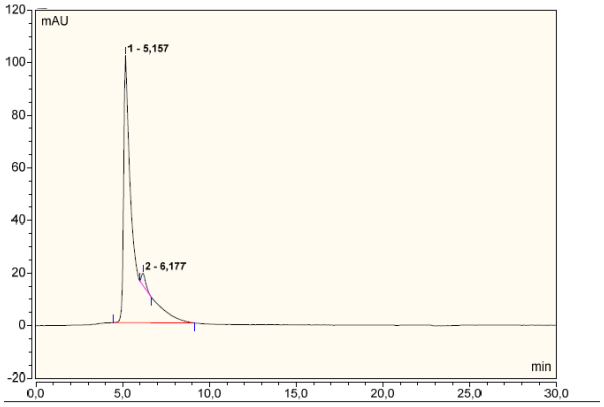

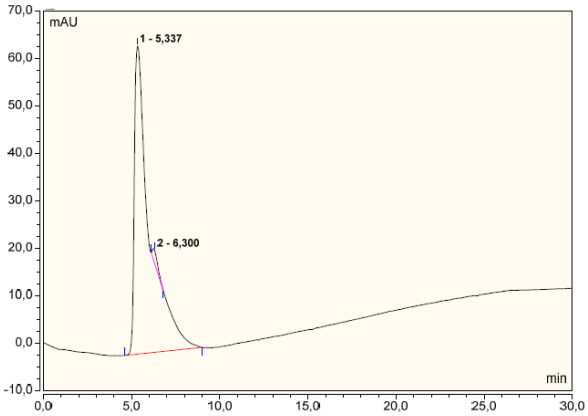

mp580

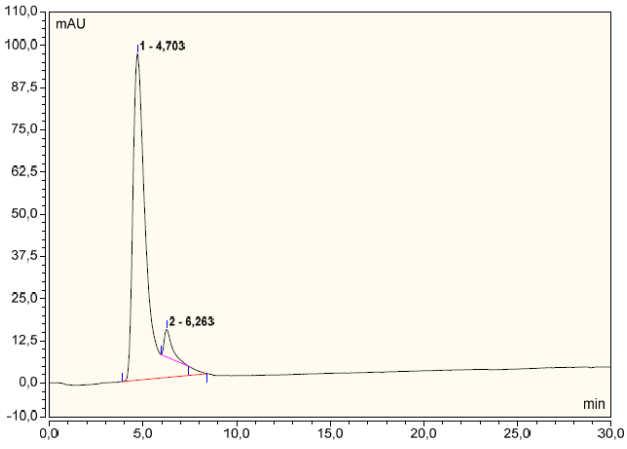

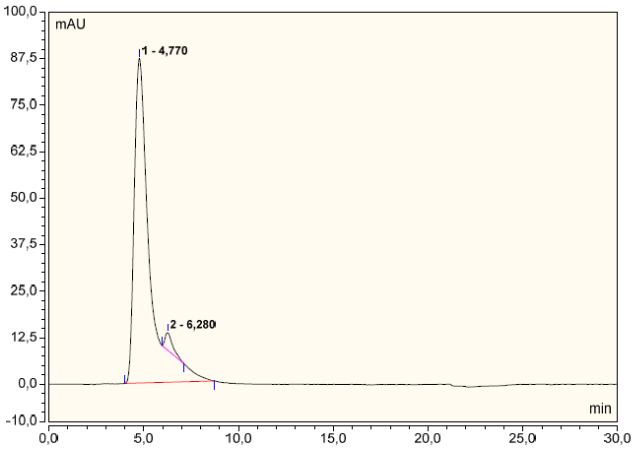

mp1060

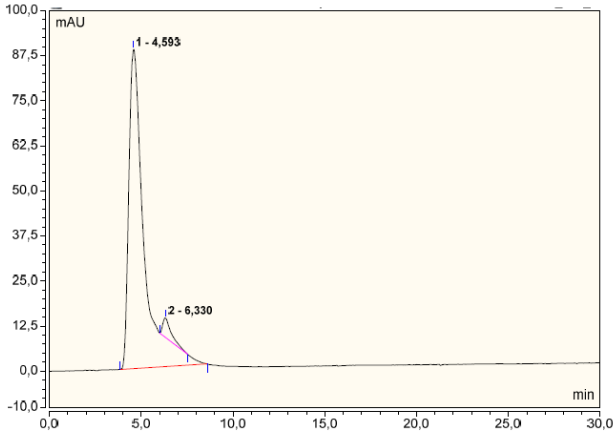

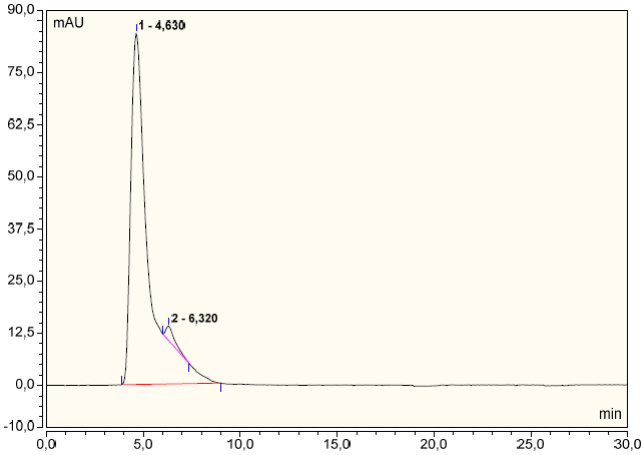

mp1480

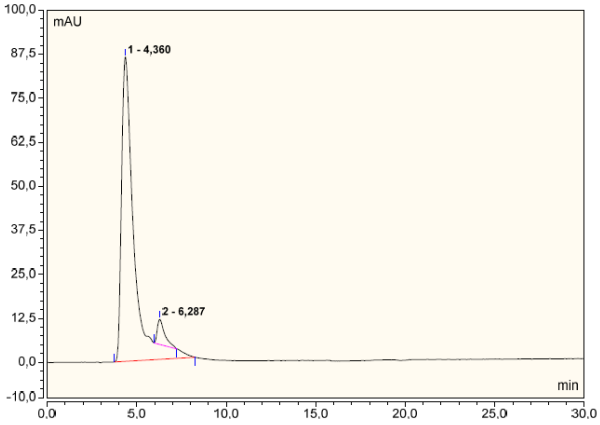

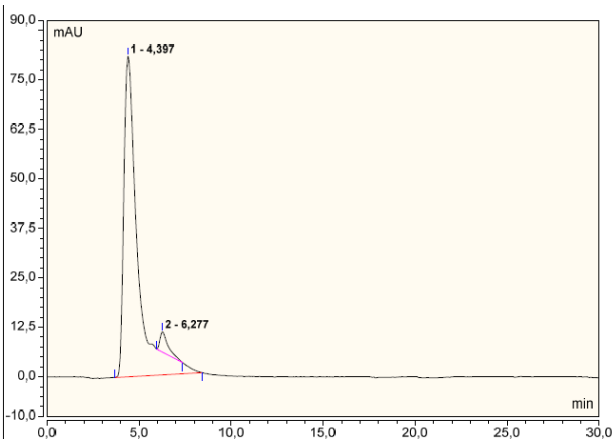

mp2360

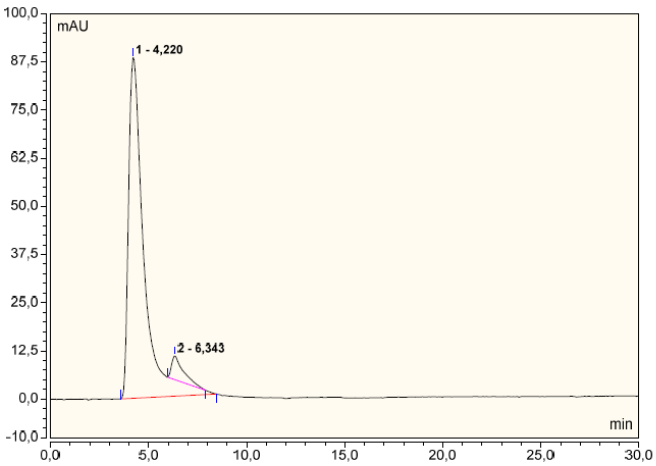

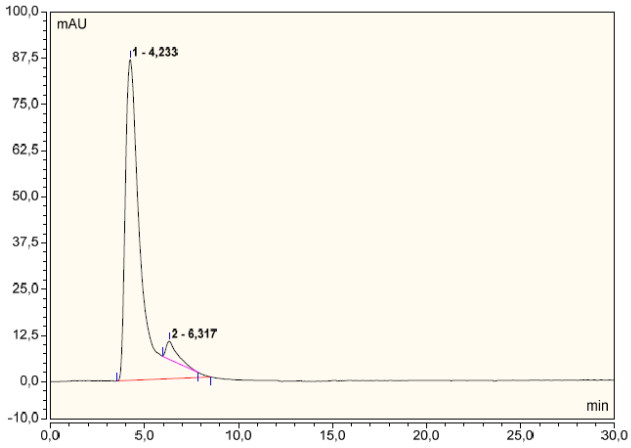

B2. Oil samples

NoCat

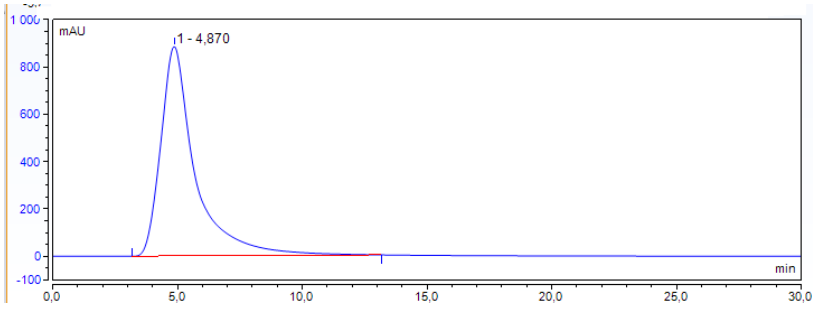

SZr4-1

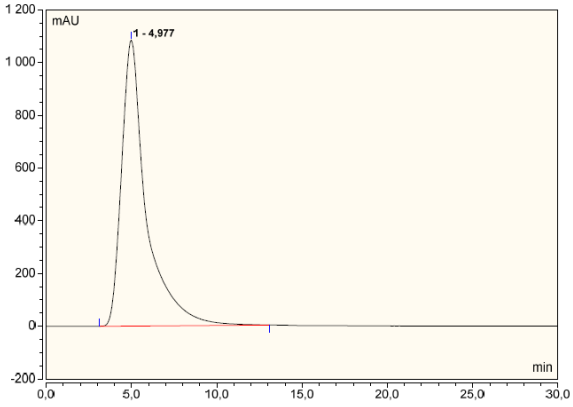

SZr4-2

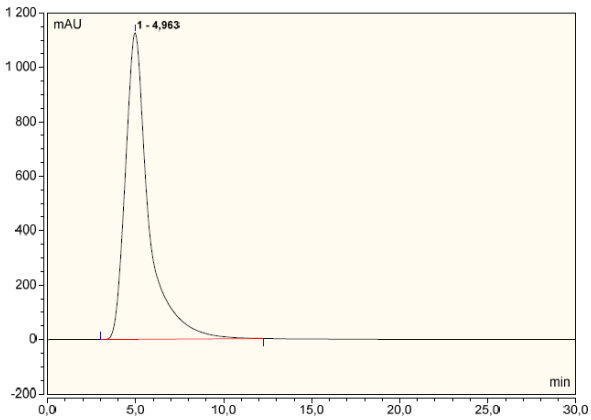

NMzr4

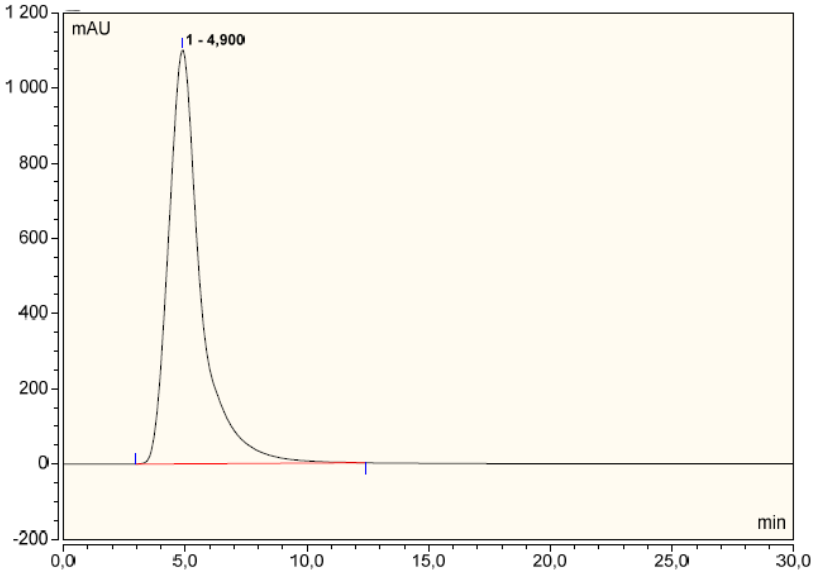

H300-2

H300-6-1

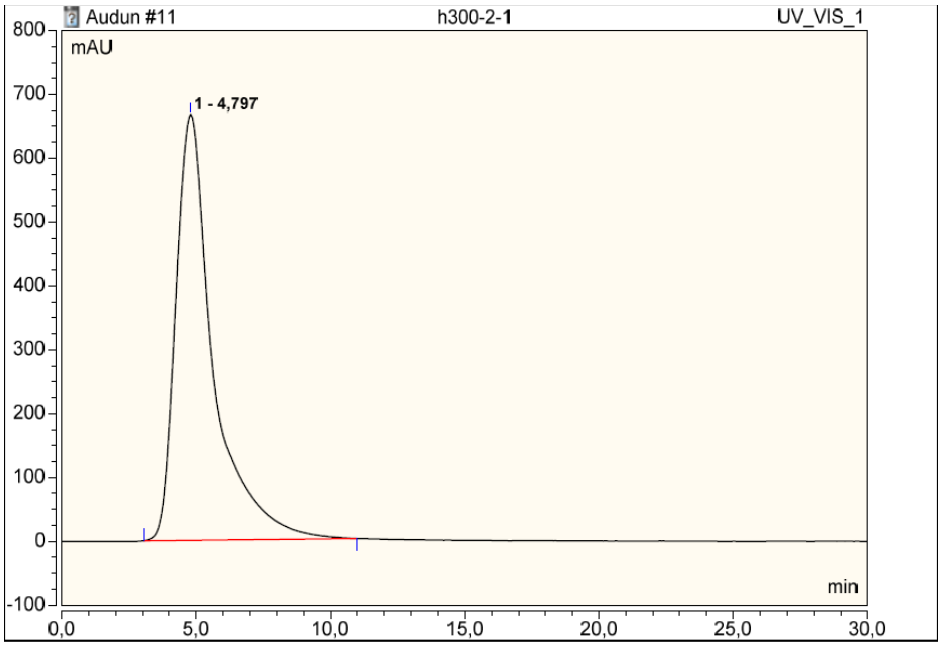

H300-6-2

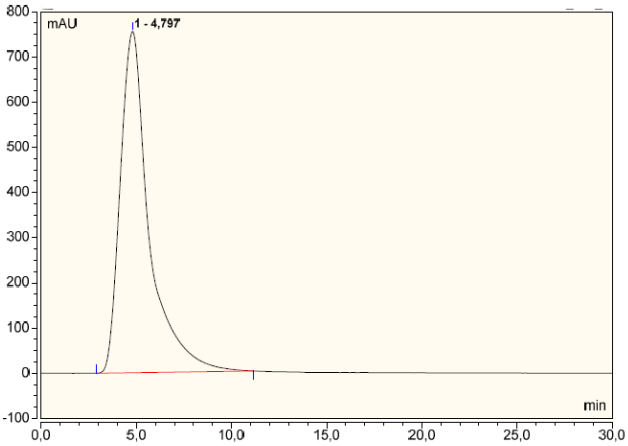

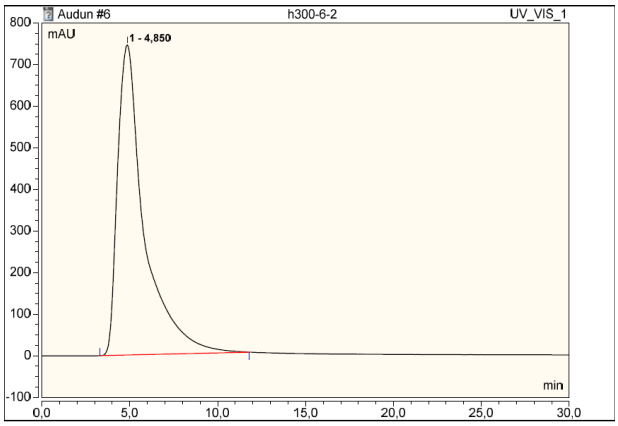

H300-10-1

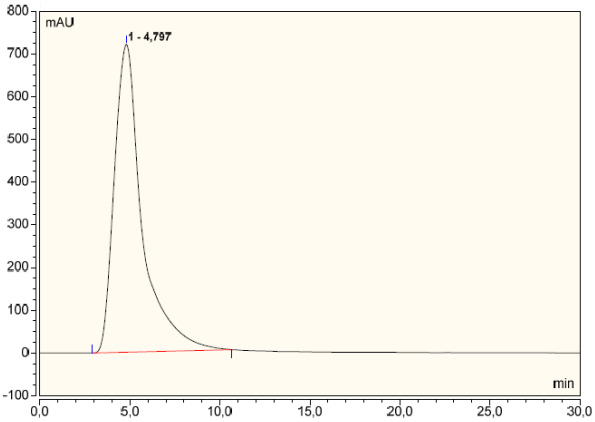

H300-10-2

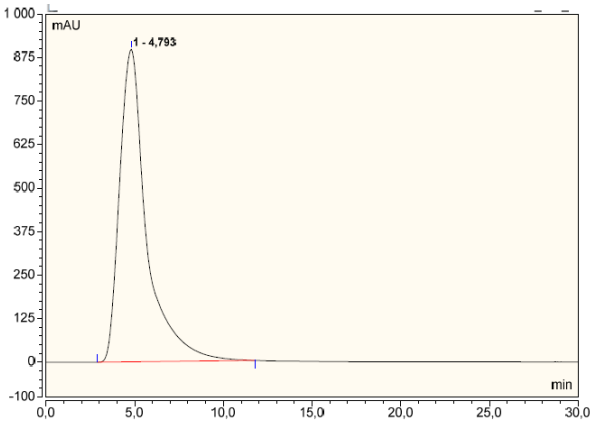

H340-2-1

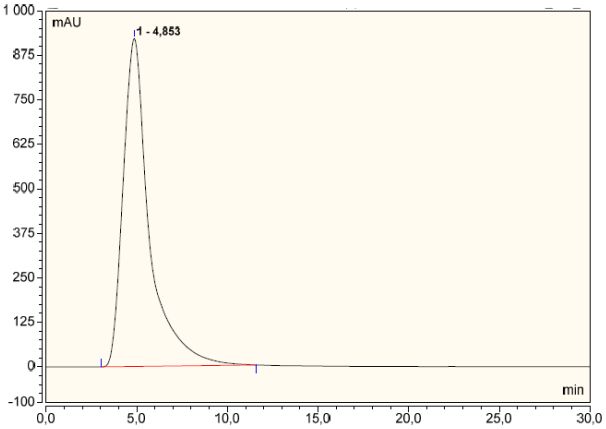

H340-6-2

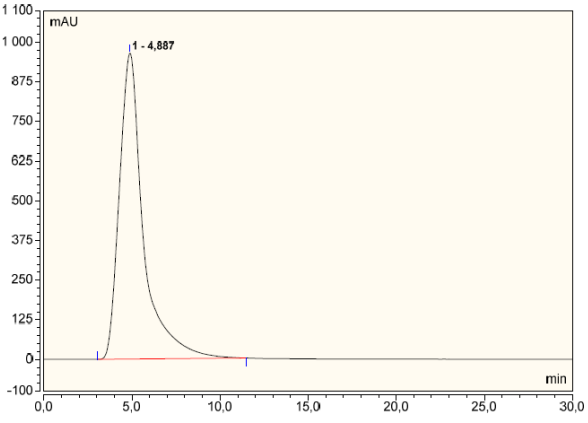

H340-10-1

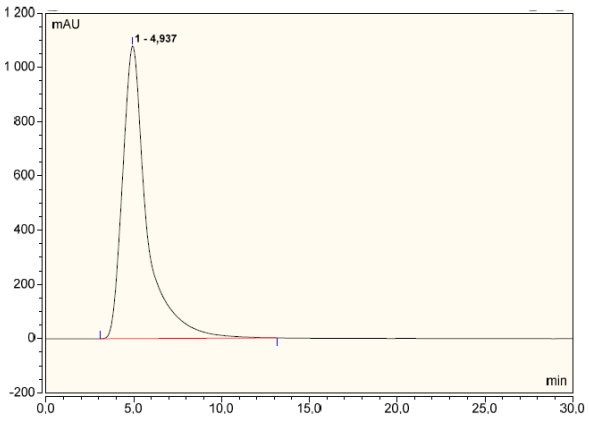

H380-2.1

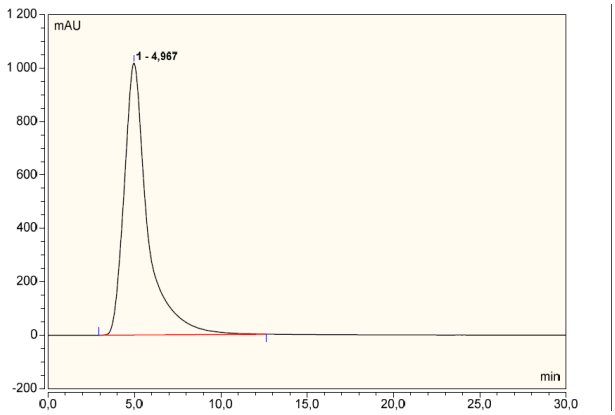

H380-6-1

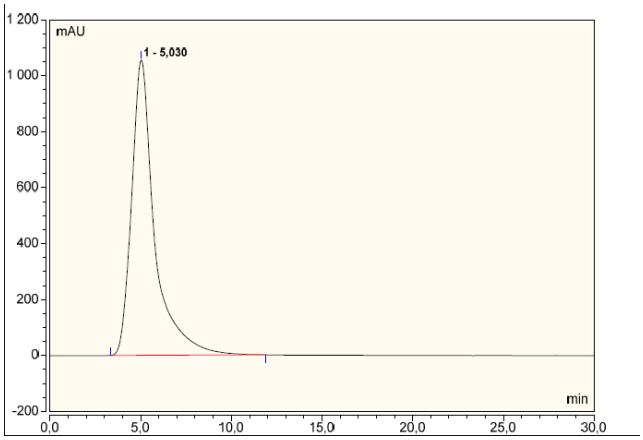

H380-10-1

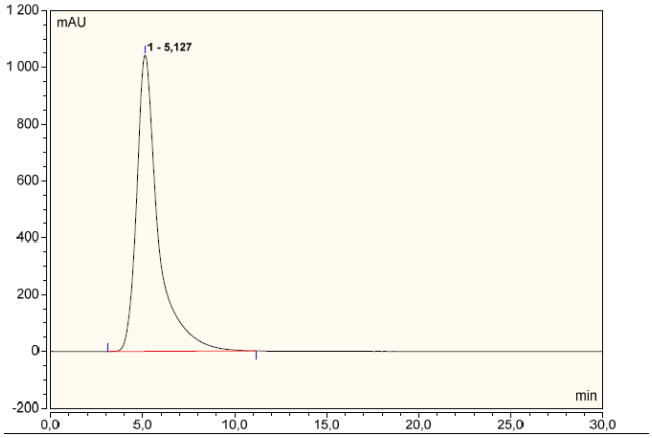

C. GC-MS: Chromatograms

Standard.1

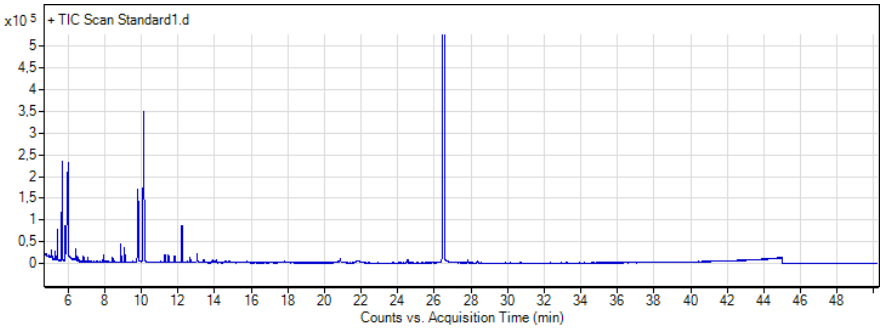

H300-2-1

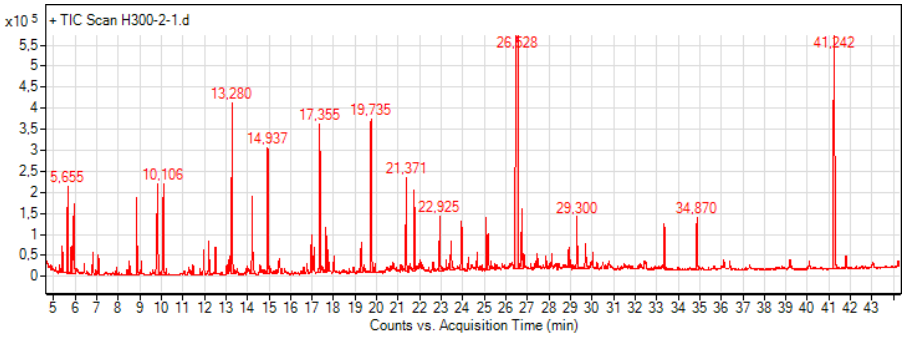

H300-6-2

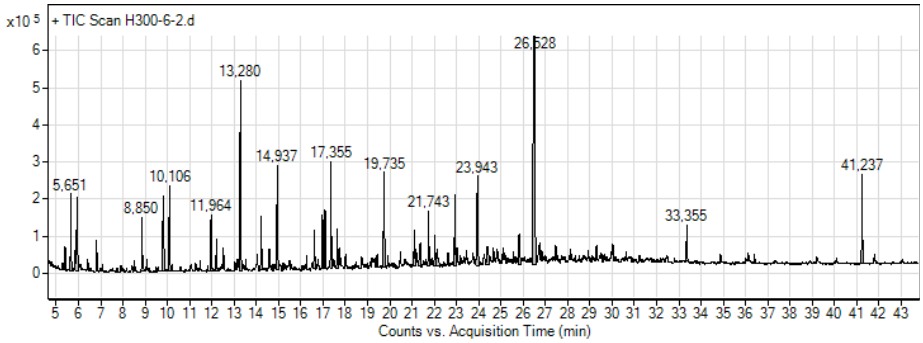

H300-10-1

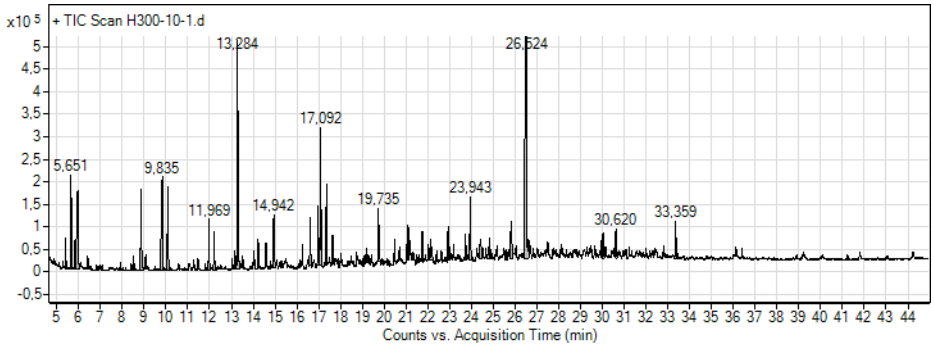

H300-10-2

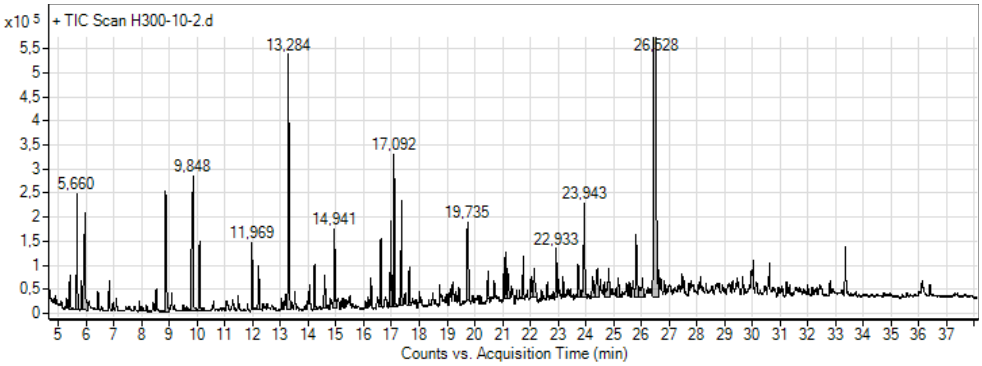

H340-2-1

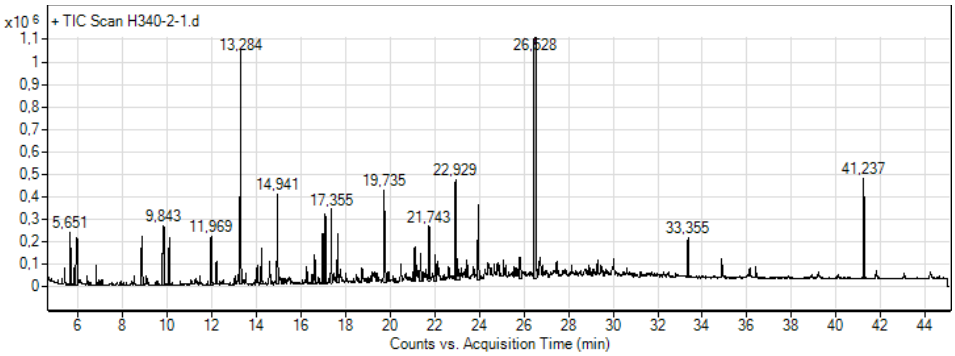

H340-6-2

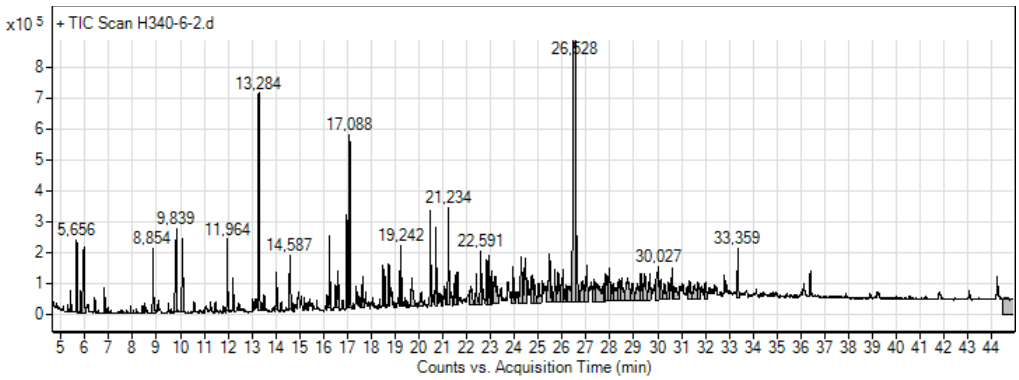

H340-10-1

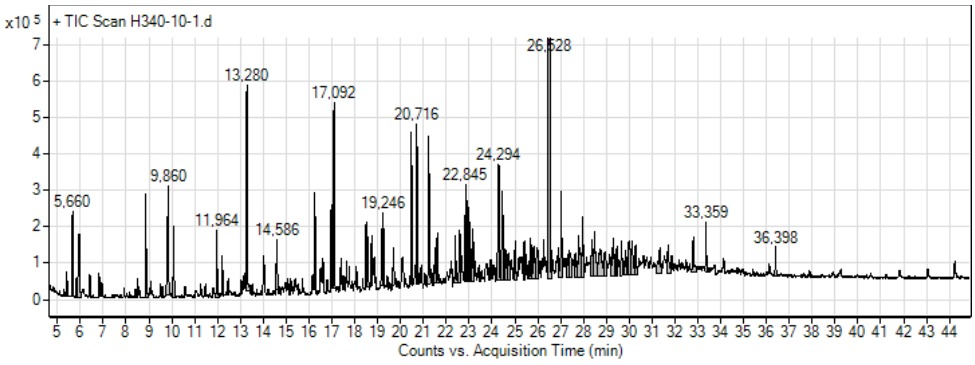

H380-2-1

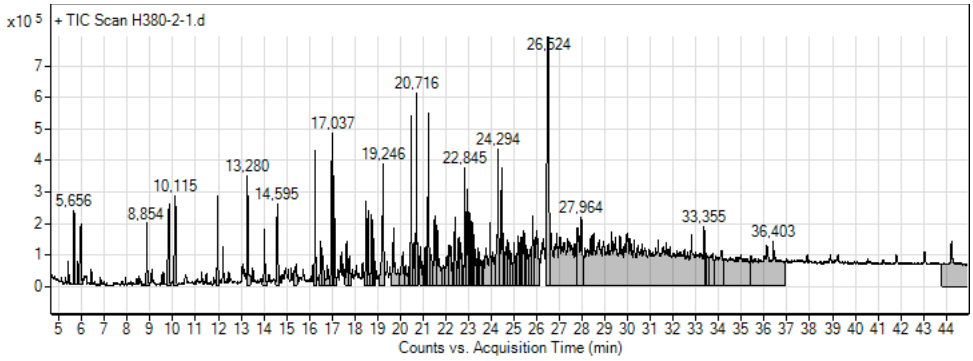

H380-6-1

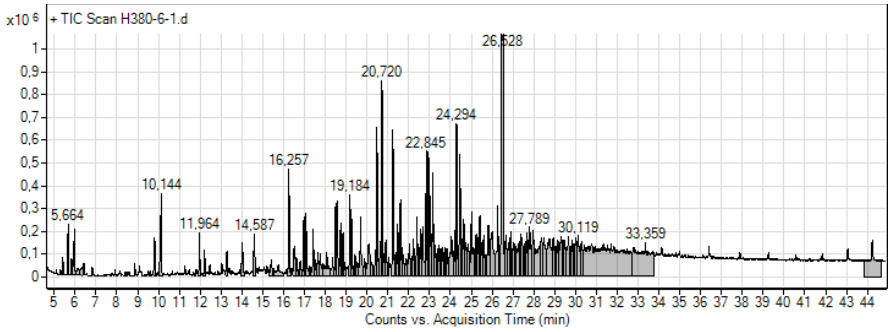

H380-10-1

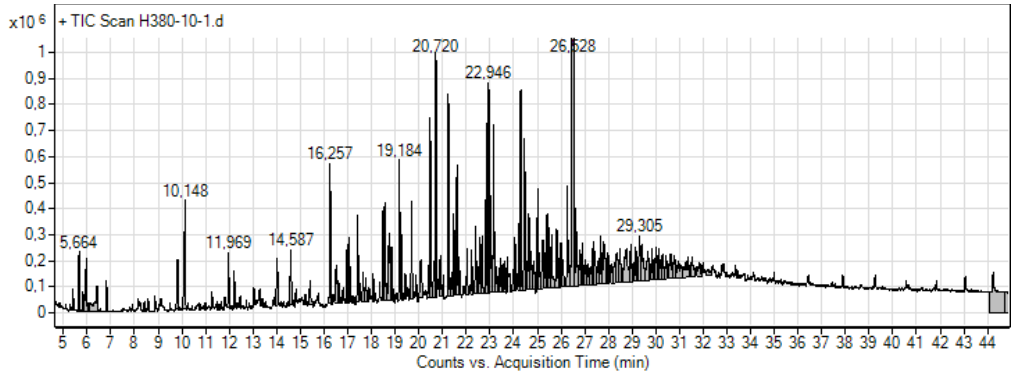

HNMZr4

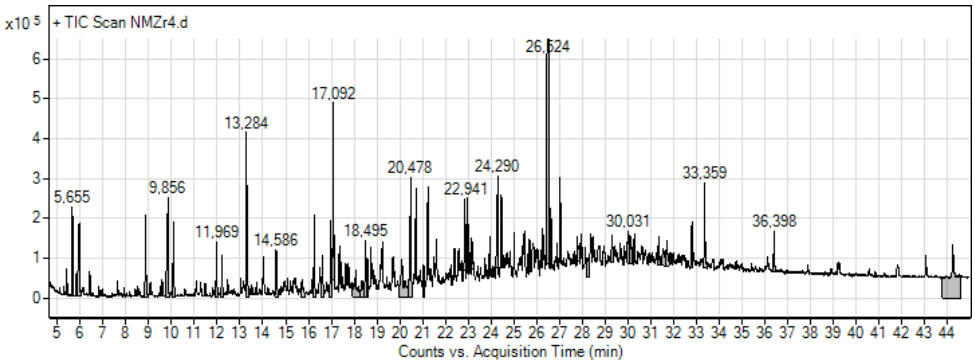

SZr4-1

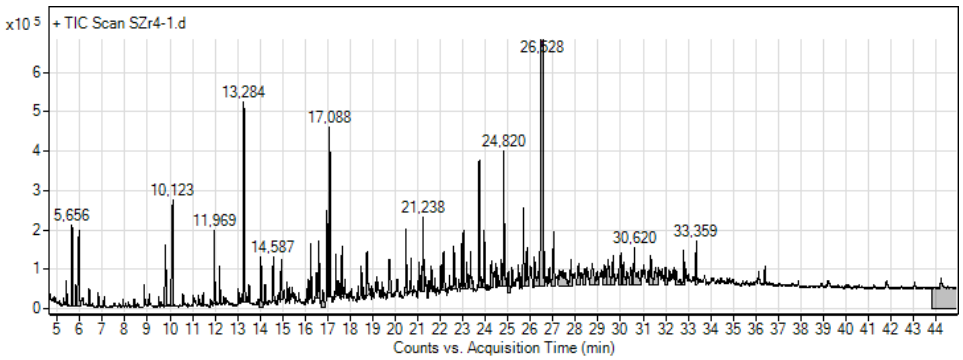

D. ESI-MS: Spectra
D1. Oil spectra

H300-2-1

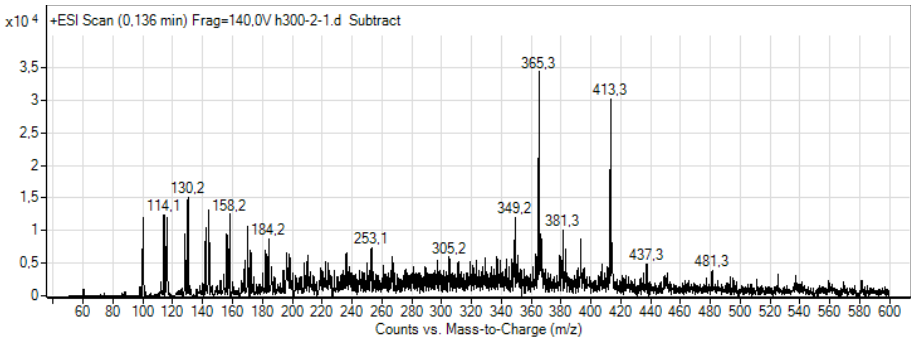

H300-6-2

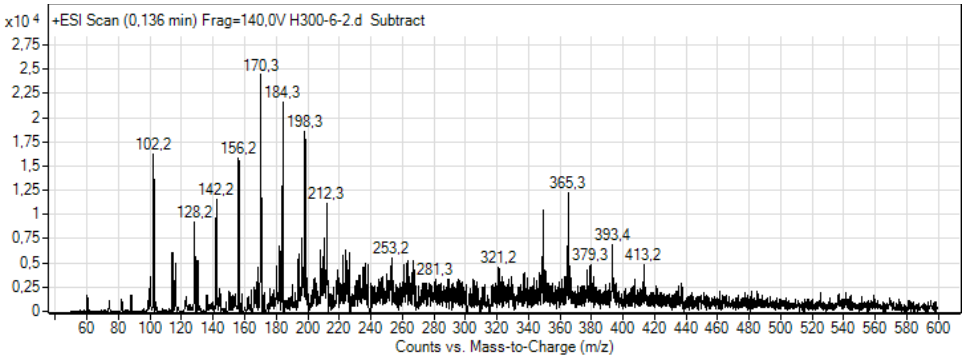

H300-10-1

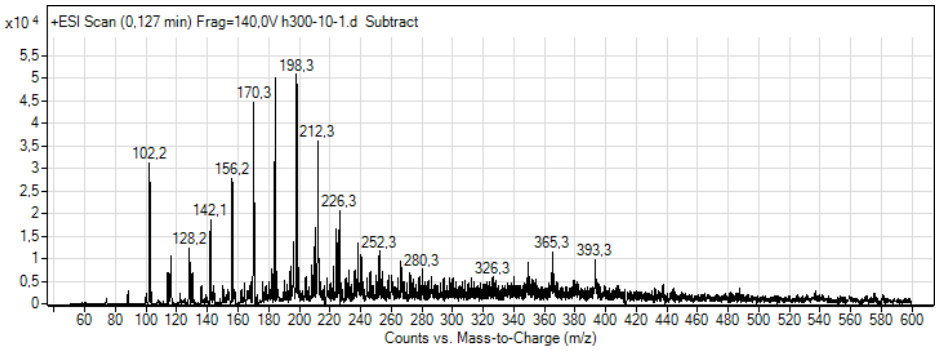

H340-2-1

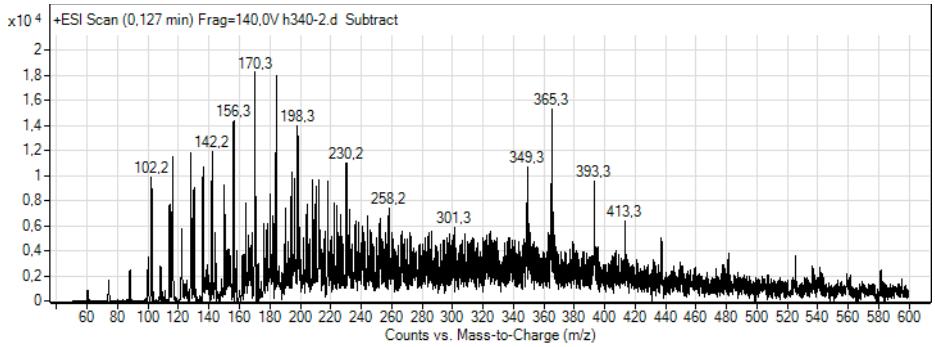

H340-6-1

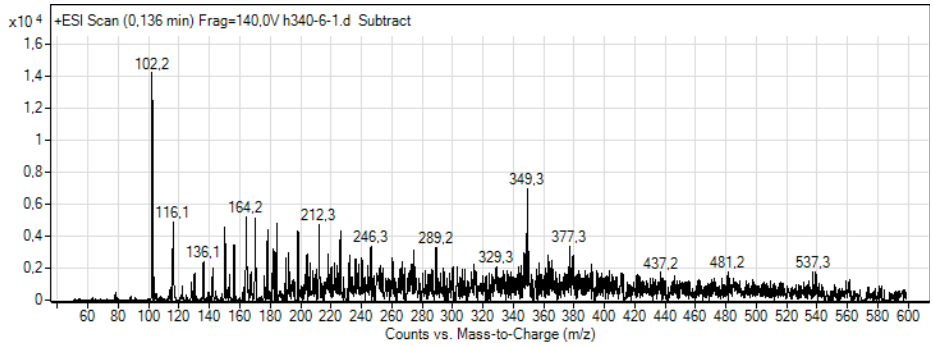

H340-10-1

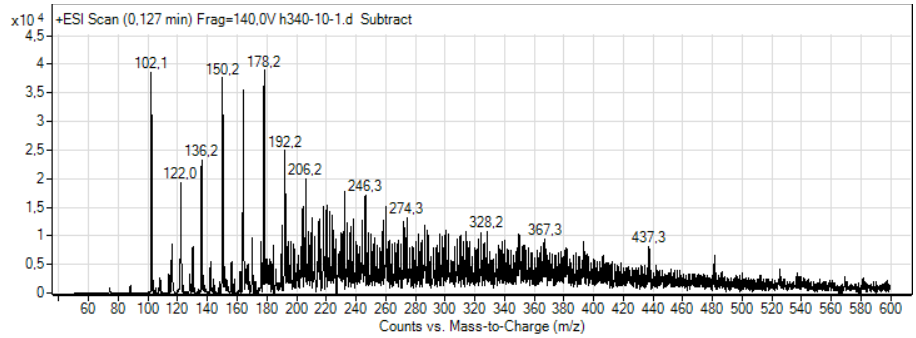

H380-2-1

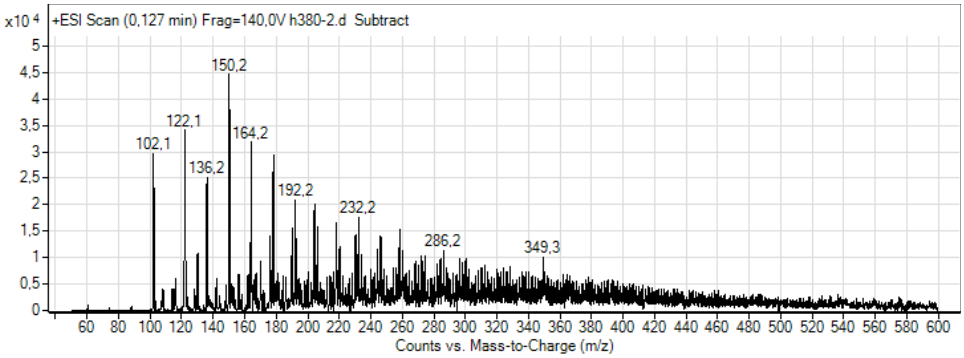

H380-6-1

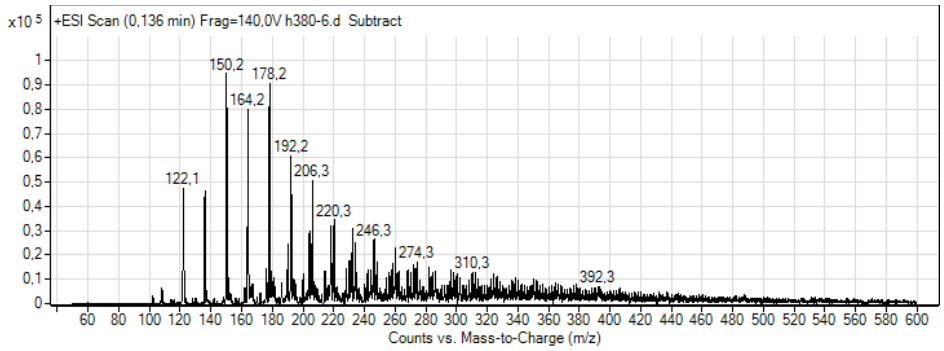

H380-10-1

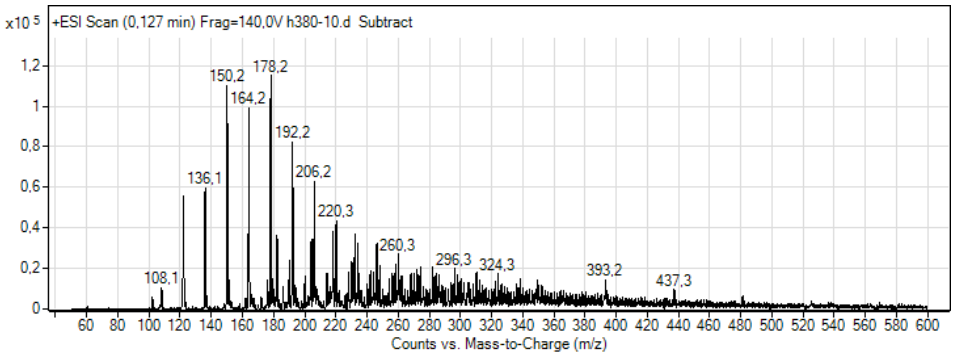

NMzr4-2

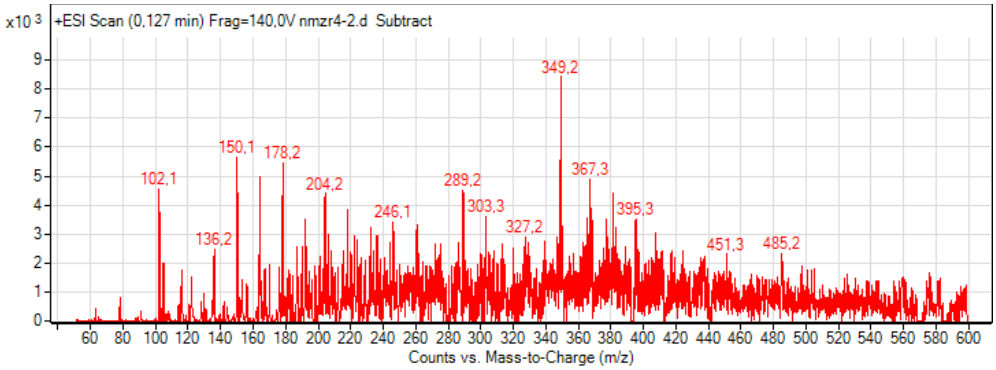

NoCat

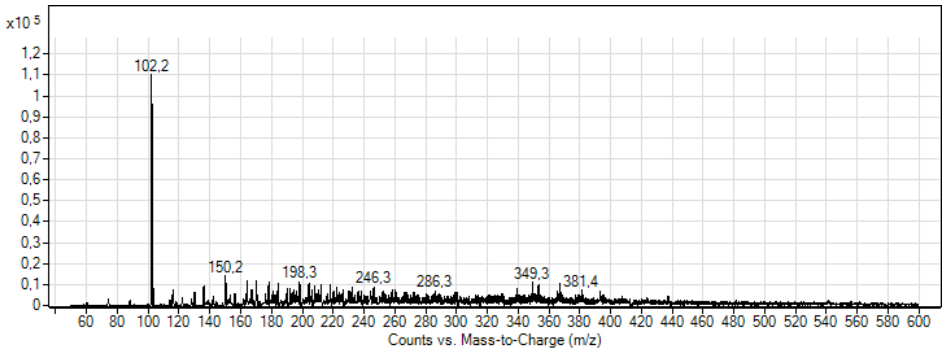

SZr4-1

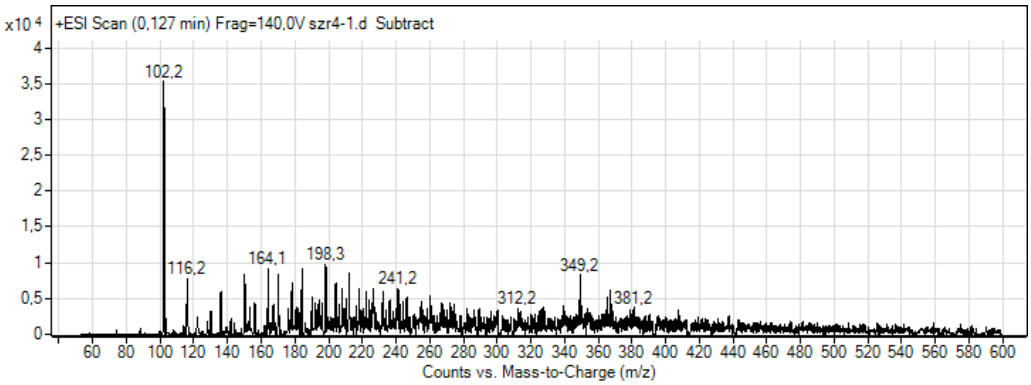

D2. Standards

Triethylamine

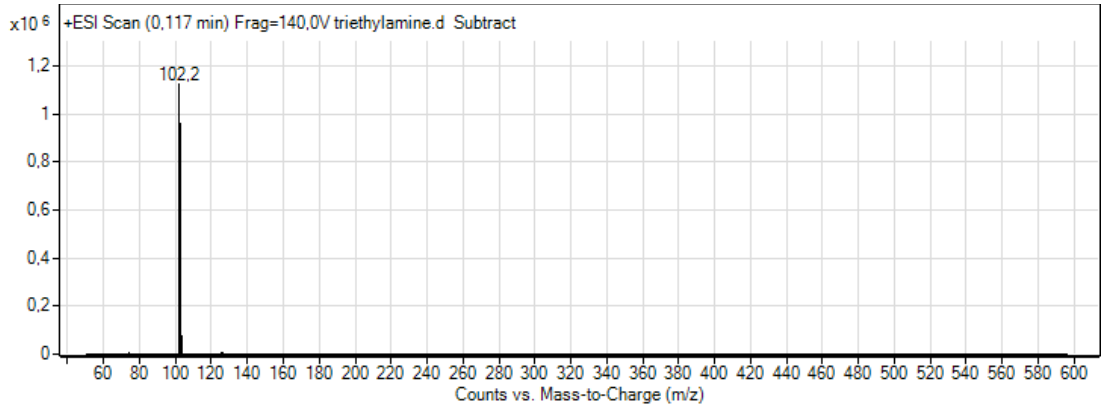

o-nitrophenol

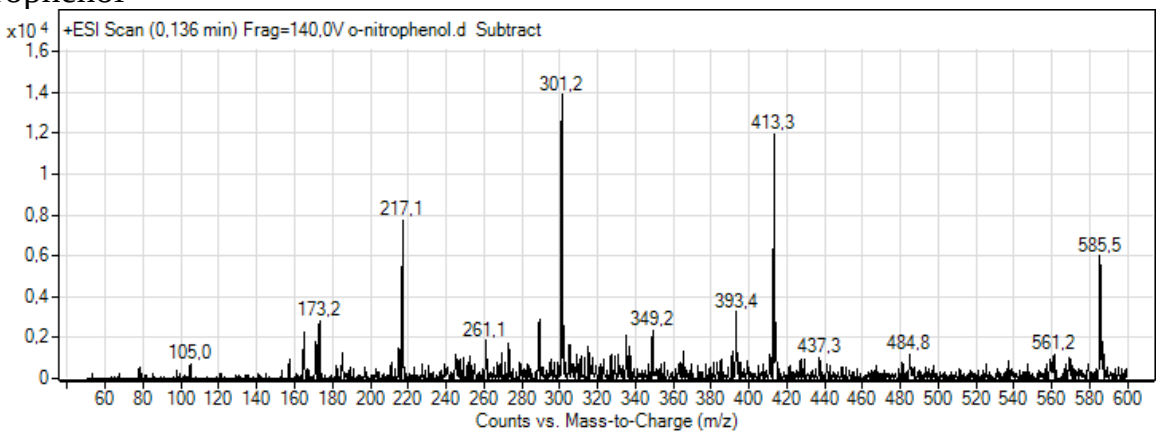

3-aminophenol

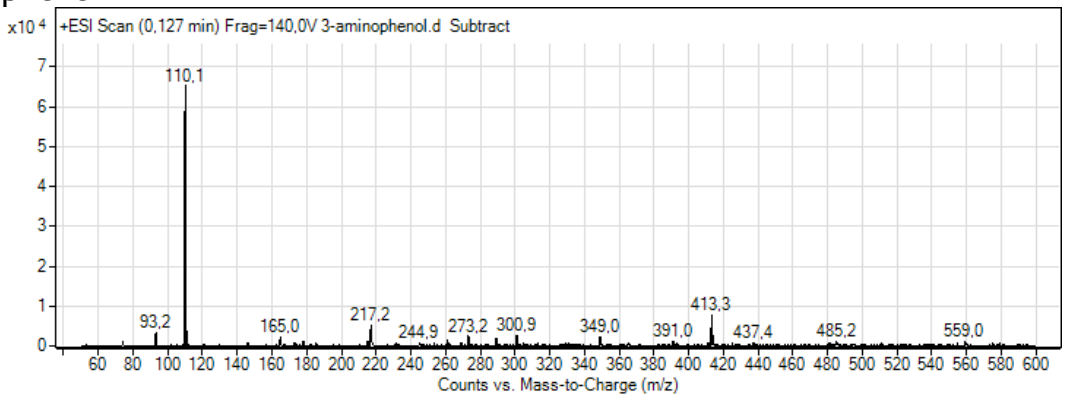

2,6-dimethylphenol

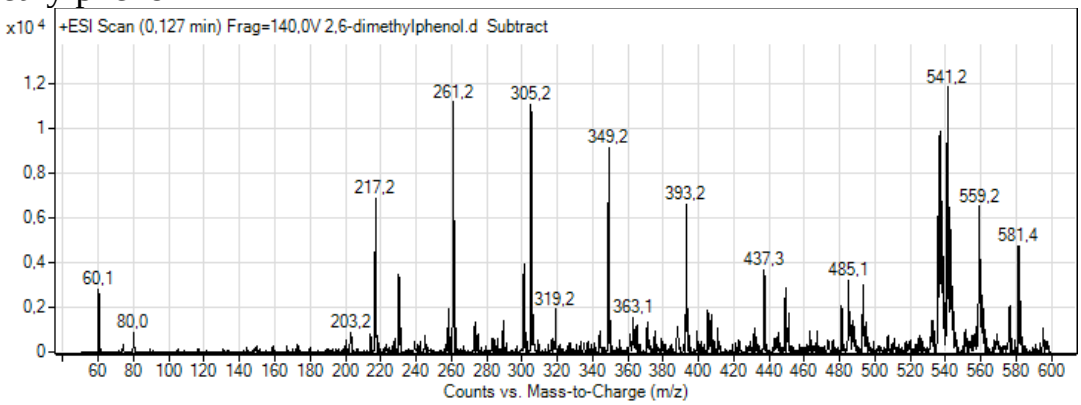

Pyridine

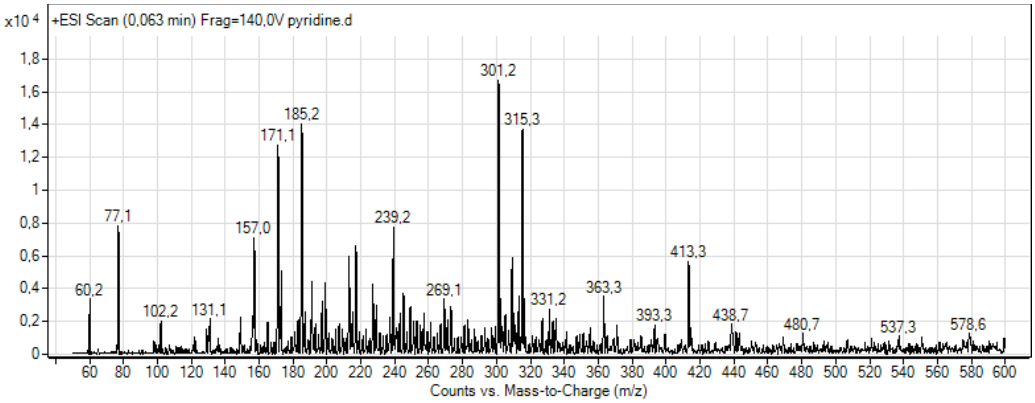

Quinoline

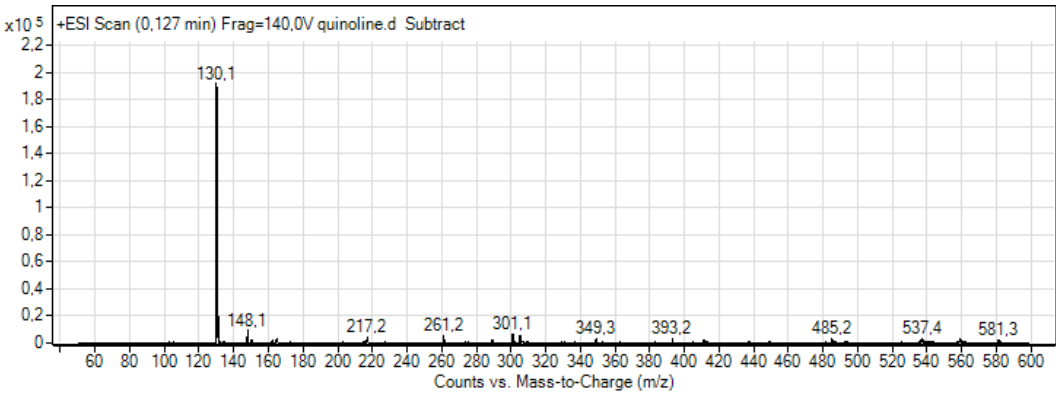

Carbazole

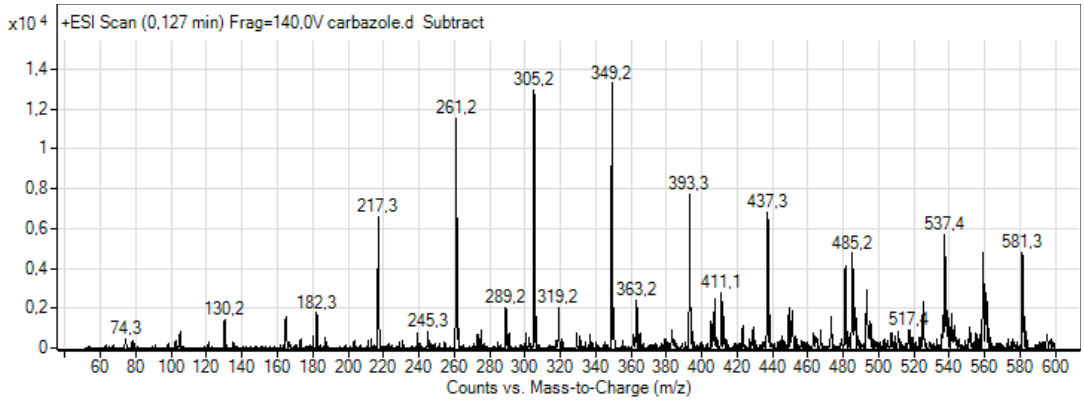

Guaiacol, 2-isopropylphenol and 2,6-diisopropylphenol

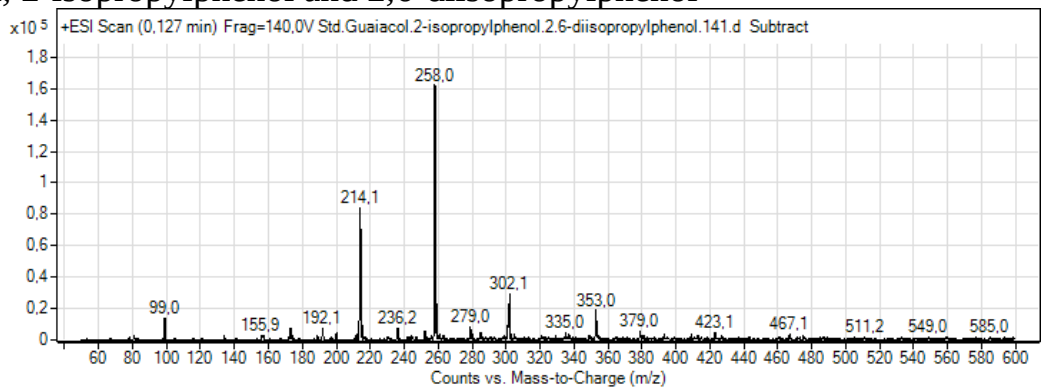

D3. Variation of fragmentor value

All spectras are taken of H300-2-1

Fragmentor: 40

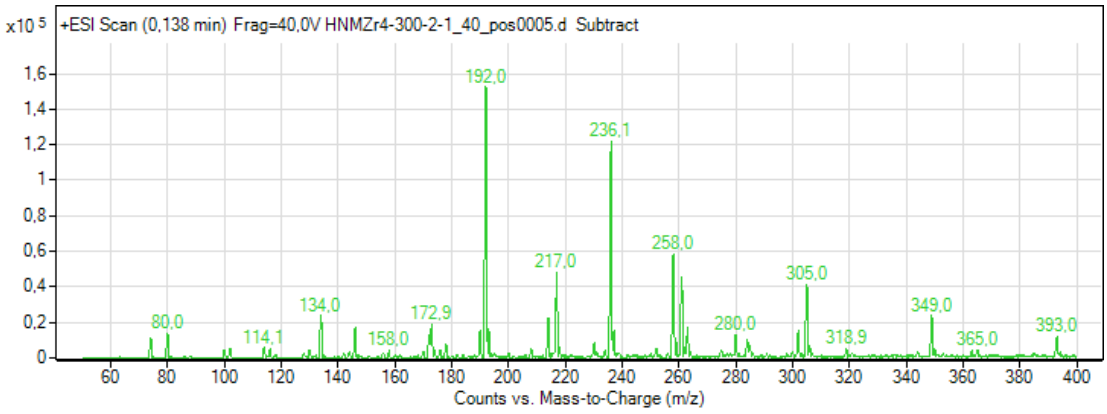

Fragmentor : 100

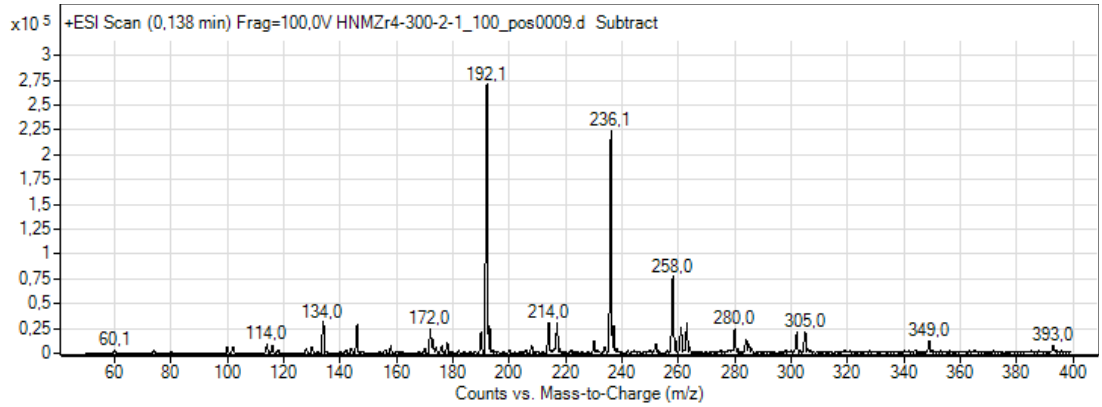

Fragmentor: 120

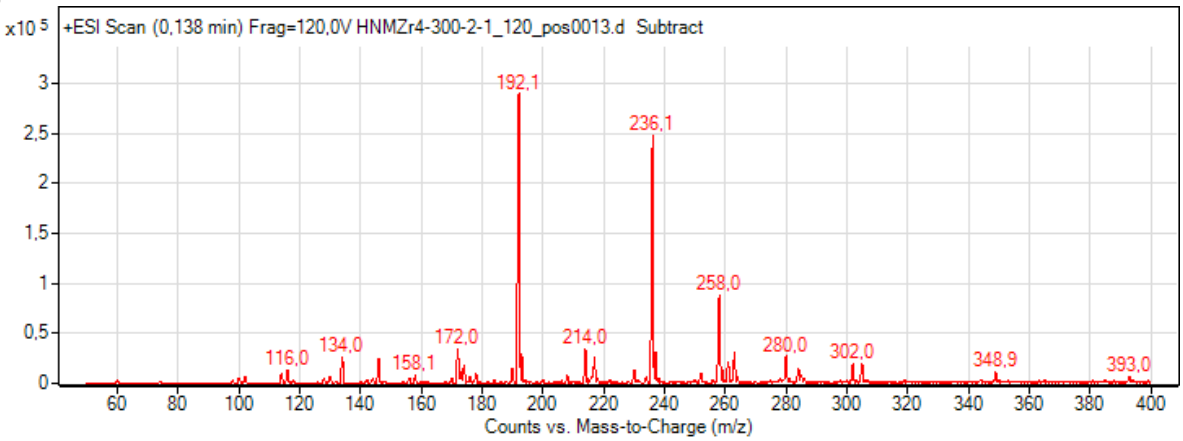

Fragmentor: 140

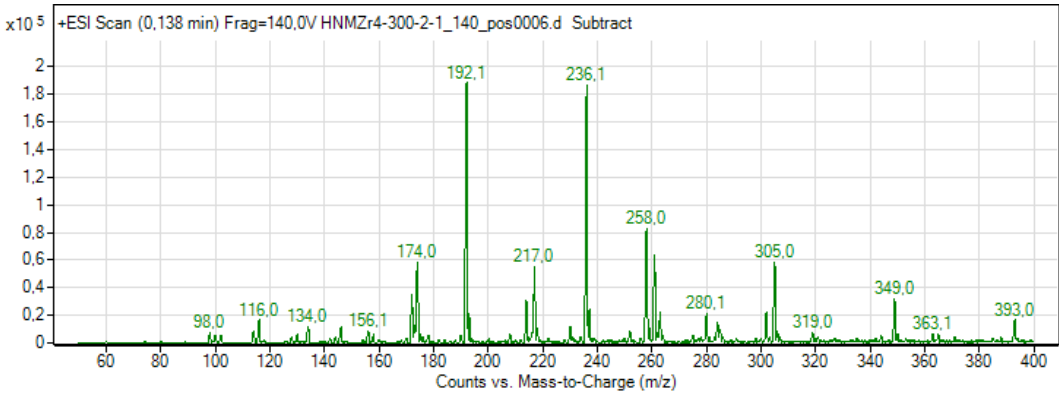

Fragmentor: 180

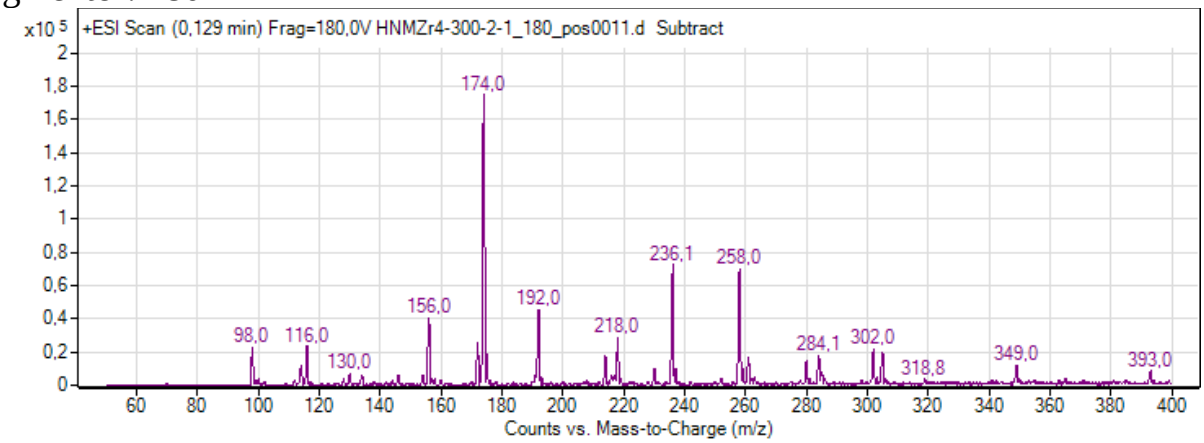

Fragmentor: 200

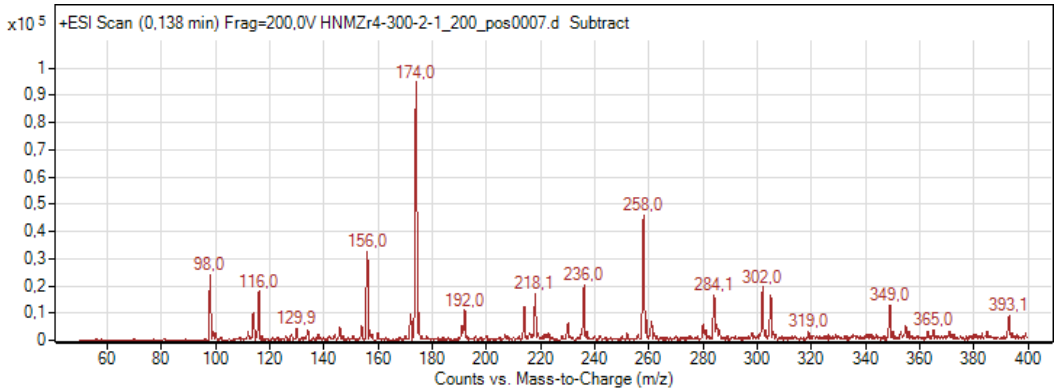

D4. Spectras captured with 0,1% formic acid in the methanol

H300-6-2

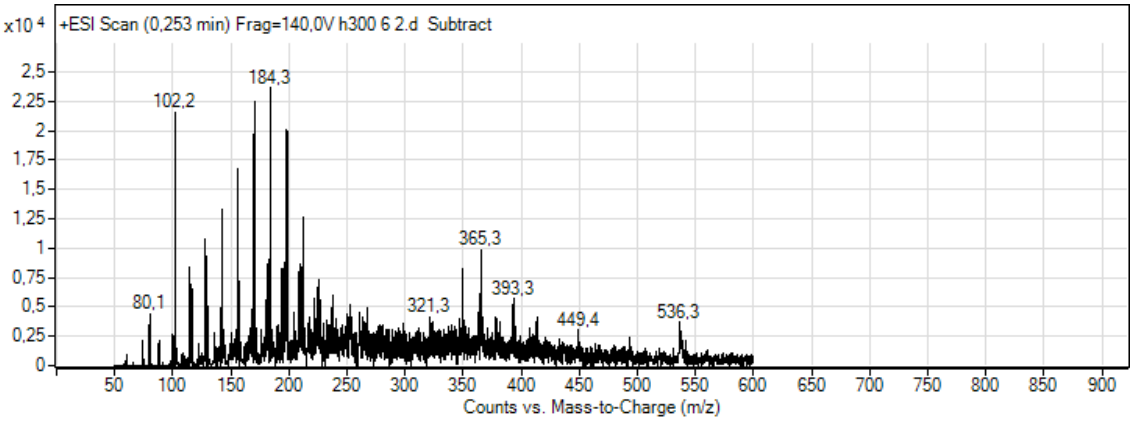

H340-2-1

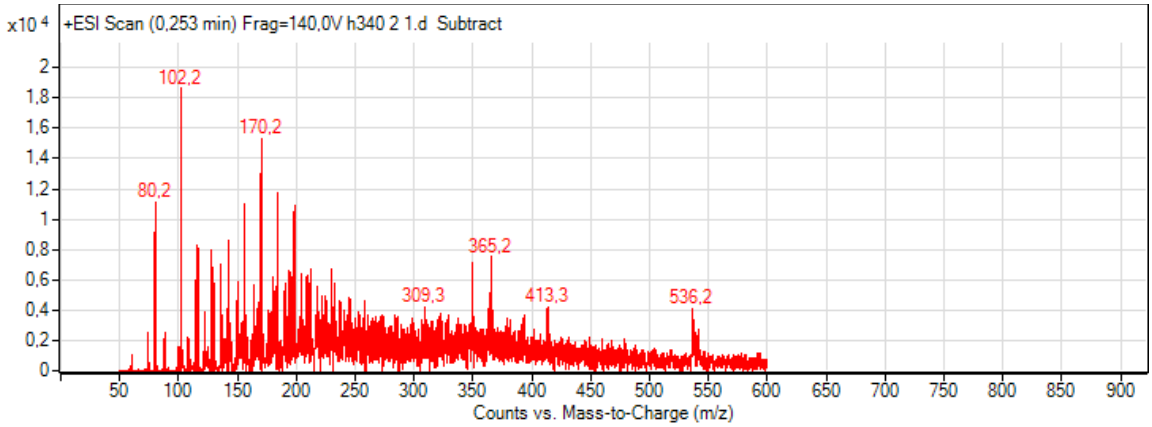

H340-6-1

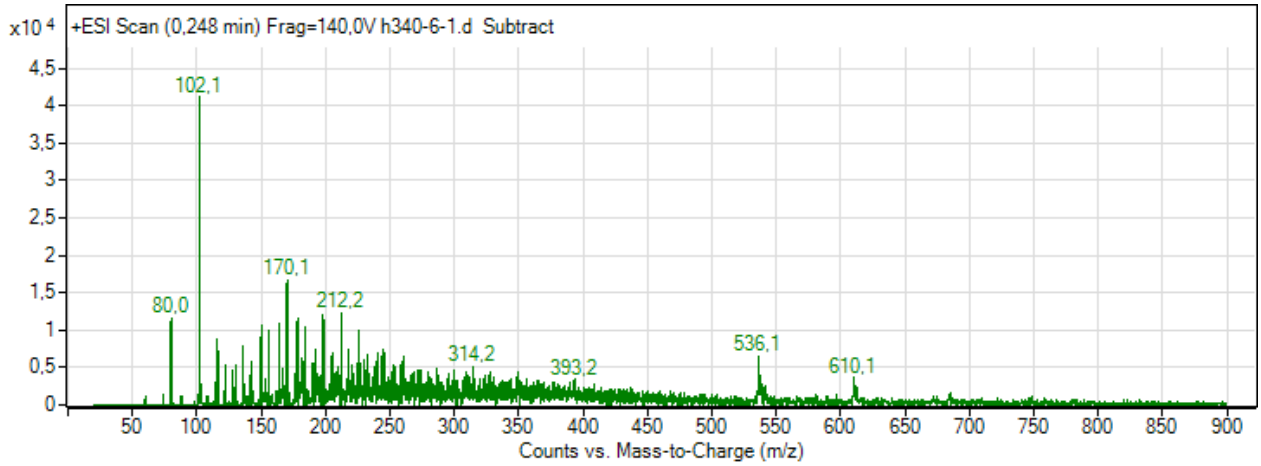

H380-2-1